UNIVERSIDADE ESTADUAL PAULISTA
"Júlio de Mesquita Filho"
Instituto de Geociências e Ciências Exatas
Câmpus de Rio Claro

HENDRYK GEMEINER

ASSESSMENT OF LABILITY AND BIOAVAILABILITY OF METALS IN A URANIUM MINING RESTORATION SITE USING DGT AND *PHYTOSCREENING* TECHNIQUES

Orientador: Prof. Dr. Amauri A. Menegário
Coorientador: Prof. Dr. Chang Hung Kiang

Rio Claro - SP
2021

UNIVERSIDADE ESTADUAL PAULISTA
"Júlio de Mesquita Filho"
Instituto de Geociências e Ciências Exatas
Câmpus de Rio Claro

HENDRYK GEMEINER

ASSESSMENT OF LABILITY AND BIOAVAILABILITY OF METALS IN A URANIUM MINING RESTORATION SITE USING DGT AND *PHYTOSCREENING* TECHNIQUES

Tese de Doutorado apresentada ao Instituto de Geociências e Ciências Exatas do Câmpus de Rio Claro, da Universidade Estadual Paulista "Júlio de Mesquita Filho", como parte dos requisitos para a obtenção do título de Doutor em Geociências e Meio Ambiente

Orientador: Prof. Dr. Amauri A. Menegário

Coorientador: Prof. Dr. Chang Hung Kiang

Rio Claro - SP

2021

G322a

Gemeiner, Hendryk

Assessment of Lability and Bioavailability of Metals in a Uranium Mining Restoration site using DGT and Phytoscreening techniques / Hendryk Gemeiner. -- Rio Claro, 2021

144 p.

Tese (doutorado) - Universidade Estadual Paulista (Unesp), Instituto de Geociências e Ciências Exatas, Rio Claro

Orientador: Amauri A. Menegário

Coorientador: Chang Hung Kiang

1. DGT. 2. Soil contamination. 3. Phytoscreening. 4. Metal lability. 5. Bioavailability. I. Título.

Sistema de geração automática de fichas catalográficas da Unesp. Biblioteca do Instituto de Geociências e Ciências Exatas, Rio Claro. Dados fornecidos pelo autor(a).

Essa ficha não pode ser modificada.

HENDRYK GEMEINER

ASSESSMENT OF LABILITY AND BIOAVAILABILITY OF METALS IN A URANIUM MINING RESTORATION SITE USING DGT AND *PHYTOSCREENING* TECHNIQUES

Tese de Doutorado apresentada ao Instituto de Geociências e Ciências Exatas do Câmpus de Rio Claro, da Universidade Estadual Paulista "Júlio de Mesquita Filho", como parte dos requisitos para obtenção do título de Doutor em Geociências e Meio Ambiente.

Comissão Examinadora

_____

Prof. Dr. AMAURI ANTONIO MENEGÁRIO

_____

Prof. Dr. PAUL NICHOLAS WILLIAMS

_____

Profa. Dra. ANNE HÉLÈNE FOSTIER

_____

Prof. Dr. MARCO TADEU GRASSI

_____

Dr. ELIAS HIDEO TERAMOTO

Conceito: Aprovado.

Rio Claro/SP, 23 de fevereiro de 2021

Dedicated to the memory
of my father Frank Gemeiner (1959 – 2019)

Acknowledgements

I would like to express my sincere and deeply appreciation to:

The organizations of Coordenação de Aperfeiçoamento de Pessoal de Nível Superior - Brasil (Capes) and Petrobras together with Fundação para o Desenvolvimento da UNESP (FUNDUNESP - grant number 2017/00061-0, process 2017/00135-4) for the financial support of this work. (This study was financed in part by the Coordenação de Aperfeiçoamento de Pessoal de Nível Superior - Brasil (CAPES) - Finance Code 001).

My supervisor, Prof Amauri A. Menegário, for the constant effort and support over the years, constructive feedback, excellent supervision, guidance, motivation, and conveying excitement regarding research and teaching.

My co-supervisor, Prof Chang Hung Kiang, for the guidance, giving me new insights and perspective regarding research, and the huge support in a difficult time.

All operator and staff members of INB Caldas for giving access to the study site and supporting the field work. Here, incredibly special thanks to Amália and Fábio for the hospitality, as well as their unflagging efforts and cooperation.

My dear colleagues from the GEMB research group, in the names of Amanda, Alfredo, Cristiane, Edson, Gabriel, Guilherme, Ingrid, Jorge, Lucas, Melina, Silmara and Vania for all the support and cooperation in the field and laboratory. Thank you for making sure that CEA was and is always a place where productive research is realized in a very pleasant working environment.

All technical staff members of CEA, especially Gleide, Eleni and Marcos for all the technical assistance.

All researchers and technical staff members of LEBAC/RAIH for the warm reception, assistance, and the exhibited professionalism. Special thanks to Roger for sharing his knowledge with the XRF as well as to Cris, Luciana, Bruno, Dagmar, Elias, Hernan and Miguel for providing all laboratory infrastructure in the RAIH facilities.

The head of the postgraduate programme of “Geociências e Meio Ambiente”, Prof César A. Moreira, for his support as well as for the excellent organization of the programme and his efforts to improve the programme.

The secretary of the postgraduate programme, Rosangela, for helping with all the paperwork and reminding me of all deadlines.
Prof Silvio Govone, Prof Didier Gastmans, Prof Paul Williams, Prof Marcelo L. Garcia and Dr Eduardo Almeida for giving me insights in the university teaching and sharing knowledge in their respective fields of work.
My dear friends Adriano, Antonio, Eduardo, Henrique, Jorge and Juliana (and families), Juan and Karina, Lucas and Lilian, Thiago and Roberta, Vania, and Vitoria. Thank you for making life outside the university so enjoyable which gave me strength for mastering the challenges of the professional life.

Most importantly, my dear family in the names of my mother Sylvia and my father Frank, my brother Holger and his wife Anne, and my grandparents Christa, Lilo and Wolfgang for all the motivation, comprehension, love, support, encouragement, and inspiration.

Assessment of Lability and Bioavailability of Metals in a Uranium Mining Restoration site using DGT and *Phytoscreening* techniques

Abstract

The technique of *diffusive gradients in thin films* (DGT) has been shown to be a promising tool to assess lability and bioavailability of metals in soils in a variety of studies. In the present work, paired topsoil and tree core samples from a reference area and three mining impacted areas at the Uranium mining complex of Poços de Caldas in Southern Minas Gerais (Brazil) were collected. Soil samples were analysed for their total content of Al, Co, Cu, Fe, Mn, Ni, Pb, Zn and U by XRF and subsequently, the lability and potential environmental bioavailability of these metals were investigated by DGT and pore water analysis using ICP-MS. In addition, results were compared with metal concentrations obtained by *Tree Coring* from the forest vegetation to potentially evaluate the soil-plant-transfer of these metals. In all sampling areas, mean total concentrations of the elements U ($C_{tot.}$= 100.5 ± 66.5 mg kg^{-1} to 129.6 ± 57.1 mg kg^{-1}), Pb ($C_{tot.}$= 30.8 ± 12.7 mg kg^{-1} to 90.8 ± 90.8 mg kg^{-1}), Zn ($C_{tot.}$= 91.5 ± 24.7 mg kg^{-1} to 99.6 ± 10.3 mg kg^{-1}), Cu ($C_{tot.}$= 26.3 ± 4.8 mg kg^{-1} to 27.9 ± 4.0 mg kg^{-1}), Ni ($C_{tot.}$= 49.1 ± 8.7 mg kg^{-1} to 73.7 ± 17.4 mg kg^{-1}), Co ($C_{tot.}$= 73.8 ± 25.5 mg kg^{-1} to 119.7 ± 26.4 mg kg^{-1}) and Mn ($C_{tot.}$= 554.0 ± 163.6 mg kg^{-1} to 1080.4 ± 697.9 mg kg^{-1}) in soils were explicitly higher than quality reference values for soils from Minas Gerais. Study results suggest that influence of AMD effluents caused the increase of relative labile concentrations of Zn in AMD affected soils. High labile fractions of the elements Pb (R= 62 ± 34 % to 81 ± 29 %), U (R= 57 ± 20 % to 77 ± 28 %) and Zn (R= 21 ± 25 % to 34 ± 31 %) in soils together with high bioconcentration factors found in wood samples for Pb (BCF= 0.04 ± 0.03 % to 0.26 ± 0.33 %) and Zn (BCF= 1.2 ± 1.3 % to 2.5 ± 2.1 %) indicate a high toxic potential of these elements to living organisms in the soils of the study site. The combination of pore water and DGT analysis with *Tree Coring* showed to be a useful approach to specify the risk of metal polluted soils. However, the comparison of the results from DGT and *Tree Coring* could not predict the uptake of metals into the xylems

of the sampled tree individuals and are thus limited to assess environmental and toxicological bioavailability.

Keywords: DGT, soil contamination, *Phytoscreening*, metal lability, bioavailability, Uranium mining

Avaliação de labilidade e biodisponibilidade de metais em um local de restauração de mineração de urânio utilizando a técnica DGT e *Phytoscreening*

Resumo

A técnica *difusão em filmes finos por gradientes de concentração* (DGT) mostrou ser uma ferramenta promissora em vários estudos para avaliar a labilidade e biodisponibilidade de metais no solo. No presente trabalho, foram coletadas amostras pareadas do solo e núcleo de árvores de uma área de referência e três áreas impactadas pela mineração no complexo de mineração de urânio de Poços de Caldas no sul de Minas Gerais (Brasil). As amostras de solo foram analisadas quanto ao teor total de Al, Co, Cu, Fe, Mn, Ni, Pb, Zn e U por XRF e, posteriormente, a labilidade e potencialmente a biodisponibilidade ambiental desses metais foi investigada pela técnica DGT e análise da água intersticial usando ICP-MS. Além disso, os resultados foram comparados com a concentração de metais obtida pela técnica de *Tree Coring* da vegetação florestal, a fim de avaliar a transferência solo-planta desses metais. Em todas as áreas de amostragem, as concentrações totais médias dos elementos U ($C_{tot.}$= 100.5 ± 66.5 mg kg^{-1} até 129.6 ± 57.1 mg kg^{-1}), Pb ($C_{tot.}$= 30.8 ± 12.7 mg kg^{-1} até 90.8 ± 90.8 mg kg^{-1}), Zn ($C_{tot.}$= 91.5 ± 24.7 mg kg^{-1} até 99.6 ± 10.3 mg kg^{-1}), Cu ($C_{tot.}$= 26.3 ± 4.8 mg kg^{-1} até 27.9 ± 4.0 mg kg^{-1}), Ni ($C_{tot.}$= 49.1 ± 8.7 mg kg^{-1} até 73.7 ± 17.4 mg kg^{-1}), Co ($C_{tot.}$= 73.8 ± 25.5 mg kg^{-1} até 119.7 ± 26.4 mg kg^{-1}) e Mn ($C_{tot.}$= 554.0 ± 163.6 mg kg^{-1} até 1080.4 ± 697.9 mg kg^{-1}) nos solos foram explicitamente superiores aos valores de referência de qualidade para solos do estado de Minas Gerais. Os resultados do estudo sugerem que a influência dos efluentes da drenagem ácida causou o aumento das concentrações lábeis de Zn nos solos afetados pela drengaem ácida. Frações altamente lábeis dos elementos Pb (R= 62 ± 34 % to 81 ± 29 %), U (R= 57 ± 20 % to 77 ± 28 %) e Zn (R= 21 ± 25 % to 34 ± 31 %) juntamente com altos fatores de bioconcentração encontrados em as amostras de madeira dos elementos Pb (BCF= 0.04 ± 0.03 % to 0.26 ± 0.33 %) e Zn (BCF= 1.2 ± 1.3 % to 2.5 ± 2.1 %) indicam um alto potencial tóxico desses elementos no solo para a biota em todas as áreas de amostragem do local de estudo. A combinação de análise de água intersticial e

DGT com *Tree Coring* mostrou ser uma abordagem útil para especificar o risco de solos poluídos por metais. No entanto, a comparação dos resultados de DGT e *Tree Coring* não podia prever a absorção de metais nos xilemas dos indivíduos dos árvores amostrados e, portanto, é limitado para avaliar a biodisponibilidade ambiental e biodisponibilidade toxicológica.

Palavras-chave: DGT, contaminação de solo, *Phytoscreening*, metais labeis, biodisponibilidade, mineração de urânio

Table of Contents

List of Figures

List of Tables

List of Abbreviations and Acronyms

AMD - Acid Mine Drainage

ATSDR - Agency for Toxic Substances and Disease Registry

BCF - Bioconcentration factor

BMUB – German Ministry for Environment, Conservation and Nuclear Safety

CETESB - Companhia Ambiental do Estado de São Paulo (Environmental Company of State of São Paulo)

CIPC - Poços de Caldas Mining-Industrial Complex

CNA – Canadian nuclear Association

CONAMA - Conselho Nacional de Meio Ambiente (Brazilian Environment Council)

COPAM - Conselho Estadual de Política Ambiental (Political Environmental State Council of Minas Gerais)

DGT - Diffusive Gradients in Thin-films

DMT - Donnan membrane technique

FOEFL - Swiss Federal Office of Environment Forests and Landscape

GWRTAC - Ground-Water Remediation Technologies Analysis Center

ICP-MS – Inductively coupled plasma mass spectrometry

INB - Indústrias Nucleares do Brasil (Brazilian Nuclear Industries)

ISO - International Organization for Standardization

LD – Limit of Detection

LQ – Limit of Quantification

USEPA - United States Environmental Protection Agency

WNA- World Nuclear Association

XRF - X-ray fluorescence

1 INTRODUCTION

Since the industrial revolution, soil ecosystems on earth have been increasingly exposed to a variety of potentially hazardous elements through anthropogenic activities. Soil contamination can be defined as the occurrence of pollutants in soil above a certain level causing the deterioration or loss of one or more soil functions. The contamination of soils poses vast risks and hazards to terrestrial and aquatic ecosystems and further to human health (PANAGOS et al., 2013). The implication of contaminated soils to human health can be directly through contact with the contaminated soil or indirectly over the food chain (soil-plant-human or soil-plant-animal-human), or over the consumption of contaminated groundwater. Furthermore, soil contamination causes a reduction in food quality (safety and marketing) through phytotoxicity and a reduction in land applicability for agricultural production, causing food insecurity and land tenure problems (MCLAUGHLIN et al., 2000; LING et al. 2007). Soil quality research is facing a major technological challenge and a number of actions are being taken to assess, correct and reduce the risk of soil contaminants (PASCUCCI, 2011).

Metals represent one of the most frequent contaminant groups globally. The particular interest in metals is since they constitute a group of hazardous inorganic chemical elements and are often abundantly found in contaminated sites, such as the elements lead (Pb), chromium (Cr), arsenic (As), zinc (Zn), cadmium (Cd), copper (Cu), mercury (Hg) and nickel (Ni) (GWRTAC, 1997; ADRIANO, 2003, DESAULES, 2012). Soils are the main destination for metals released into the environment due to anthropogenic activities and, unlike organic contaminants, most metals do not undergo microbial or chemical degradation (KIRPICHTCHIKOVA et al., 2006). The total concentration of metals in soils persists long after introduction (ADRIANO, 2003).

The distribution of metals in the environment is strongly influenced by biological and geological cycles. Factors such as pH, ionic strength, redox potential, organic and inorganic chelating activity and biological processes directly influence the concentration and behaviour of metals. Thus, changes of geochemical conditions in the environment affect the behaviour of metals by

leading to changes in their speciation conditions, significantly influencing their lability, bioavailability and thus toxicity (ARAIN et al., 2008).

However, total concentrations of metals in the soil do not provide information on the lability and bioavailability of these elements. The lability of metal complexes is referred to association and dissociation kinetics of the volume complexation reaction, and to the interfacial flux of free metals due to dissociation of complex species (VAN LEEUWEN, 2000). The International Organization for Standardization (ISO) defined bioavailability in the guidelines of 17402 as “the degree to which chemicals present in the soil may be taken up or metabolised by human or ecological receptors or are available for interaction with biological systems”. Here, bioavailability was described in three conceptual steps: (1) environmental availability, (2) environmental bioavailability and (3) toxicological bioavailability (ISO, 2008). It was shown that in polluted soils, the lability and bioavailability of metals were highly dependent on their form of association and that the most labile forms of metals represented potentially available fractions. Therefore, it is necessary to obtain information on the distribution of elements of environmental concern among the different soil phases and determine forms of association (MAIZ et al., 2000; HARMSEN, 2007; KIM et al., 2015).

Sources of metal contamination in soils are mainly anthropogenic and arise from industrial discharges, dry or wet deposition of coal ashes, urban refuse, agricultural and animal wastes, fertilization with sewage sludge, pesticide application or irrigation with wastewater (KABATA-PENDIAS, 2011; MOUSAVI et al., 2013). One of the most serious sources of metal contamination in soils is mining. In mining areas, structures such as tailing dams, mine pits and spoil piles can represent major sources of contamination through the generation of acid mine drainage (AMD). The term AMD describes metal-rich water formed from chemical reaction between water and rocks containing sulfur-bearing minerals (AKCIL & KODAS, 2006). In AMD areas, a reduction in pH of the effluents in the mining complex is caused by the oxidation of sulphide minerals and the following formation of sulfuric acid with consequent dissolution of metals, especially aluminium (Al), cobalt (Co), copper (Cu), iron (Fe), manganese (Mn), uranium (U), zinc (Zn) and other metals associated with rock matrices. This leads to various hazardous environmental impacts around the mining areas (NÓBREGA et al., 2008; FERNANDES & FRANKLIN, 2001).

In Brazil, one of the areas where the phenomenon of AMD can be found is the Poços de Caldas Mining-Industrial Complex (CIPIC) in the south of the state of Minas Gerais. The main activity performed at CIPIC was the mining and processing of uranium ore which is used in the production of fuel for nuclear power plants. Due to the depletion of the deposit, the CIPIC mining complex was deactivated and is nowadays undergoing a decommissioning and environmental recovery plan conducted by the Brazilian Nuclear Industries (INB) (FRANKLIN, 2007).

2 SIGNIFICANCE OF THE STUDY

Since the 1990s, guidelines and limit values of potentially toxic elements in soils were established by the worldwide and national legislative authorities. These guidelines have the aim of protecting soils and managing contaminated soils (BMUB 1999; EA 2004, 2009; USEPA 2002, 2005). In 2002, the Environmental State Agency of São Paulo (Companhia Ambiental do Estado de São Paulo - CETESB) published a list of areas with soil and groundwater contamination recording 255 areas in the state of São Paulo. This list was updated in 2011, registering 4131 contaminated and rehabilitated areas (CETESB, 2011). These national and international regulations are mostly based on the total metal content in the soil. The total metal content in soil itself is useful to indicate the saturation level of metals in the soil matrix and gives a first impression of soil contamination. However, it does not give a proper evaluation of adverse effects on the soil ecosystem triggered by the contamination of metals. Furthermore, a variety of studies have shown that organisms are not impacted by the non-available fraction of the total metal content in the soil which is irreversibly bounded to the soil matrix, but are adversely affected by the biological available (bioavailable) fraction of the total metal content in the soil (BLUME & BRUEMMER, 1991; BRUEMMER et al.,1986; KIM et al., 2007; LANNO et al., 2004; RIEUWERTS et al., 1998) Thus, risk assessment based alone on total metal concentrations can cause misinterpreting or overestimating the potential risk of the contamination, which can lead to unnecessary, improper and/or expensive remediation actions (MCLAUGHLIN et al., 2000; MEERS et al., 2007, KIM et al., 2015). Several countries like Australia or South Korea moved towards

a risk-based approach in the recent past with highly considering bioavailability for the frameworks of the assessment and remediation of contaminated soils. Furthermore, more and more new methods for the prediction and assessment of bioavailability of metals in soils have been proposed recently (HARMSEN, 2007; ZHANG et al., 2014; KIM et al. 2015). Though, these methods still have to be standardized in order to use the concept for a proper risk assessment. The development and standardization of such tools which accurately predict metal bioavailability is indispensable in order to provide risk assessments of the potential exposure for soil–crop–human transfer. This approach can highly contribute to the protection of ecosystems and human health (HARMSEN, 2007; ZHANG et al., 2014; KIM et al. 2015). Therefore, the present study combined the analysis of total metal content in contaminated soil samples from a uranium mining area together with the extraction and analysis of soil pore water as well as the *diffusive gradients in thin films* techniques (DGT) in order to measure the labile and bioavailable fraction of the total metal content in the soils. Furthermore, results were compared with those results obtained by the analysis of tree cores sampled at the forest vegetation of the study site to gain insight if the predicted metal bioavailability is correlating with metal contents in the vegetation. If a correlation between the resulting chemical values and an effect or accumulation has been demonstrated in the tree cores, it can be an indicator that DGT is applicable as a tool for the prediction of environmental bioavailability. Furthermore, this study will provide a database of metals analysed in tree cores for further studies as this is the first work of analysing metals in tree cores in the southern hemisphere and tropical vegetation.

3 LITERATURE REVIEW

3.1 Sources of metal contamination in soils

A variety of metal elements are classified as biological essential (like Co, Cu, Fe or Zn) as they are micronutrients for living organisms. However, these elements can show toxic effects in high concentrations. On the other hand, non-essential elements, like Pb or U, can be toxic to living organisms in low concentrations (BOLAN et al., 2013). Though occurring naturally, anthropogenic

pollution emissions can raise the concentrations of metals to dangerous concentrations in the environment (ADRIANO, 2003). The distribution of metals in the environment depends on the emission sources but also on the media that is being assessed. Soils are a main receptor of metal contaminants, even if emissions are airborne. As the soil matrix has several constituents interacting with cations, metal complexes can be found in different fractions and in mobile or immobile forms (WUANA & OKIEIMEN, 2011; VAREDA et al., 2019). Naturally, metals are deposited in soils through their release by weathering from rocks of the Earth's crust. Other natural sources are windblown dusts, volcanogenic particles, landslides, debris flow and forest wildfires (NAGAJYOTI et al., 210, LUOMA & RAINBOW, 2008). The natural concentration of metals in soils largely depends on the parent material. Thus, most metals are enriched in soils after parent material composition or volcanic activity. This results in high baseline metal concentrations in volcanic soils (ZHANG et al., 2018; ADUMITROAEI et al., 2018; MEMOLI et al. 2018).

Generally, anthropogenic sources of metal contamination have a much greater impact on the living and non-living parts of soil ecosystems than natural sources. This is because human activities enhance metal inputs to the environment and affect their natural concentrations. Anthropogenic sources of metal contamination are often considered to be more serious than natural sources as a higher amounts of labile and bioavailable metals are released in soils by anthropogenic activities like mining, use of pesticides or fossil fuel combustion (ADRIANO, 2003; KABATA-PENDIAS, 2011; WUANA & OKIEIMEN, 2011) Thus, it is indispensable to gain adequate knowledge about biogeochemical cycles of metals in the environment in order to determine possible effects of metal contamination on human health. Most industrial, commercial, and domestic appliances are made of metals with their disposal potentially contaminating the environment. Serious anthropogenic sources of metal contamination arise from industrial discharges, dry or wet deposition of coal ashes, burning of fossil fuels, urban refuse, agricultural and animal wastes, fertilization with sewage sludge or pesticide application. Wastewaters usually contain toxic metals and the irrigation of soils with these waters can lead to biomagnification on plants and effects in food safety (ADRIANO, 2003; KABATA-PENDIAS, 2011; MOUSAVI et al., 2013).

Mining represents one of the most serious metal contamination sources through the large-scale exposure of metal-rich rocks from the Earth's crust and the abundant formation and release of acid metal-rich mine effluents into the environment. The most commercially exploitable sources are metal sulphides containing zinc (Zn), cobalt (Co), lead (Pb), nickel (Ni), iron (Fe) and uranium (U) (NÓBREGA et al., 2008, FERNANDES & FRANKLIN, 2001). Panagos et al. (2013) stated that mining and metal processing is responsible for 48 % of the total release of contaminants in the European industrial sector.

3.2 Open pit uranium mining as source of metal contaminants

3.2.1 Overview about open pit uranium mining

Uranium (U) is one of the world's most important energy minerals. Besides the main use for nuclear fuel, U can also be used for the production of medical isotopes. The primary mined uranium ore mineral is uraninite (UO_2). Currently, U is mined in 20 countries (WNA, 2019). Over 53,498 t of U were produced worldwide with 51 % of the world production coming from just ten mines in four countries in the year 2018. The countries with the largest U reserves are Kazakhstan, Australia, Russia and Canada (WNA, 2019). The countries with the largest production of U from mines are Kazakhstan, Canada and Australia with a combined production of 44,940 t of U in 2016. Most of uranium ore deposits represent average grades of 0.1 % of U, though some Canadian deposits hold grades in excess of 20 %. However, there are mines which still can be operated at very low grades of about 0.02 % (CNA, 2019; WNA, 2019).

U ores are mined and processed in a similar manner as other metal ores unless the U ore grade is very high. Nowadays, U is globally extracted from the earth crust by In-situ leaching (55 % of world U production), open pit/ underground mining (39 %) or as by-product from the treatment of other ores like copper (7 %). While the removal of U minerals from the ground in the In-situ leaching method is realized without any major ground disturbances, the production of U by underground and especially open pit mining represents a huge environmental impact as enormous amounts of waste rocks has to be removed from the earth's surface and accumulated in waste rock piles. Here, a very high

stripping ratio - the ratio of the amount of waste rock that has to be removed to the amount of ore mined – is critical (DNPM, 2009; COMMITTEE ON URANIUM MINING IN VIRGINIA, 2011).

Generally, uranium is typically extracted by open pit mining when uranium ore with a sufficient grade is found near the surface in a depth of less than 100 m. Ore grades of U are normally below 0.5 % in open pit mines (CNA, 2019). Open pit mining starts with the removal of surficial soil and uneconomic rock in order to expose the hard rock with the ore. Afterwards, a pit is excavated to access the ore and the walls of the pit are mined in a series of benches or steps. The resulting amounts of waste rocks or overburden are mounted near the pit in waste rock piles. The walls of the pit must be constructed and angled so that they are strong enough to support a safe slope (COMMITTEE ON URANIUM MINING IN VIRGINIA, 2011). For the mining of each bench, holes are drilled in the rock and loaded with explosives in order to break the rock. The ore fragments are then hauled by trucks and transported to the ore processing area, where their size is reduced by crushing and they are afterwards mounted to heaps. These heaps receive an alkaline or acidic solution, e.g., sulfuric acid, through tubes in a process called *heap leaching*, which separates uranium from the ore and is dissolved into the solution (INB, 2018).

The pregnant leach liquor containing uranium is then pumped through an internal circulation system to the surface and directed to the uranium recovery unit. This unit normally is located within the mining site. Here, the pregnant liquor is purified, and the uranium separated by precipitation triggered by the addition of e.g. ammonia, caustic soda or lime and solid-solid separation using vacuum filters (INB, 2018). The resulting product is ammonium diuranate ($(NH_4)_2U_2O_7$), a yellow powder containing up to 90 % of uranium compounds (U_3O_8, UO_2 or UO_3) commonly known under the name *yellow cake* (ABDEL-RAHMAN & EL-MONGY, 2017). In the further steps for the nuclear fuel fabrication, the *yellowcake* has to be converted into gaseous UF_6 and the isotope U^{235} has to be enriched up to a percentage of at least 3 % in the compound. After the reconversion to solid UO_2, the compound is pressed in pellets with a diameter of 1 cm, which are the basis for the nuclear fuel assembly. These operational steps are normally realized in facilities outside of the mining site (DNPM, 2009; COMMITTEE ON URANIUM MINING IN VIRGINIA, 2011; INB, 2018).

3.2.2 Uranium mining in Brazil

Brazil has significant uranium reserves and holds about 5 % of the worldwide U reserves with an estimation of 309,000 t of U (INB, 2018). The most important deposits are in south-east Bahia (Caetité, Lagoa Real), in the north of Ceará (Santa Quitéra), north of Paraná (Figueira) and south of Minas Gerais (Poços de Caldas). However, just one third of the country's territory were subject of research in pursuit of Uranium ore. Huge deposits are already identified in central Amazonas (Pitinga) and central Pará (Rio Cristalino). In the constitution of 1988, the federal government of Brazil reserved a monopoly over all uranium resources and its development. Thus, all exploration and ore processing activities are realized by the national owned enterprise *Indústrias Nucleares do Brasil (INB)* until today (ALBERTI, 2017; INB, 2018).

Uranium mining in Brazil started in 1982 with the inauguration of the open pit mine *Osamu Utsumi* in Poços de Caldas (Minas Gerais). The deposits of the reserve show an average content of U of 800 mg kg^{-1} in their ores. Between 1982 and 1995, about 1200 t of yellowcake were produced in this mining area. The production of U in the Poços de Caldas Mining-Industrial Complex (CIPC) was abandoned in 1995. In the year 2000, the open pit mine Lagoa Real/Caetité in the Cachoeira metasomatite deposit (Bahia) started the production of U. The deposit shows an average uranium content of 3000 mg kg^{-1} and has an estimated production capacity of 400 t of U per year. At the moment, the complex of Lagoa Real/Caetité is the only place in Brazil where Uranium is still actively mined. Furthermore, uranium is produced as a by-product of phosphate in the open pit mine in Santa Quitéria (Ceará) (DNPM, 2009).

Brazil is ranked 17th in the worldwide production of U_3O_8 with an estimated production of 44 t in 2016. The expected production of U_3O_8 for 2018 is 250 t, while production in 2017 was 150 t. This quantity is enough to supply the demand for medical and agricultural research as well for the demand of nuclear fuels of the only two nuclear power plants in Brazil, *Angra 1* and *Angra 2* (state of Rio de Janeiro). Though Brazil is self-sufficient in the production of yellowcake, the operation steps of conversion, enrichment, and reconversion in order to produce pellets for the nuclear fuel rods are realized abroad as no respective facilities nor

environmental legislation for their operation exists yet in the country (DNPM, 2009; ALBERTI, 2017; INB, 2018).

3.2.3 Environmental impacts of open pit uranium mining

Huge amounts of overburden material, spoil piles and tailings are generated when uranium is mined in open pits or underground mining. Stripping ratios for open pit uranium mines can range from 10:1 to 80:1 with an average of around 30:1 (USEPA, 1983). Mine pits, tailings and spoil piles not only represent immense alterations of the lands surface, but also are major sources for the release of highly hazardous contaminants like radionuclides, most important Radon (^{222}Rn) as well as its short-lived daughter isotopes, and metals like U, Ni, Cd, As, Mo, Hg, Zn, Fe and Al into the environment. Overburden, mineralized waste and barren waste rocks are generally low in their uranium contents and are left at the mine site (FERNANDES et al., 1995). The economically valuable ore is stockpiled and processed at the mill site. The resulting residual waste (tailings) is then normally disposed near the mill site. As most of these tailings contain radionuclides with long half-lives (>1000 years), these weakly radioactive waste materials are often placed back into the open pit, underground workings or in above ground surface impoundments in order to isolate the toxic heavy metals and the radioactive elements from the environment (FERNANDES et al., 1995).

As the original host material is altered physically (crushing) and chemically (milling and heap leaching) at the mining site in order to extract uranium, environmental media such as air, surface water or groundwater interacts with the material at each of these processes and potentially disseminates contaminants to human and environmental receptors (IAEA, 2005).

In several uranium mines around the world, the presence of oxidizing sulphides in open pits, tailings and waste rocks is the cause of the most serious environmental problems (FERNANDES et al. 1998). The phenomenon related with this oxidation of sulphides causing serious contaminations of the environment is called *Acid Mine Drainage* (AMD). AMD is defined as “metal-rich water formed from the chemical reaction between water and rocks containing sulfur-bearing minerals” by the Environmental Protection Agency of the USA (USEPA, 2003). AMD can cause long-term impairment to waterways and

biodiversity. In 1989, it was estimated that ca. 19,300 km of streams and rivers, and ca. 72,000 ha of lakes and reservoirs worldwide had been seriously contaminated by mine effluents (FERNANDES et al. 1998; JOHNSON & HALLBERG, 2005).

AMD is formed when sulfur-bearing minerals (e.g. pyrite - FeS_2) are exposed by mining and react with air and water to form sulfuric acid (H_2SO_4). Although this process also occurs naturally, mining can accelerate this process by simply increasing the amount of sulfides exposed. As many metals occur as sulfide ores and tend to be associated with pyrite, these metals are dissolved from the rocks, forming acidic waters rich in metals (Fe, Al, Mn and other heavy metals) and metalloids (especially As with the element of greatest concern). When this acid runoff drains out the mine, the dissolved metals react with O_2 from the air and form distinctive reddish, yellow or brown sediments (Figure 1). This acid runoff further dissolves the metals and metalloids into the ground or surface water and soils, posing severe contaminations for the environment (JOHNSON, 2003; JOHNSON & HALLBERG, 2005; AKCIL & KODAS, 2006).

Figure 1: Example of typical sediments formed by AMD, INB Caldas (MG, Brazil). (Gemeiner, 2018).

The fundamental reaction for the generation of AMD is the oxidation of pyrite (FeS_2) into dissolved iron, sulphate and hydrogen (Reaction I).

$$4\,FeS_2 + 15\,O_2 + 14\,H_2O = 4\,\mathrm{Fe(OH)_3} + 8\,\mathrm{SO_4^{2-}} + 16\,\mathrm{H^+} \quad \text{(I)}$$

This reaction equation is very simplified as the oxidation of pyrite is a multi-step process involving oxygen-independent and oxygen-dependent reactions. Furthermore, natural bacteria can accelerate this process by assisting in the breakdown of sulphide minerals. At pH values above 4, the regeneration of ferric ion, the key reaction for the ongoing oxidation of FeS_2, is promoted by iron-oxidising bacteria (e.g., *Gallionella ferruginea*). On the other hand, at pH below 4, acidophilic iron-oxidising bacteria are eminent for the formation of AMD. Thus, the chemical composition of AMD is controlled by the pyrite oxidation rate, which is a function of temperature, pH, the concentration of oxygen in the water and gas phase, composition and amount of infiltrating water, the surface area of the exposed metal sulfide and bacterial activity (FERNANDES et al., 2006). Iron sulfides are the most common but there are many other sulfide minerals (e.g. chalcocite - Cu_2S; galena – PbS; sphalerite - ZnS) that also can be the source of producing AMD (JOHNSON & HALLBERG, 2005; AKCIL & KODAS, 2006).

Acid mine drainage or also called “acid rock drainage” can also be neutral to alkaline rather than acid. The pH of these waters can be above 6 at the point of discharge (where dissolved oxygen concentrations are frequently very low). This is related to the fact that the total (or net) acidity derives both from proton acidity (i.e., hydrogen ion concentration) and mineral acidity (the combined concentration of soluble metals, notably Fe, Al and Mn, that produce protons when they hydrolyse) (JOHNSON & HALLBERG, 2005).

AMD emanating from open pit mines are under great concern since large volumes of rock are initially subjected to an oxidizing environment in this mining method. As the acid-generating minerals are more disaggregated and concentrated in open pits, waste rock piles and tailings; acidic-metal rich waters formed in these structures are potentially more aggressive than AMD’s from mine shafts of underground mining. Furthermore, production of AMD can continue for many years after open pit mines are closed and tailing dams are decommissioned, demonstrating a serious long-term pollution problem. The timescales for acid production and pollution generation can vary from 10 to 100 years (FERNANDES et al., 1998; FERNANDES & FRANKLIN, 2001; AKCIL & KODAS, 2006).

The true scale of the environmental pollution caused by AMD is difficult to assess accurately as every mine is unique in terms of its AMD potential. This

means that the nature and size of environmental contamination caused by AMD vary from site-to site (MORRISSEY, 2003; AKCIL & KODAS, 2006). There are no standardized methods for ranking, measuring and reducing the risk of AMD. Thus, predictions of AMD can be exceedingly challenging and related with high costs. Site-specific research has to be undertaken where AMD is inevitable or likely. For the restoration of mining sites, adequate techniques and equipment has to be available in order to monitor the scale of contamination by AMD and to subsequently minimize and control AMD impacts on life forms and their environment. In mining regions where AMD has not been formed yet, research should be carried out to identify ways in which AMD can be prevented (MORRISSEY, 2003; AKCIL & KODAS, 2006).

3.3 Metal speciation

The interaction of metals with their surrounding media depends on its chemical form or the so-called speciation. Metals can exist in different chemical forms in soils, e.g., as inorganic and organic complexes or as free ions in the soil solution. The importance of each metal species in their respective environment is dependent on the physical and chemical properties of the metal (e.g., size and oxidation state) as well as the physicochemical parameters of its surrounding media (e.g., pH, alkalinity, ionic strength, temperature, etc.) (PRICE et al., 2013).

Since industrialization, high metal concentrations are consistently introduced to soil environments globally. This increase of metal emissions demands the need to identify and quantify those metal species in soils that pose the greatest potential risks for organisms and their environment (ROBERTS et al., 2005). Furthermore, identification of metal species in soils is eminent for research in soil fertility, land-use planning, water quality, environmental risk assessment, soil ecology and soil remediation. The ubiquity of metals combined with the complexity of soils makes studying metal speciation a particularly important task in the field of soil chemistry. Metals are present in soils as a result of both natural and anthropogenic processes. Figure 2 shows the possible fate of metals once introduced into a soil from both natural and anthropogenic sources (ROBERTS et al., 2005; PRICE et al., 2013).

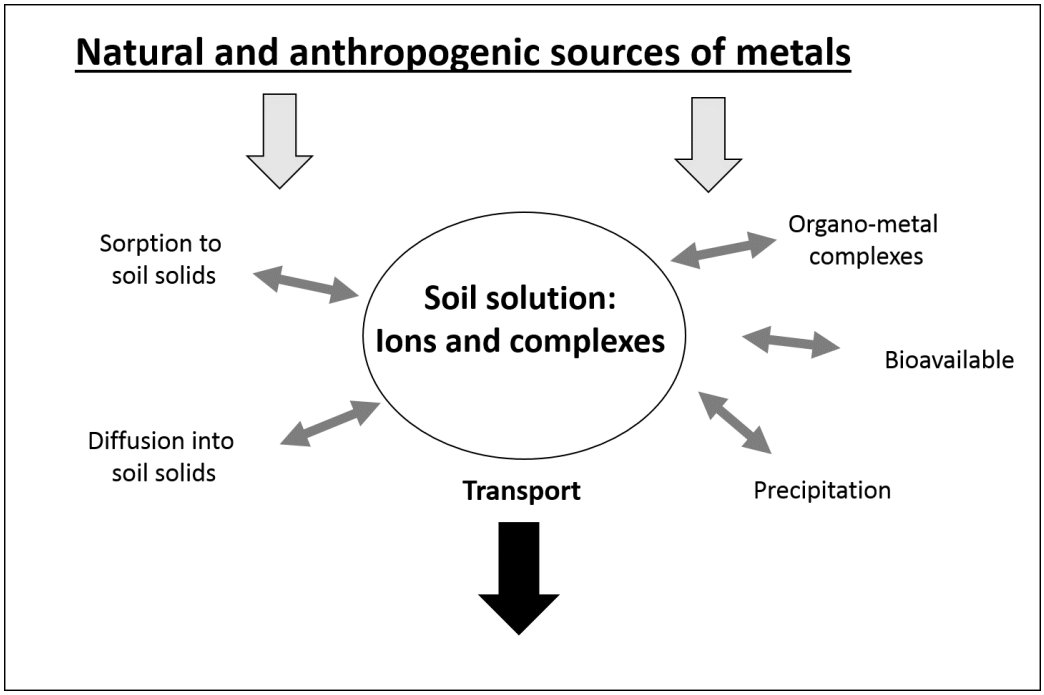

Figure 2: Possible physical and chemical pathways of metal ions once introduced into soil (adapted from ROBERTS et al., 2005)

Once the primary phase is dissolved, metal ions may enter the pore water and are subjected to various pathways, which can be overlapping. All pathways shown in Figure 2 can be divided into various complex reactions with different kinetics and mechanisms. The metal can be present in the soil solution as a free ion or as a complex with inorganic or organic ligands. In both cases, the metal can be exposed to one of several pathways, e.g., uptake by plants, mineral surfaces, and organic matter; transport through the vadose zone (unsaturated zone); precipitation as solid phase; and diffusion into porous material. Also, reverse reactions can occur, which turn metal behaviour in soils into a vibrant process influenced by plurality of physical and chemical processes. Thus, there are three pools in a soil where a metal can be found: the soil solution (pore water), the sorbed solid phase and as part of the structure of solid phases (ROBERTS et al., 2005).

The term *speciation* is difficult to attach to a single definition. The term *metal speciation* in soils includes the chemical form of the metal in the soil solution (either as free ion or complexed to a ligand), in the gaseous phase and distributed amongst solid phases within the soil. Thus, all the phases a metal may inhabit has to be addressed in metal speciation studies. However, the solid phase contains the majority of metals in soils and supplies the other two phases. Thus,

the long-term bioavailability of metals to organisms is determined by the re-supply of the metal to the mobile pool (soil solution) from more stable phases (metals in and associated with solid species). The quantitative speciation of metals, as well as their variation with time is an important concept in environmental soil chemistry. The accurate description of the partitioning of metal contaminants between the solid and solution phases is necessary in order to develop methods for the prediction of the fate of these contaminants in the soil (SCHULZE & BERTSCH, 1995; ROBERTS et al., 2005).

Speciation incorporates the chemical and physical form an element assumes in a geochemical setting. For a detailed definition of speciation, the following components are needed: identity of the contaminant of concern, the oxidation state of the contaminant, the valency associations and complexes to solids and dissolved species (surface complexes, metal-ligand bonds) and the molecular geometry and coordination environment of the metal. Many of these components can be linked to each other and are often difficult to distinguish. As more of these parameters can be identified, a better prediction of the potential bioavailability and thus toxicity to an organism by a metal contaminant can be realized (BROWN et al., 1999; ROBERTS et al., 2005).

3.4 Lability and bioavailability of metals in soils

Heavy metal toxicity in soils is related to their lability and bioavailability, which depend on the specific forms of metals in the soil. The lability of metal complexes is referred to association and dissociation kinetics of the volume complexation reaction, and to the interfacial flux of free metals due to dissociation of complex species (VAN LEEUWEN, 2000). The term *lability* loosely describes a relatively unstable and transient chemical species but also can be used to describe a relatively stable but reactive species. The term must therefore not be used without explanation of the intended meaning (IUPAC, 1994). In general, the term *lability* refers to how easily metal bonds in complexes are broken. A compound in which metal bonds are easily broken is referred to as labile. This is a compound that undergoes reactions with a relatively high rate of substitution. A compound where metal bonds are more difficult to break is described as inert. It

is a compound which undergoes reactions with a slow rate of substitution (TAUBE, 1984; SCHALLER, 2019).

Similar to the term *lability*, numerous definitions for the term *bioavailability* exists in the literature. Over the last two decades, scientists have been engaged to develop conceptual definitions of bioavailability combined with operational aspects. This approach has the objective to allow the mechanistic understanding of bioavailability and the standardization of measurement tools for bioavailability (KIM et al., 2015). Gary et al. described bioavailability as a flux of contaminants to the biota (GARY et al., 1999). Warrington and Skogley suggested in 1997 the definition of bioavailability as “the amount of chemicals in the soil that are present in forms and amounts that plants or other organisms can take up during the time they are living” (WARRINGTON & SKOGLEY, 1997). Shor and Kosson defined bioavailability as “the rate at which a chemical compound can be transported to the specified biological population” (SHOR & KOSSON, 2000). These definitions can be grouped in definitions that describe bioavailability as flux or rate (mol m^{-2} s^{-1}) or are defined in terms of content (mol kg^{-1}).

Hund-Rinke and Koerdel (2003) defined bioavailability as a complex dynamic process strongly controlled by the type of organism, type of exposure and metal speciation. The principle of a dynamic process was adopted by the National Research Council (NRC) which defined bioavailable processes as “the individual physical, chemical and biological interactions that determine the exposure of organisms to chemicals associated with soils and sediments” (NRC, 2003). Here, the following five processes were included: (1) contaminant release from the soil solid phase, (2) transport of the released contaminants or (3) transport of the bound contaminants to the membrane of an organism, (4) the passage across a physiological membrane and (5) the incorporation into a living system through metabolic processes (NRC, 2003).

Harmsen (2007) emphasized that it is more constructive to present bioavailability as a concept and relate it to specific chemical extractions or bioassays. Thus, bioavailability has to be defined conceptually and operationally (HARMSEN, 2007). Based on this emphasis, the International Organization for Standardization (ISO) established a definition for bioavailability in the guidelines 17402 for the selection and application of methods for the assessment of bioavailability of contaminants in soils. Here, bioavailability was defined as “the

degree to which chemicals present in the soil may be taken up or metabolised by human or ecological receptors or are available for interaction with biological systems" (ISO, 2008). Further, bioavailability was described in three conceptual steps: (1) *environmental availability*, (2) *environmental bioavailability* and (3) *toxicological bioavailability* (Figure 3).

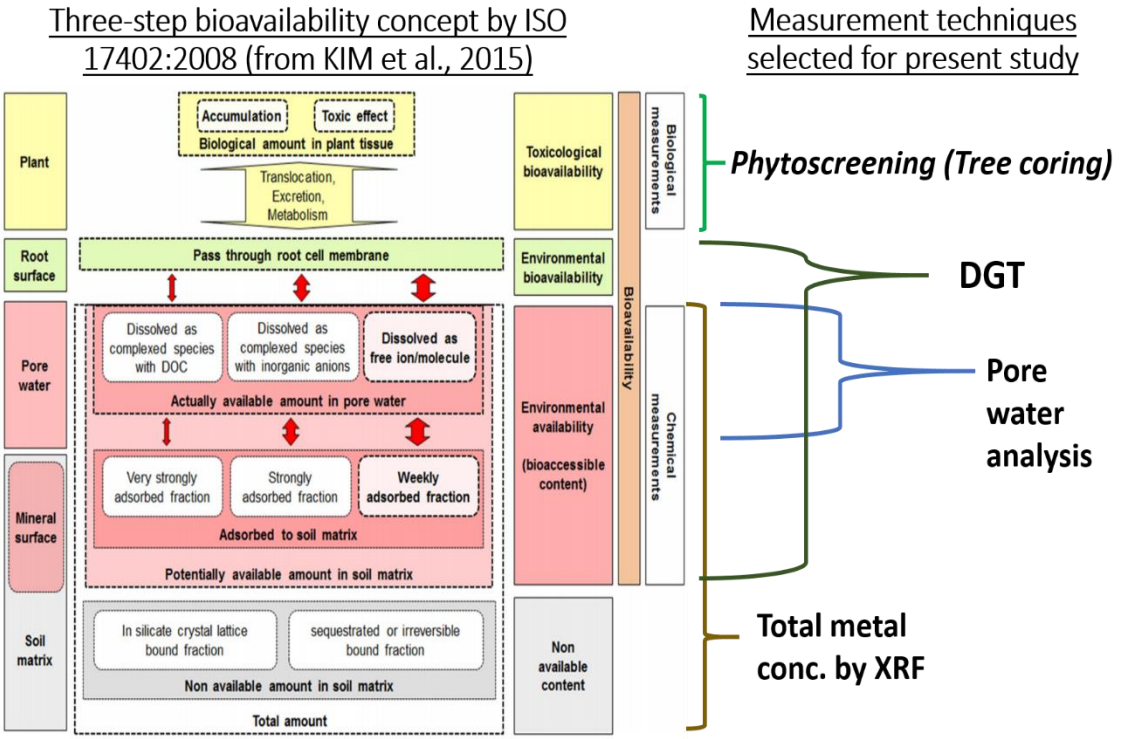

Figure 3: Three-step concept of heavy metal bioavailability in soils for plants established by ISO 17402:2008 as guideline for the selection of the measurement techniques of the present study (adapted from KIM et al., 2015).

Environmental availability describes on the one hand the available amount of the total metal content in the soil including both the actual available fraction dissolved in the pore water. This can be e.g., the heavy metal concentration in the pore water. On the other hand, the term also includes the potential available fraction absorbed in the soil matrix (e.g., specific and non-specific absorbed, organically bound, surface-precipated amounts). The potential available fraction is determined as the maximum amount which can be desorbed from the soil matrix under defined conditions and exposure time being in equilibrium with the dissolved fraction in the pore water (KIM et al., 2015). *Environmental bioavailability* is the fraction of dissolved metal species in the pore water which can be taken up by plants or other soil organisms. Thus, this step is controlled by physiological processes and depends on the transfer from the pore water to the

plant roots and uptake mechanisms specific to plant and metal species. Finally, the *toxicological bioavailability* describes the amount of the metal fraction which can physiologically induce bioaccumulation or other effects within the plant depending on translocation, metabolism and detoxification (ISO, 2008; KIM et al. 2015).

Solubility and mobility of metals in the soil as well as translocation of these metals in the plants is dominated by specific and non-specific adsorption and different complexation affinities for inorganic and organic ligands, thus the speciation of the metal. These factors depend to a large degree on soil pH (KIM et al., 2015). In general, bioavailability is considered dependent to the specific soil or organism, but some plants are able to modify soil characteristics like pH which turns metal contaminants more or less available. All these parameters constitute uncertainties when assessing bioavailability (HARMSEN, 2007).

3.5 Tools for bioavailability assessment in soils

Figure 3 established by Kim et al. (2015) indicates that there are two complementary ways to assess bioavailability: chemical and biological measurements. Chemical measurements used in the soil matrix, e.g., extraction methods, determine a defined fraction of a well-defined class of contaminants assumed to be available for specific receptors. Most of these methods were developed to predict the amount of contaminants by organisms. These analytically determined values can be correlated with effects and bioaccumulation in organisms. Biological measurements use organisms exposed to soil or soil eluates to monitor effects of contaminant exposure on these respective organisms. If effects or bioaccumulation is encountered (e.g., growth inhibition or mortality), bioavailable contaminants are likely to be present even they cannot be chemically identified (HARMSEN, 2007; KIM et al., 2015).

Chemical methods for the measurement of environmental availability promise to predict the uptake of contaminants after soil ingestion, plant uptake, transport of the contaminant in pore water (leaching), biodegradation and effects on soil organisms (HARMSEN, 2007). The main principles that are used in these methods are (1) the measurement of the total amount of the contaminant in the pore water or its chemical activity, (ii) the extraction of the contaminant by a

solvent or adjusting temperature and time during extraction and (iii) the use of an adsorbent for extraction in an equilibrium with the water phase (HARMSEN, 2007).

Frequently used chemical methods for measuring available metal contents are extraction-based methods. A commonly used type of these methods is the measuring of the actual available metal concentration in the pore water. Here, the total dissolved metal concentrations are extracted by unbuffered neutral salt solutions such as 0.001-0.01 M $CaCl_2$, 0.1 M $NaNO_3$ or 1.0 M NH_4NO_3 (HOUBA et al., 1996; GRYSCHKO et al. 2005; MEERS et al., 2007; MENZIES et al. 2007). These three extraction methods are already established in regulatory framework of the national environmental agencies in the Netherland, Switzerland and Germany, respectively (HOUBA et al., 1996; FOEFL, 1998, BMUB, 1999). Several authors argued that a batch or leaching test using neutral salt solution such as $CaCl_2$ or NH_4NO_3 with a solution/soil ratio of 2:1 is sufficient to measure the bioavailable fraction of relatively high mobile metals such as Cd, Ni or Zn (GRYSCHKO et al. 2005; MEERS et al., 2007; MENZIES et al. 2007). The authors Houba et al. (1996), Meers et al. (2007) and Pueyo et al. (2004) suggested the preferential use of 0.01 M $CaCl_2$ solution instead of 1 M NH_4NO_3 solution as the ionic strength of 0.01 M $CaCl_2$ is similar to pore water. Furthermore, the ion Ca^{2+} has a better ability to displace metals like Cd or Zn from exchange sites than NH_4^+. Furthermore, the low salt concentration reduces the analytical interferences during the sample analysis by ICP-MS or ICP-OES (HOUBA et al. 1996; MEERS et al. 2007; PUEYO et al., 2004).

Other types of extraction methods measure the potential available contents in the soil solid phase. In these approaches, extraction either by exchange with strong acids such as 0.1 M HCl and 0.43 M HNO_3, or by chelation with strong complexing organic agents like 0.05 M EDTA and 0.5 M DTPA is realized. These methods show better correlation of strongly absorbed metals such as Cu, Cr and Pb with the actual uptake (MACHOLZ et al., 2011). On the other hand, organic chelating agents such as 0.5 M DTPA are supposed to mimic organic exudates produced by plants, which are capable of removing metals more aggressively from exchange sites into soil solutions (FANG et al., 2007; HAN et al., 2006).

A different model for the assessment of bioavailability in soils are specific diffusion separation techniques like DGT (*Diffusive Gradients in Thin films*) or DMT (*Donnan Membrane Technique*). These techniques are able to measure free ion concentrations and weak complexes with organic and inorganic ligands in pore water (DAVISON & ZHANG, 1994; ZHANG et al., 1998; WENG et al. 2002). Furthermore, a determination of strongly chelating metals such as Cu can be realized with these methods. The diffusion separation model provides significant advantages for measuring bioavailability compared with the methods above such as only free metal ions are measured selectively by DGT and DMT. Furthermore, DGT and DMT are able to determine strongly chelating metals such as Cu (DEGRYSE et al. 2009; AGBENIN & WELP, 2012). However, both techniques are not yet implemented for routine regulatory national frameworks (with exception to Australia) as they are time-consuming procedures and require specialized equipment (BRAND et al., 2009; KIM et al., 2015). The DGT technique is described specifically in the following chapter. The *Donnan membrane technique* is based on the theory of the Donnan membrane equilibrium. Using a cell containing an acceptor solution and a negatively charged cation exchange membrane, cationic metal species are separated from a substrate solution (donor solution) during analysis. When the Donnan membrane equilibrium is attained, the activity ratios (corrected for charge) of the ions in the donor solution and in the acceptor solution are equal (WENG et al., 2002). In most applications in soil, artificial solutions or soil extracts separated from the soil phase were used (SALAM & HELMKE, 1998; TEMMINGHOFF et al., 2000). The main problem here is the limited buffering capacity of the solution for trace metals, which can lead to changes of the chemical equilibrium (WENG et al., 2002).

3.5.1 Diffusive Gradients in Thin Films (*DGT)*

Principles of DGT

The technique *diffusive gradients in thin films* (DGT) was first proposed in 1994 by Zhang and Davison as a passive in-situ metal sampling technique in aquatic systems. The technique is based on the use of plastic devices containing a diffusive layer and a binding layer that accumulates metals in a controlled

manner. In their conventional (commercially available) forms, DGT is able to sample chemical species that are bioavailable present in solutions, sediments and soils. This includes all inorganic species in solution and most organic complexes (DAVISON & ZHANG 1994; ZHANG & DAVISON 1995; ZHANG et al. 2014).

The devices used in DGT are made of polypropylene and basically consists of two parts, a clip and a piston. The piston has a diameter of 2.5 cm on its circular top. The clip of the device has an open window with a diameter of 2.0 cm and is deposited directly onto a filter membrane within hydrogel (diffusive) layer and a binding layer (gel supported), which are previously stacked on the surface of the piston. The basic structure of a stacked DGT is shown in Figure 4 (ZHANG & DAVISON, 1998). The basis layer of each DGT device is a binding layer, usually an ion exchange resin (or a chelating agent impregnated within a hydrogel) in order to accumulate solutes. The analytes that can be measured by DGT are determined by the binding agent in use. On top of the binding agent, a diffusive layer consisting of a hydrogel will be installed. The diffusion layer is generally made of polyacrylamide and induces that the transport of the ions in the solution (in which the DGT device was deployed) to the binding agent occurs exclusively by molecular diffusion. The establishment of a constant concentration gradient in the diffusive layer is the basis for measuring metal concentrations in solution quantitatively without the need for separate calibration. Thus, Fick's first law can be used to calculate the concentration of the analyte in the solution. The upper most layer of a DGT device is the filter membrane. This membrane has the function of protecting the underlying diffusive layer. The filter membrane usually consists of cellulose acetate or cellulose nitrate (DAVISON & ZHANG, 1994; DGT RESEARCH, 2003; ZHANG et al. 2014; DE SOUZA et al. 2014; MENEGÁRIO et al. 2017).

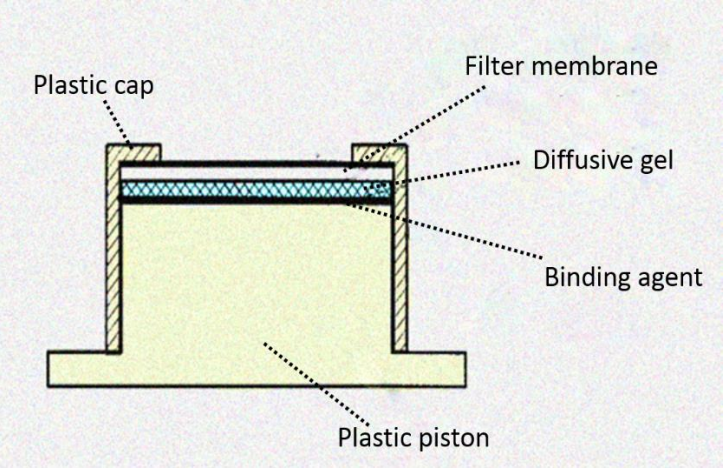

Figure 4: Structure of a *DGT* device (adapted from ZHANG & DAVISON, 1998).

When deployed in aquatic systems with high flow conditions, DGT measures labile species. Above a low threshold value, the measurement is independent of solution flow (ZHANG & DAVISON, 1995; DGT RESEARCH, 2003). In the conventional use of the DGT technique for the in-situ determination of metals (Al, Mn, Fe, Co, Cu, Zn, Ni, Cd and Pb) in aquatic systems, a Chelex-100® resin is used as binding agent, polyacrylamide gel as diffusive layer and a cellulose nitrate filter as the filter membrane (ZHANG & DAVISON, 1995).

Application of DGT in soils

When assessing the availability of toxic metals or nutrients in soils, mobility, lability and solution-to-solid phase exchange kinetics should be considered. The DGT technique accumulates metals in a well-defined geometry that allows the quantification of the supplies of metals from the solid phase. (ZHANG et al. 2014). When DGT is deployed into sufficiently wetted soils (at field capacity), the concentrations of metal ions in the soil adjacent to the DGT device are lowered. Here, the respective labile metals are removed from the soil solution (or also called pore water) by binding to the resin gel of the DGT device. This triggers a resupply of metals from the bulk solution by diffusion and further the desorption of metal ions from the solid phase to the pore water in the layers of soil near to the device. Thus, DGT measures directly the mean flux of labile species to the DGT device during the time of deployment. This flux can be interpreted directly as the mean concentration of labile metals at the interface between the surface

of the DGT device and the surrounding soil during the time of deployment (DGT RESEARCH, 2003). Summing up, for a given device and deployment time, the interfacial concentration can be related directly to the effective concentration of labile metal, C_E. The concentration C_E (or as in this study denominated as C_{DGT}) represents as a concentration the supply of metals to any sink, be it DGT or a plant, that comes from both diffusion in solution and release from the solid phase. Thus, C_{DGT} can potentially be a proxy for the environmental bioavailability of the analysed metals in the soil to the plants (DGT RESEARCH, 2003).

The DGT technique is based on Fick's first diffusion law. Thus, when applying the DGT device in a solution or soil, simple metal ions diffuse through the diffusive gel, which has a defined thickness of Δg, and are quickly retained by the binding layer. As long as the capacity of the binding agent is not exceeded, the concentration on the binding layer surface will effectively maintained zero throughout the immersion, creating a steep concentration gradient in the diffusive gel layer. If the concentration gradient remains constant over the immersion time (t), the flux (F) of a metal ion can be calculated by Equation (1) (DAVISON & ZHANG, 1994):

$$F = DC/\Delta g \qquad (1)$$

where C is the concentration of free ions in the soil solution of the studied metal; D, the diffusion coefficient of the metal ion in the diffusive gel, which should be approximately the value of the diffusion coefficient of the analyte in water (ZHANG et al., 1998).

The flux is also defined as (Equation 2):

$$F = M/(At) \qquad (2)$$

The mass (M) of a metal ion diffused through permeable diffusive gel with a defined area (A) and a defined thickness (Δg) after a defined deployment time (t) is given by Equation (3):

$$M = D.C.t.A/\Delta g \qquad (3)$$

The ion mass accumulated in the resin layer (M) can be obtained using appropriate elution and analytical procedures and applying Equation 4 (DGT RESEARCH, 2003):

$$M = Ce(V_{HNO3}+V_{gel})/fe \qquad (4)$$

where Ce is the concentration of metals in the 1M HNO_3 elution solution (in µg l^{-1}), V_{HNO3} is the volume of HNO_3 added to the resin gel, V_{gel} is the volume of the resin gel and fe is the elution factor for each metal.

Therefore, the in-situ concentration of the analyte in the solution can be obtained using a rearranged version of Equation (3):

$$C_{DGT} = F.\Delta g/D \qquad (5)$$

The flux of metal ions from solution to binding agent measured by DGT can be interpreted as an in-situ concentration of the analyte in the soil solution, assuming that the concentration gradient in the diffusive gel remains constant over the deployment period. However, if this concentration gradient changes by depletion of metal ions near the gel, Equation (5) cannot be used to obtain the actual concentration (HOODA et al., 1999).

To assess bioavailability of metals by DGT in soils, it is particularly important to consider the extraction and the kinetics of metal resupply from solid phase to soil solution (also called pore water) (HOODA & ZHANG, 2008). However, the bioavailability of metals in soils is both dependent on their concentration in the soil solution and their rate of transport through the soil (HOODA & ZHANG, 2008). DGT measures directly the mean flux of labile species in soils to the device during the deployment. This fact can be interpreted as the mean concentration of labile metals at the interface of the DGT device and soil during the time of deployment. Thus, for a given device and deployment time, this interfacial concentration can be related directly to the effective concentrations of labile methods. This concentration represents the supply of a metal to any sink (like a DGT device or a plant) coming from both diffusion in solution and release from the solid phase (DGT RESEARCH, 2003). Therefore, DGT provides a promising approach for the measurement of bioavailable metal concentrations in soils (ZHANG et al., 2001). By comparing the concentration of the analyte in soil pore water (C_{sol}) and the

concentration of the analyte measured by DGT (C_{DGT}), at least three conditions associated with desorption (or replacement) kinetics and metal flow can be established (Figure 5). In the “fully sustained case (i)”, where $C_{DGT} \cong C_{Sol}$, ions removed from the soil solution by DGT are rapidly resupplied from the soil solid phase. In the second case, the “unsustained case (ii)”, where $C_{DGT} < 0{,}06\ C_{Sol}$, no resupply occurs from the soil solid phase to the solution. Here, the accumulation of the ions on the DGT binding agent will only occur by diffusion of the ions present in pore water. On the other hand, in the “partially sustained case (iii)”, where $6\ \% < C_{DGT} < C_{Sol}$, some resupply of ions from soil to solution is occurring, but this resupply is insufficient to sustain the initial bulk concentration and to satisfy fully the DGT demands. This information is extremely relevant for the assessment of the lability and bioavailability of metals in contaminated soils, and thus for the assessment of the degrees of metal contamination in the environment (ZHANG et al., 1998).

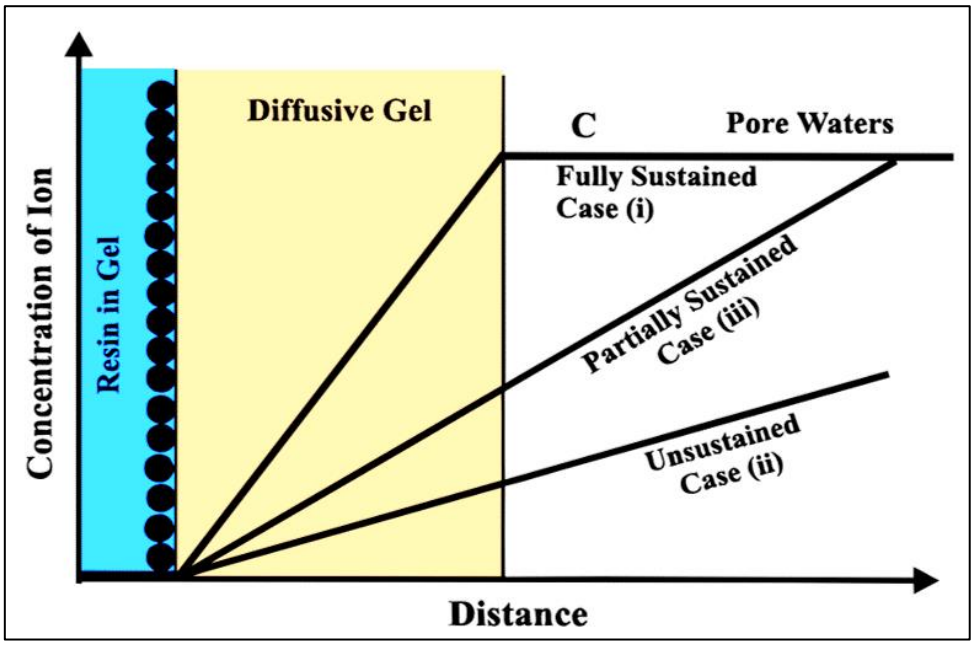

Figure 5: Schematic representation of the concentration gradient in a DGT assembly in contact with soil pore waters where the concentration of ions is fully sustained (i), unsustained (ii) or partially sustained (iii) by resupply of the soil solid phase (adapted from ZHANG et al., 1998).

The above-mentioned insights were elaborated in the study by ZHANG et al. 1998, where DGT was used to measure the maximum potential fluxes of metals available in arable and deforested soils which were variously treated with sewage sludge containing different metal concentrations. Zn and Cd

concentrations in soil pore water were shown to have higher resupply rates from the soil solid phase when the soils received no sludge (or a low sludge dose). This study provided the first fully quantitative in situ measurements by DGT of the potential resupply flux of metals from soil to solution (ZHANG et al., 1998).

A limitation of the DGT devices using a Chelex resin as binding agent is the reduced performance at low and high pH values. For most metals, the Chelex resins functions best at pH ranges of 5 to 9. Below a pH of 5, the adsorptive capacity of the resin diminishes. At pH values greater than 9, the resin can swell which affects its physical characteristics (INAP, 2002).

A study to assess the attenuation of metal bioavailability in acidic multi-metal contaminated soil which were treated with fly ash and steel slag was carried by Qui et al. (2012). A significant increase of the soil pH reduced the labile concentrations of the metals (Pb, Cd, Cu and Zn) in the contaminated soil. In this case, DGT was shown to be a good bioavailability indicator as metal concentrations correlated well with plant uptake as determined by digested biomass analysis and using the DGT technique (QUI et al., 2012).

It has been shown that the effective concentration of metals in soil measured by DGT gives a better correlation to plant uptake than any other measurement technique (ZHANG et al. 2004; NOLAN et al., 2005; KOSTER et al., 2005). The main reason for this is that DGT mimics the plant uptake of metals as it locally lowers the concentration of the respective metal and induces a diffusive supply and release from the soil solid phase (LEHTO et al. 2006). This accounts for all soil properties including soil pH and organic matter content (ZHANG et al., 2014).

The paper of Degryse et al. (2009) concluded that the assessment of metal bioavailability by DGT is most accurate where the diffusive transport of an element from soil to the plant roots is rate-limiting for its uptake. If plants have small affinity for an element or when supply is large and the plant uptake is saturated, the DGT flux and plant uptake do not correlate well (DEGRYSE et al. 2009).

Conesa et al. (2010) investigated the suitability of DGT for the assessment of metal bioavailability in mine tailings. Here the DGT performance were tested at extremely acidic soils with a pH of 3. It has been concluded that at low soil pH values, competition with other cations that are present at very high metal

concentrations may hinder the accumulation of ions at the chelating resin in the DGT. It showed that the performance of binding layers is often dependent on the pH. It was also stated that DGT deployment under water saturated conditions yielded higher metal concentration values (C_{DGT}). This indicated the importance to adequately control the moisture content in soils before and during the application of DGT (CONESA et al., 2010).

The work of Hooda et al. (1999) also emphasized the effect of soil moisture on DGT performance for the determination of metal bioavailability in soils. DGT was used to measure Cd, Co, Cu, Ni, Pb and Zn fluxes in a sludge-treated soil at various moisture contents (27-106 %). For moisture contents above field capacity (42 %), DGT fluxes reflected the metal concentrations in pore water. With moisture contents below field capacity, the measured DGT flows were below the expected metal concentrations in pore water. These results showed that soil moisture should be between field capacity and maximum water holding capacity in order to maintain contact with the membrane. For the element Cd, DGT fluxes reached the highest levels at maximum water holding capacity (HOODA et al. 1999). Therefore, soil moisture always should be considered and preferably consistent when assessing metal bioavailability in soils by DGT (ZHANG et al. 2014).

The study of Mundus et al. (2012) focused on the assessment of bioavailability of Mn by DGT in Scandinavian agricultural soils. It was stated that the DGT prediction of plant availability was much more appropriate in anaerobic soil conditions rather than in aerobic soil conditions (MUNDUS et al. 2012). Agbenin and Welp (2012) compared the performance of DGT in soils with plant uptake by *Sorghum bicolor* and *Lactuca sativa* in the field and in the greenhouse. DGT showed to be fairly predictive for bioavailability of Cd, Cu, Pb and Zn in the greenhouse, but not under field conditions (AGBENIN & WELP, 2012). Williams et al. (2012) evaluated the DGT technique for the prediction of Cd concentrations in Chinese-field cultivated rice. Thus, Cd concentrations measured by DGT in soil and Cd concentrations in grain of rice from 77 paired samples were compared. It was stated that the deployment of DGT in dried and homogenized soil wetted to maximum water holding capacity offered to be a better screening tool for Cd uptake in rice than the DGT deployment in situ in the field due to the inherent heterogeneity of the rice rhizosphere soils (WILLIAMS et al. 2012). In the study

of Ferreira et al. (2013), DGT measured Cu concentrations were compared with plant uptake by aquatic mosses. It was concluded that an approach of coupling DGT data and a cationic-effect model can be considered to be a good surrogate for evaluating Cu bioavailability in aquatic mosses (FERREIRA et al. 2013).

The mentioned studies show that the DGT technique provides a promising approach for the assessment of environmental availability and, potentially, environmental bioavailability of metals in soils. However, further work is required where more plant species are tested, and more metals are analysed under various different field conditions to validate and standardize this method for metal bioavailability assessment (ZHANG et al. 2014).

3.5.2 *Phytoscreening*

Phytoscreening is a commonly used monitoring method in Europe that allows the identification of contaminants and the demarcation of the contamination plume (VROBLESKY, 2008). Generally, the term *Phytoscreening* describes the use of vegetation as bioindicators to detect subsurface pollutants (HOLM et al., 2011). One method of *Phytoscreening* is *Tree Coring*, where wood extracted from the tree trunk is used as a bioindicator. *Tree Coring* is an inexpensive, non-invasive screening tool that can be applied for the localization and mapping of underground pollution based on chemical analysis of tree core samples. The technique uses the natural ability of trees to absorb water, nutrients and potential pollutants from soil and groundwater through their roots. From the roots, pollutants can be translocated to the xylem and retained for a short time (such as volatile organic compounds) or linked (such as heavy metals) to the wood structure (NIELSEN & TRAPP, 2014).

The application of *Tree Coring* is relatively simple as the main sampling instrument is an increment borer, a tool which is normally used by foresters to examine wood quality and growth rates of the trees (Figure 6). For sampling of tree cores, the increment borer is simply screwed in the stem and with the help of an inserted core retractor, the tree core sample is released out of the stem (NIELSEN & TRAPP, 2014).

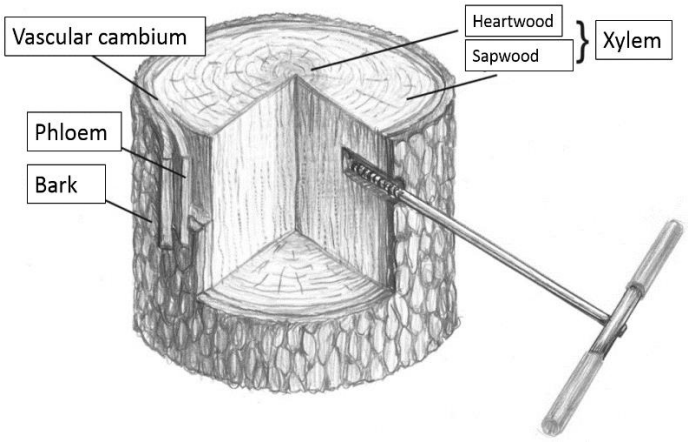

Figure 6: Schematic illustration of tree core sampling by an increment borer (adapted from HOLM et al., 2011).

The ability to investigate groundwater contamination by volatile chlorinated hydrocarbons without producing groundwater sampling wells and without taking groundwater samples based solely on wood core measurements was developed in the 1990s in the US. (VROBLESKY & YANOSKY, 1990; VROBLESKY, 1998; VROBLESKY et al., 1999). *Phytoscreening* of volatile organic compounds in soil and groundwater is today a scientifically validated and accepted method (GOPALAKRISHNAN et al., 2007). The technique can be used to explore contamination plumes of volatile chlorinated hydrocarbon, tetrachloroethylene, trichlorethylene and cis-1,2-dichloroethene (SOREK et al., 2008). It has also applications for exploring contaminant entry points and demonstrating processes of natural soil microbial degradation (natural attenuation) (LARSEN et al., 2008). Furthermore, the technique can be used for the monitoring of heavy metals in soil and groundwater (NIELSEN & TRAPP, 2014). Sampling of tree cores for the screening of heavy metals in the soil was performed by Algreen et al. (2012) and Algreen et al. (2014). *Phytoscreening* is a semi-quantitive tool which can be initially applied for the location and mapping of pollution. The method is appropriate for large contamination sites as well as for single contamination hotspots (NIELSEN & TRAPP, 2014).

The advantage of *Tree Coring* is that it represents a simple, fast, inexpensive and mobile sampling method as only a tree borer and some storage material is needed for sampling. Furthermore, the technique has minimal impact on the site and its environment. Due to the large root system of trees, one tree core sample represents a large volume of the subsurface. Regarding this fact and

the low cost of sampling, a high number of samples can be taken with a high density. This allows to detect single contamination hotspots. In this way, *Tree Coring* can serve as an initial screening tool to give a fast overview about the spreading of pollutants. Overall, the method gives information about plant uptake of metals which can be useful in terms of planning for further remediation (HOLM et al., 2011; NIELSEN & TRAPP, 2014).

The *Tree Coring* method is limited by the fact that it requires the presence of trees at the contamination site. But a lack of trees can be just due to toxic levels of the contamination site. Because of this, the method can be limited by phyto-toxic levels. Also, results of metal concentrations in the wood can vary with tree species, age and tree size as well as with soil properties and groundwater levels. Soil grain size (clay or other impermeable layers), chemical properties of the pollutants or physical properties can limit the availability of pollutants for the root system and their mobility inside the tree. Thus, these pollutants may not be detected by *Tree Coring*. Furthermore, *Tree Coring* is only applicable for shallow pollutants as pollutants in soil depths down to 19 m can be detected by *Tree Coring*. All these limitations make *Tree Coring* a semi-quantitive method for investigating pollution levels. Because of this, results of *Tree Coring* should always be compared with quantitive screening methods such as groundwater and soil sampling (HOLM et al., 2011; NIELSEN & TRAPP, 2014).

In principle, only dissolved and labile metals can be incorporated into plants. Thus, only bioavailable metals can be detected by *Phytoscreening*. Although this technique is advantageous for risk assessment, the reference values are usually based on the total metal content. This does not always correlate with the dissolved bioavailable fraction. Generally, plant samples have lower metal contents than soil samples (bioconcentration factor often below 0.01) (HOLM et al., 2011).

The first approach for the evaluation of *Phytoscreening* as a screening tool for metals in the subsurface was realized by Algreen et al. (2012). Here, tree core samples from several tree species of a reference site and a contaminated former dump site for waste oil and oil distillery wastes in Norway were analysed for As, Cd, Cr, Cu, Ni and Zn. It was shown that mean metal concentrations in the wood from the polluted dump site were higher than those from the reference site. However, differences between the tree species were higher than differences

between the polluted and the reference site. This fact showed that the metal bioconcentration in the wood depends on the tree species and that it is thus important to investigate intraspecific differences of the metal concentrations in the wood (ALGREEN et al. 2012).

In the study by Algreen et al. (2014), the viability of *Phytoscreening* was tested for evaluation of an area contaminated by heavy metals. For this, the concentrations of heavy metals were determined from tree cores of willow and poplar wood collected from a strongly (sludge disposal site), a moderately (dump site for steel scrap and dross) and a slightly polluted site (wood proofing site), as well as from three reference points. The concentrations of Cd, Cu, Ni and Zn in willow wood sampled at the highly polluted site were significantly elevated compared to those found at the reference site. This result showed that *Tree Coring* in willows can be successfully used to identify highly polluted soil by metals such as Cd, Cu, Ni and Zn. Furthermore, regressions were calculated for metal concentrations measured in wood and measured in soil. However, regressions only provided reasonable predictions for very high contaminated spots (ALGREEN et al., 2014). Yet, very few data on heavy metal in woods is published, though more literature regarding the uptake of metals into smaller plants or other plant parts as leaves or roots are available (MCLAUGHLIN et al. 2011; ZACCHINI et al. 2011; DJINGOVA et al. 2004). To the authors knowledge, there are no studies published yet involving *Tree Coring* as screening tool for metal contamination in soil in Brazil nor the southern hemisphere, nor the tropical regions.

In Brazil, *Phytoscreening* was used in the study by Ferraz et al. (2017) to investigate the applicability and effectiveness of this technique to determine contamination plumes in an area impacted by organochlorine hydrocarbons in a tropical environment in Porto Feliz (SP), Brazil. Here, *Phytoscreening* proved to be a fast and economical method for detecting contaminated areas by organochlorine hydrocarbons (FERRAZ et al., 2017).

4 OBJECTIVES

The objective of the present work was to evaluate the lability and environmental availability (and thus the possible environmental bioavailability) of

the metals Al, Co, Cu, Fe, Mn, Ni, Pb, Zn and U in topsoil at sites with different mining impacts (reference area, area of acid mine drainage and two waste rock areas) at the former uranium mine of the Poços de Caldas Mining-Industrial Complex (INB Caldas - Minas Gerais) using the *diffusive gradients in thin films* technique. In addition, these results were compared with metal concentrations obtained by the analysis of tree core samples to potentially evaluate the soil-plant-transfer and potentially toxicological bioavailability of these metals. These approaches aimed to realize a specified risk assessment for the metal contaminated soils of the study site.

5 STUDY AREA

5.1 Geographical and geological background

5.1.1 Location

The study area is located at the former uranium mining and milling site of INB Caldas at the Poços de Caldas plateau, in the Southeast region of Brazil in the state of Minas Gerais (Figure 7). The area is located between the coordinates 21°56'36 S, 46°30'51 W and 21°58'31 S, 46°29'10 W. The altitude varies between 1300 m and 1450 m above sea level.

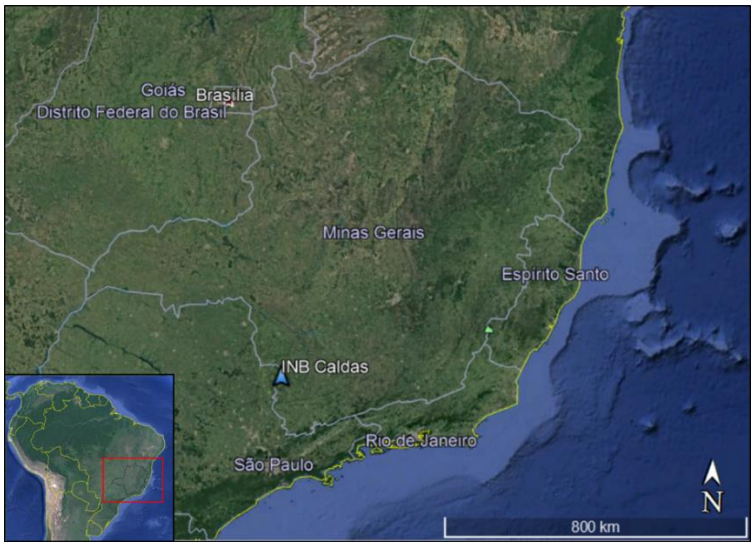

Figure 7: Location of the study site inside the state of Minas Gerais (map generated by GoogleEarth Pro software).

5.1.2 Climate

Regarding the climate classification of Köppen, the climate in the Poços de Caldas region is classified as Cwa – Subtropical climate of altitudes. The annual average temperature is 18.3°C, with maximum temperatures of up to 36°C and minimum temperatures of 1°C. The warmest month is January with a medium temperature of 21°C, while the coldest month is July with a medium temperature of about 15°C. The region is subjected to a distinct seasonality in dry season and rainy season. The total maximum precipitation is 1686 mm with more than 120 days of rain per year. The precipitation is concentrated in the months of November, December, January and February accounting for 1245 mm, while January shows the highest precipitation with 310 mm. In contrast to this, the months of June, July and August are the driest month showing each a precipitation total of under 30 mm (FERNANDES et al., 1998).

5.1.3 Geology

The study area is placed in the Poços de Caldas plateau which is considered as one of the most important alkaline intrusions in the world, a round caldera with a diameter of 35 km and an area of 1000 km² (Figure 8). This volcanic structure was formed in successive steps in the upper Cretaceous from 87 ma until 60 ma ago (WABER et al., 1993, FERNANDES & FRANKLIN, 2001). The host rocks consist of hydrothermally and metasomatically altered intrusive bodies and flows of volcanic to subvolcanic phonolites. These rocks mainly contain mafic minerals and nepheline syenites (WABER et al., 1993). The intrusion is rounded by the levelling of bed rocks composed of granite and gneisses which are frequently cut by diabase dykes, amphibolites and gneisses (FERNANDES & FRANKLIN, 2001). The uranium enrichment at the Poços de Caldas complex is related to hydrothermal events (primary mineralisation) and to weathering processes (secondary mineralisation). Pyrite represents the main ore mineral inside the hydrothermally altered phonolites. These minerals were basically formed during a potassium-rich hydrothermal event and occur as finely disseminated mineralisation throughout the phonolites (WABER et al., 1993; FERNANDES et al., 1998). Furthermore, cryptocrystalline uranium minerals

occur in the phonolites as finely disseminated impregnation. Uranium minerals even can be found in higher concentrations in association with pyrite. These aggregates can be observed finely distributed throughout the phonolites, in veins and along fractures (FERNANDES et al., 1998). Latter weathering processes of the uppermost exposed rocks resulted in a laterization. A secondary supergene enrichment of U along redox fronts is also observed which is assumed to be a result of downward migration of groundwater (WABER et al., 1993). The mining complex of Poços de Caldas covers an area of about 2.5 km² and has been divided into three mineralised units for ore exploitation, designated as ore bodies A, B and E. The lithology of ore body A and E is composed of tinguaites and phonolites. Thus, the ore bodies are assumed to belong to the internal part of one of the many occurring secondary volcanic pipes. The ore body B is located at the external part of a secondary pipe. It corresponds to a pyroclastic deposit which is limited in its lower part by a foiaitic intrusion. The lithology of this ore body shows a high diversity including porphyritic phonolites, pseudo-leucitic phonolites, breccias, ashes and ultrabasic rocks appearing as dikes crossing the ore body (FERNANDES et al., 1998; FERNANDES & FRANKLIN, 2001). The average elemental concentrations of Uranium for ore body A, B and E are 89 ± 57 ppm; 538 ± 958 mg kg^{-1} and 279 ± 619 mg kg^{-1}, respectively (FERNANDES & FRANKLIN, 2001).

The mine is crossed by two watersheds, the rivers of Rio das Antas and Rio Verde. Both watersheds are just fed by fluviometric precipitation. The Rio das Antas drains about 75% of the Poços de Caldas plateau and flows from the water reservoir of the mine to the Bortolan dam in the urban area of Poços de Caldas. The Rio Verde is responsible for 20% of the drainage of the plateau. Waters from both rivers are used for irrigation in local agriculture and cattle farming (FERNANDES et al., 1998; FERNANDES & FRANKLIN, 2001).

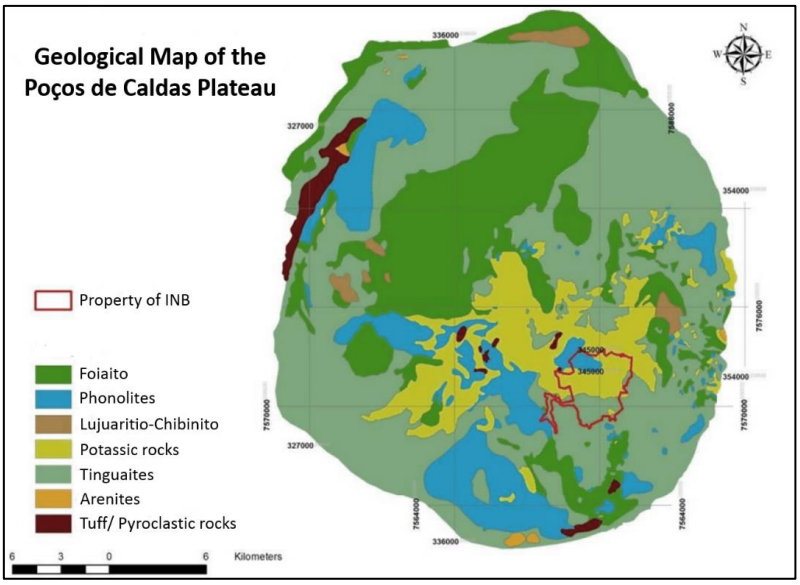

Figure 8: Geological map of the Poços de Caldas Plateau (adapted from FRAENKEL et al., 1985).

5.1.4 Pedology

Red and yellow latosols are one of the predominant soils in the south-west of Minas Gerais (AGEITEC, 2019). They can form on flat land, slopes and hilly landscape. They have a clayish texture and are rich in Al and Fe oxides, especially in the A layer. These soils are normally depleted in Ca, Mg, Na and K. The formation process of latosols is called latolisation and is characterized basically by the removal of SiO_2, Ca^{2+}, Mg^{2+} and K^{+} from the soil profile after the transformation of the primary mineral constituents, leaving only Al and Fe oxides inside the soil (AGEITEC, 2019).

Red and yellow latosols are subdivided in six different types. They are profound soils with depths of over 2 m and show a low differentiation between the A, B and C horizons. The A horizon is normally darker while the C horizon is clearer. The B horizon is very deep and uniform in texture due to intense leaching in high temperatures. The content of silt in red and yellow latosols is normally about 20%. Latosols are very weathered soils having a small storage of nutrients accessible for plants with a small to media capacity of cation exchanges. The humus content of latosols is very low as organic material is rapidly breakdown, but humus is quickly absorbed by plants. Though dense rainforest grows on these soils, once the forest vegetation is removed, the soils show a very low fertility

(IAC, 2019; AGEITEC, 2019). The soils in the study area are mainly dystrophic red and yellow latosols (FEAM, 1980). Dystrophic red and yellow latosols are one of the most common latosols in Brazil. They are acidic with a pH between 4.0 and 5.5 and have a low content of phosphor with a media concentration of < 1mg dm^{-3}. The soils show clay accumulations in the superficial layer or also the B horizon until depths of 200 cm. Also, there can be found fragments of rocks and less altered minerals between the superficial layer and depths of 200 cm. The clayish fraction is generally composed of kaolinite, iron oxides (goethite or hematite) and aluminium oxides (gibbsite) (IAC, 2019; AGEITEC, 2019).

5.1.5 Vegetation

According to the maps of the biomes of Brazil, the area of INB Caldas is located in the biome of the Atlantic rainforest (IBGE, 2004). Though the area is near the transition zone between the Atlantic rainforest and Cerrado biome.

The biome of the Atlantic rainforest is considered as one of the 34 hotspots of biodiversity of areas which lost over 70% of their original extension but host together over 60% of all land species of the earth (MITTERMEIER et al. 2004). In relation to the flora, the Atlantic rainforest is one of the biomes on earth with the highest diversity counting 15,782 registered plant species which makes up 5% of all flora species on earth. Of this species, 45% are endemic to the Atlantic rainforest (STEHMANN et al., 2009). The predominant phyto-physiognomies in the study area are semi-deciduous forests and natural open areas (“campos”) forming vegetational mosaics inside the forest areas. These open areas are found on hill tops, slopes and especially on areas were pedologic factors were affected. They are low grasslands with sporadic presence of shrubs and half-shrubs. The semi-deciduous forests are typical for the Atlantic rainforest. The tree canopies in these forests show irregular heights between 15 to 20 m, though trees with heights of over 30 m can occur. Canopies are normally wide, thin and tucked up. The trunks of the trees are profiled with a thick bark and twisted branches (IVANAUSKAS & ASSIS, 2012). Due to the seasonality of the climate with a distinct dry and rainy season, between 20% and 50% of the tree species drop their foliage during dry season. Besides the native forests and open areas,

plantations of exotic tree species like eucaplyptus and pine trees were installed sporadically at the site (INB, 2015).

In the area of INB Caldas, in total 138 plant species are registered distributed between 58 botanic families. The tree species with the highest abundance and highest phytosociological importance are *Piptocarpha macropoda*, *Clethra scabra*, *Myrsine coriacea* and *Myrsine umbellata*. Some forest areas of the site are preservation areas even showing the presence of endangered flora species (INB, 2015).

5.2 Mining activities and resulting contamination areas

The Caldas Mining-Industrial Complex (INB Caldas) (Figure 9) was established and is still hold until today by the governmental nuclear energy company of *Indústrias Nucleares do Brasil* (INB). The industrial production of uranium at INB Caldas began in 1982 with open-pit mining and the physical and chemical processing of uranium ore to obtain ammonium diuranate ($(NH_4)_2U_2O_7$ or commonly *yellowcake*). On-site activities were discontinued between 1990 and 1992 due to reduced ore demands and high production costs. In 1993, mining and production of yellowcake continued but the mining activities were finally stopped in 1995 (FERNANDES et al., 1998; FERNANDES & FRANKLIN, 2001; FRANKLIN, 2007).

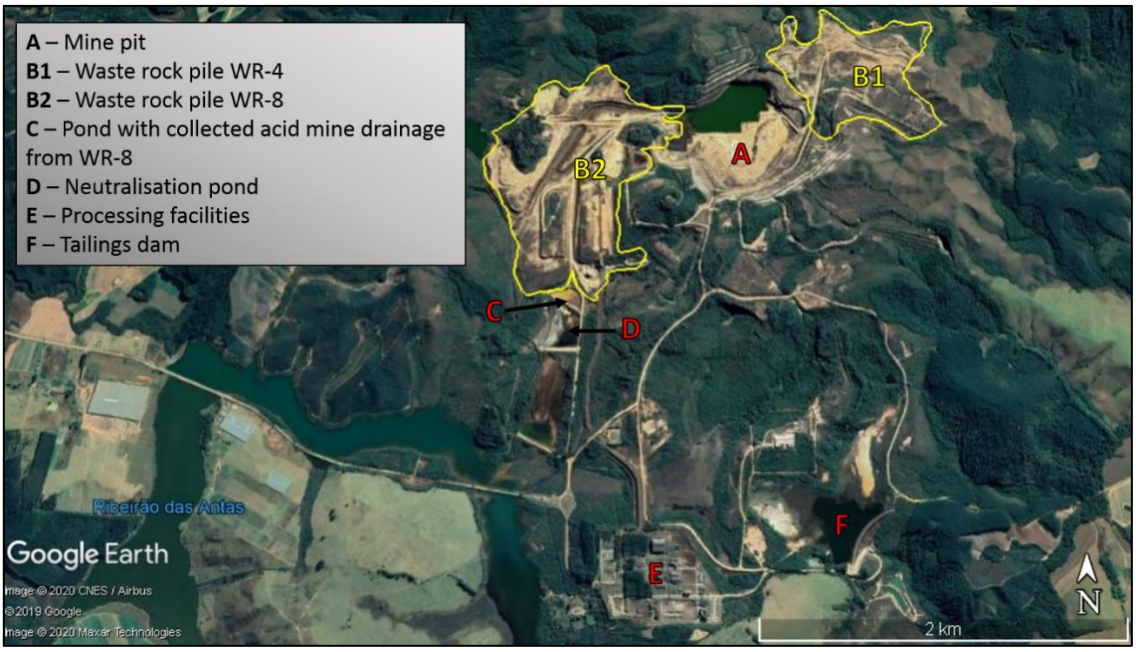

Figure 9: Map of INB Caldas (generated by Google Earth Pro software).

During the 13 years of activity, 1.172 t of U_3O_8 were produced in INB Caldas. For this, a volume of 94.5 x 10^6 m^3 of rocks were removed from the earth's surface, where only 2% of it were designated for physical and chemical processing. (FERNANDES et al., 1998; FERNANDES & FRANKLIN, 2001). The open pit has a circular form with a diameter of about 1.2 km, having slopes with widths of each 5 to 6 m and heights of 16 m. The maximum difference between the deepest excavated point and the original surface is 125 m (ALBERTI, 2017). The waste rocks which were generated at the excavation of the open pit were used as building materials (road, ponds, etc.). The rest, a volume of 44.8 x 106 m^3, were disposed at the site in piles and dumps without compaction control (FRANKLIN, 2007; SOUZA et al., 2013). In the mining complex exists eight waste rock pile areas, highlighting WR-4 and WR-8 as the piles with the biggest volume (12.4 and 14.8 million m^3, respectively) (Figure 9). Together with the open pit and tailings, these areas are serious sources of acid mine drainage. It was reported that pyrite oxidation mostly through the reaction with oxygen is the main driving force for radionuclides and heavy metals mobilisation at the site (FERNANDES et al., 1996; FERNANDES, 1997). WR-4 and WR-8 are located at the water divide of the two main river basins of Rio Verde and Rio das Antas. Despite proofed impermeability at the base of the waste rock piles, there is still a risk of contamination by percolating acid drainage fluids (SOUZA et al., 2013). Drainage

from the mine is retained inside the open pit by an energetic trench. All drainage from WR-4 is collected in a single holding pond and pumped out to the open pit where it is mixed with the mine drainage. From WR-8, just a part of the drainage is collected in a near artificial pond. Those waters are pumped to a neutralisation pond. There, the drainage is chemically treated with the addition of $CaCO_3$ and CaO. This neutralisation unit has a capacity of 250 $m^3\ h^{-1}$. The overflow leaves the neutralisation unit with a pH varying between 10 and 12 (Fernandes et al. 1998). In this pH range, metals and radionuclides precipitate and can be removed easily. The treated water is then released in the Rio das Antas river. The remaining sludge containing calcium diuranate, $CaSO_4$, aluminium hydroxides, and iron is then discarded in the tailing dam (FERNANDES et al., 1998; FERNANDES & FRANKLIN, 2001; FRANKLIN, 2007; ALBERTI, 2014).

For the chemical ore processing, an oxidant (pyrolusite) was added to the crushed ore on heaps and subsequently H_2SO_4 was added for the acid leaching of the uranium from the ore. Afterwards, the pregnant solution was mixed with an organic solvent and NH_4OH in order to extract and precipitate the uranium from the solution. The chemical processing operations generated large quantities of liquid and solid wastes which were neutralised by $CaCO_3$ and CaO to a pH of 9. Subsequently, these wastes were discharged in the tailings dam for solid deposition. The liquid effluent was treated with $BaCl_2$ in order to precipitate Ra which is then removed and stored in two settlement ponds. The liquid effluent is then released into the environment (FERNANDES et al., 1995).

According to Franklin (2007), the area of the mine is under the influence of two main unconnected water systems. The first system is situated between the spoil piles and a transition material (alterated rocks, soil and material which were used for the earthworks) which has the comportment of a free aquifer and is lying over a confined fractured aquifer (rock mass). In this way, it favours the typical hydrolysis and oxidation reactions of weathering (FRANKLIN, 2007).

Little is known of the potential danger posed by AMD of open pit mining operations, as most mines are still being worked or maintained. Thus, INB Caldas poses a potential for pioneer studies in this field of research.

6 MATERIALS AND METHODS

The infrastructure and all the equipment needed to carry out this project were available **at** the premises and laboratories of the Environmental Studies Center (*Centro de Estudos Ambientais – CEA)* and *Laboratório de Estudo de Bacias (LEBAC)*, both being part of the São Paulo State University *Universidade Estadual Paulista (UNESP)* in Rio Claro-SP, Brazil.

6.1 Sampling

6.1.1 Sampling campaign

Soil and tree core samples were taken in November 2018 at four different areas along the study site. For each sampling area, tree cores of always two individuals of six different tree species were sampled. Sampled native tree species were the following with their respective taxonomy: *Alchornea triplinervia* (Family: *Euphorbiaceae* - Order: *Malpighiales* - Clade: *Rosids*), *Clethra scabra (*Family: *Clethraceae* - Order: *Ericales* - Clade: *Asterids*), *Myrsine coriacea*/*Myrsine gardineriana* (Family: *Primulaceae* - Order: *Ericales* - Clade: *Asterids*), *Piptocarpha axillaris/ Piptocarpha macropoda* (Family: *Asteraceae* - Order: *Asterales* - Clade: *Asterids*). Sampled exotic tree species were the following with their respective taxonomy: *Eucalyptus sp.* (Family: *Myrtaceae* - Order: *Myrtales* - Clade: *Rosids*), and *Pinus sp.* (Family: *Pinaceae* - Order: *Pinales* - Clade: *Tracheophytes*). The tree species were chosen due the fact that they are the species showing the highest abundance at the study site and are present in all selected sampling areas. For each individual tree, two replica samples of tree cores were collected accumulating a total of 24 tree core samples for each of the four study areas (total of 96 samples). Topsoil samples were collected at each sampled tree in a radius of 5 m, accumulating 12 samples for each study area (total of 48 samples).

6.1.2 Sampling areas

The study site was separated in the following four different areas regarding the supposed contamination level by metals and the existence of forest vegetation: a reference area (C), the area around the pond with the accumulated acid mine drainage of waste rock pile WR-8 (A1), the area of waste rock pile WR-8 (A2) and the area of waste rock pile WR-4 (A3) (Figure 10).

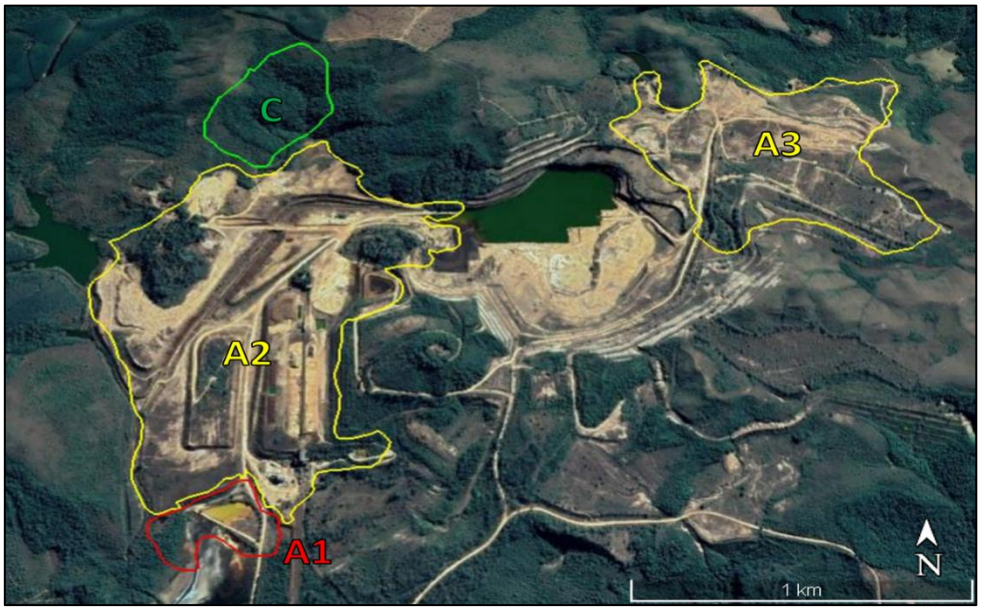

Figure 10: Map of study site inside Caldas Mining-Industrial Complex with sampling areas (generated by Google Earth Pro software).

Area C were selected as the reference area as it is a protected reserve area which hosts primary native Atlantic rainforest (Figure 11 and 12). The area is located on a hilltop north of the waste rock pile WR-4 and did not undergo any mining activities. Thus, it was supposed that the contamination by metals in soil and plants in this area is relatively low compared to the other sampling areas. The native tree species *Alchornea triplinervia*, *Clethra scabra*, *Myrsine coriacea*/*Myrsine gardineriana*, *Piptocarpha axillaris*/ *Piptocarpha macropoda* are all found here. The reference samples for the exotic tree species *Eucalyptus sp.* and *Pinus sp.* were taken in a separated area in the tree nursery of INB in the south of the INB property.

Figure 11: Sampling spots of sampling site C (generated by Google Earth Pro software).

Figure 12: Native tree vegetation of sampling site C (Gemeiner, 2018).

The sampling site A1 is the area around the pond where the AMD from waste rock pile WR-4 is collected (Figure 13 and Figure 14). Thus, this area is supposed to have a high content of metals in the soil. Adjacent to the pond with the AMD is the neutralisation pond where the AMD is treated with $CaCO_3$ and CaO. Samples were taken between the separation line of the ponds and at the adjacent forest vegetation west of the ponds. The tree species which were sampled here were *Alchornea triplinervia*, *Clethra scabra*, *Myrsine coriacea*/*Myrsine gardineriana*, *Pinus sp.* and *Piptocarpha axillaris*.

Figure 13: Sampling spots of sampling site A1 (generated by Google Earth Pro software).

Figure 14: Pond with accumulated AMD at sampling area A1 (Gemeiner, 2018).

The study areas A2 and A3 are the areas of waste rock pile WR-4 and WR-8, respectively (Figure 15 and 16). Both waste rock piles are very scarcely vegetated with tree vegetation. Thus, just few samples could be taken on top of the waste rock piles where single trees could be found (Figure 17). The majority of the samples were taken on the margin of the piles where the tree vegetation is denser. Though, all six tree species of interest could be sampled in these areas.

Figure 15: Sampling spots of sampling site A2 (generated by Google Earth Pro software).

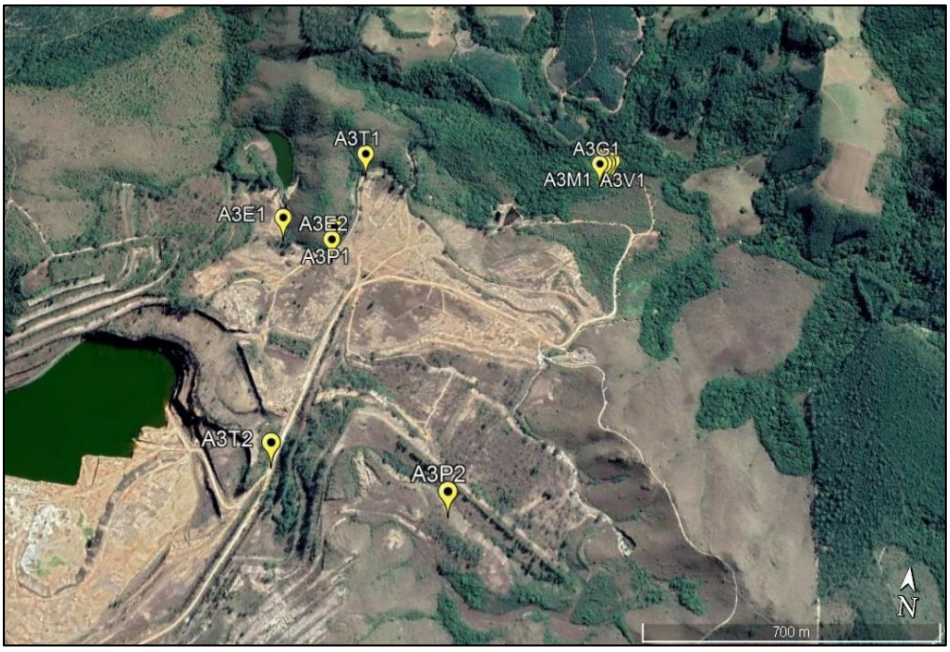

Figure 16: Sampling spots of sampling site A3 (generated by Google Earth Pro software).

Figure 17: Left: Waste rock pile WR-4 at sampling area A3 showing sporadic tree vegetation (Gemeiner, 2020). Right sampling of Pinus sp. at area A3 (Gemeiner, 2018).

6.1.3 Soil sampling

Topsoil samples were collected at each sampled tree in a radius of 5 m and on single spots with no tree vegetation. Topsoil samples were collected to a depth of 0-20 cm removing the uppermost layer by a shovel. An amount of 3 kg of soil were extracted at each sampling point and were placed in a plastic bag which were stored after transportation in a dry and dark room with an ambient temperature until sample treatment (QUI et al. 2012; WORSHAM et al. 2012).

6.1.4 Sampling of tree cores

Sampling of tree cores were based on the method of Algreen et al. (2012). Only healthy and mature trees from the species of interest were selected. Thus, trunks of the trees were required to have at least a diameter of >10 cm. All tree cores were sampled from the trunk at a height of 1 m using an increment borer (Suunto, Finland) (Figure 18). The removed tree cores had a length of 6 cm. The outer first centimetre (bark) of the sample was cut with a ceramic knife and discarded in order to avoid atmospheric contamination. The rest of the sample was placed in a dry and clean plastic bag. After each sampled tree core, the increment borer was cleaned with 92 % alcohol and ultrapure water (Milli-Q) in

order to avoid cross contamination and to obviate the displacing of pathogens from one tree to another. After sampling, tree cores were stored in the plastic bags inside a freezer at a temperature of -8°C (ALGREEN et al., 2012).

Figure 18: On-site tree core sampling of Piptocarpha axillaris at the study site (Gemeiner, 2018; Aily 2018).

6.2 Sample treatment and analysis

6.2.1 Analysis of total metal content in soils

Soil samples were dried at a temperature of 110°C in a drying chamber. Afterwards, samples were homogenized and passed through a 2-mm sieve. Following, samples were sieved to 250 µm particle size and packed into standard XRF plastic packs fitted with Mylar film. Total metal content was then determined for each sample by an X-ray fluorescence (XRF) Analyzer (Nilton XL3t Ultra, Thermo Scientific, Germany). Each sample were measured twice for 120 s respectively and afterwards an average for both measurements were calculated. Reference material NIST 2709a, RCRA App, USGS and SiO2 180-647 were used to check the precision of the equipment (ENE et al., 2009).

6.2.2 Application of DGT in soil samples

Soil samples were dried at a temperature of 110°C in a drying chamber. Afterwards, samples were homogenized and passed through a 2-mm sieve. DGT

deployment in soils were then realized regarding the method of Qui et al. (2012). For each soil sample, 50 g of sieved soil were weighed in an acid cleaned plastic container. Soils were wetted with ultrapure water (MilliQ) until a water holding capacity of 80-100%. The sample container was then closed with a plastic lid and stored for 24 h at a constant temperature of 21°C in order to establish an equilibrium into the wetted soil. Subsequent, a DGT device was deployed into each sample for 24 h (Figure 19) with the sample container closed. Each soil sample were analysed in replicas. All used DGT devices contained a filter membrane made of cellulose acetate, a polyacrylamide diffusive layer and Chelex-100 resin gel as binding agent. Filter membranes were made by cellulose nitrate (11306-25-N, Sartorius Biolab Products, Germany) and had a diameter of 25 mm and a thickness of 0.14 mm. Diffusive layers (R-GDD Standard diffusive gel disc, DGT Research, UK) had a diameter of 25 mm and a thickness of 0.8 mm. Binding agents (R-GDC Chelex gel disc, DGT Research, UK) had a diameter of 25 mm and a thickness of 0.4 mm.

Figure 19: DGT device deployed in soil sample at 100 % water holding capacity (Gemeiner, 2020).

After the deployment time, the binding agent was removed from the DGT device and placed in a clean sample tube, where it was fully immersed in 2 ml of 1M of HNO_3 solution. The gel was left for 24 h in the solution inside a sample tube which were placed in a Digital Vortexer (Orbit 300, Labnet) at 100 rpm. Afterwards, the solution was analysed for metal content by ICP-MS (ICAP Q, Thermo Scientific, Germany). The instrumental and data acquisition parameters

used for the determination of Al, Mn, Fe, Co, Ni, Cu, Zn, Cd, Pb and Zn in the sample solution are shown in Table 1. The instrument signal was optimized before every analysis using a Tune B solution containing 1 µ L^{-1} of Ba, Bi, Ce, Co, In, Li and U (Thermo Scientific, Germany). Standard solutions with concentrations of 0 ng mL^{-1}, 1 ng mL^{-1}, 10 ng mL^{-1}, 25 ng mL^{-1}, 50 ng mL^{-1}, 100 ng mL^{-1} and 500 ng mL^{-1} containing 2% of HNO_3 were analysed before the samples in order to generate an analytical curve. The accuracy of the analysis was checked by using an internal standard with a concentration of 100 ng mL^{-1} for the isotopes of ^{45}Sc, ^{73}Ge, ^{89}Y, ^{115}In and ^{159}Tb. If the signal of the internal standard varied over 20%, results were discarded. The elements Al, Mn, Fe, Co, Ni, Cu and Zn were analysed with kinetic energy discrimination (KED) process in collision mode using a collision reaction cell with helium gas. The elements Pb and U were analysed in standard mode. Due to the high content of Mn, samples had to be diluted 100 times with ultrapure water in order to determine these elements.

Table 1: Instrumental and data acquisition parameters of ICP-MS used for sample analysis.

Nebulizer		Mira Mist	**Acquisition time**	
RF Power [W]		1550	**Replicates**	3
Flow rate nebulizer gas [l min^{-1}]		0.97	**Dwell time**	0.01 s
Flow rate coolant gas [l min^{-1}]		14	**Sweeps**	10
Flow rate auxiliary gas [l min^{-1}]		0.8	**Weighting**	Absolute SD
Peristaltic pump speed [RPM]		40	**Spacing**	0.1 u
Torch	**Sample depth [mm]**	5		
	Vertical [mm]	106		
	Horizontal [mm]	72		

The concentration of the DGT labile metals were calculated using equations 4; 2 and 5, which were described in the introduction section.

6.2.3 Pore water analysis

Pore water was analysed similar described by Qui et al. (2012) and Orlowski et al. (2016). From each soil sample that were previously sampled by DGT, ten grams were placed in a 50 ml sample tube and subjected to a centrifugation system (NT 820, Marconi, Brazil) at 5000 r min^{-1} for 45 minutes. Afterwards, distant pore water was separated from soil by a clean plastic syringe and filtered

by PTFE-filters with a pore size of 0.45 µm (Analítica, Brazil). Subsequent, the filtered solution was acidified by 1M of HNO_3 and analyzed for metal content by ICP-MS (ICAP Q, Thermo Fisher Scientific, Germany). As pore water samples were analysed together with DGT elution samples in the ICP-MS, instrumental and data acquisition parameters used for the determination of Al, Mn, Fe, Co, Ni, Cu, Zn, Mo, Cd, Pb and Zn were the same as mentioned in the anterior section. Detection limits obtained in ICP-MS measurements analysing metal concentrations in pore water and DGT eluates are shown in Table S1.

6.2.4 Analysis of tree core samples

Before analysis, frozen tree core samples were thawed and dried at temperatures of 75-85 °C in a drying chamber until a constant weight. Subsequently, an amount of 0.5 g of each sample was placed together with 10 mL of sub-boiling bi-destillated HNO_3 in a clean microwave tube and was rested for 24 hours. Samples were then digested in the high-performance microwave digestion system *ETHOS-UP* by *Milestone* (Italy) with the parameter settings as shown in Table 2. The method was sufficient for a complete digestion without any solid residues.

Table 2: Parameter settings of ETHOS-UP by Milestone for the digestion of the particulate matter samples.

Steps	Temperature	Time	Power	Pressure
1	210 °C	20 min	1800 W	50 bar
2	210 °C	15 min	1800 W	50 bar

After digestion, samples were transferred to plastic tubes adjusting the volume to 50 ml with ultrapure water. Here microwave tubes were rinsed with ultrapure water for transferring the complete digest to the plastic tubes. The decontamination procedure of the microwave tubes was based on the standard method CLEANING in the equipment software, using 10 ml of sub boiling HNO_3 and parameters as shown in Table 3. This cleaning procedure was afterwards repeated applying 10 ml of ultrapure water in the tubes.

Table 3: Parameter settings of ETHOS-UP by Milestone for the cleaning of the microwave tubes.

Steps	Temperature	Time	Power	Pressure
1	160 °C	15 min	1800 W	50 bar
2	160 °C	10 min	1800 W	50 bar

After digestion, samples were analysed by ICP-MS with the same instrumental settings and data acquisition parameter as mentioned earlier. Detection limits obtained in ICP-MS measurements analysing metal concentrations in wood samples are shown in Table S1.

6.3 Statistical treatment of obtained data

The distribution of all experimental data was tested using the Kolmogorov-Smirnov test (KS-test) for continuous distributions. If the data was normally distributed, a one-factor ANOVA test with an error probability of 0.05 (α = 5%) was performed to identify statistically significant differences between the mean metal concentrations of the different sampling areas. If the equality between the data of the sampling areas was rejected, a post-hoc Tukey test was performed to investigate which area showed statistically significant differences from the other areas. If data was not normally distributed or there was a high heterogeneity of the variances between the data of the sampling area, the Kruskal-Wallis test was performed to detect significant differences between the mean metal concentrations of the different sampling areas. If inequality of the data between the sampling areas was detected, a post-hoc Student-Newman-Keuls test was performed to investigate which area showed statistically significant differences from the other sampling areas (ALGREEN et al. 2012; ALGREEN et al. 2014).

Pearson correlation coefficients were calculated to investigate correlations between metal concentrations measured by DGT and metal concentrations in soil pore water, total metal concentrations in soil and metal concentrations in tree core samples and between metal concentrations measured by DGT and metal concentrations in tree core samples.

All statistical calculations and graphic drawing were realized using Excel, Graphpad Prism 8.4.3 and BioEstat 5.3 software.

7 RESULTS AND DISCUSSION

7.1 Total metal content in soil

7.1.1 Accury of Measurements

In total, 41 soil samples were analysed for their total metal content by XRF technique counting for 10 samples in the reference area, 8 samples in area A1, 11 samples in area A2 and 12 samples in area A3. The accuracy of the measurement of the total content for every relevant element in soil samples analysed by XRF are shown in Table 4. In all samples, results for Cd were under the respective detection limit. The accuracy, which is automatically calculated by the equipment based on the counts, for the elements Mo, U, Fe, Mn and Al were high with error values under or near 10 %. For the elements Cu, Ni and Co, accuracy were lower showing relatively high errors of the measurement with over 20 %

Table 4: Accuracy of the measurement by XRF technique for every analysed element represented by the measurement error in %.

Element	Error (%)
Mo	4.2
U	8.6
Pb	12.3
Zn	9.8
Cu	44.6
Ni	31.8
Co	43.6
Fe	0.9
Mn	7.9
Al	1.6

The obtained recovery values from reference material analysis values are demonstrated in Table 5.

Table 5: Obtained recovery values from reference material analysis by XRF (n.a.= element not contained in reference material).

	Recovery (%)			
Element	USGS	NIST	RCRApp	SiO2
Pb	78.3	93.8	94.8	n.a.
Zn	91.3	89.2	n.a.	n.a.
Cu	87.5	108.3	n.a.	n.a.
Co	189.1	81.7	n.a.	n.a.
Fe	94.5	95.9	n.a.	n.a.
Mn	84.1	95.9	n.a.	n.a.
Cd	110.5	n.a.	85.6	n.a.
Al	112.5	102.2	n.a.	n.a.
Mo	130.3	n.a.	n.a.	n.a.
Si	108.4	98.7	n.a.	97.9

Results for the total content of every relevant element in every soil sample analysed is shown in Table S2 in the Supplementary Material. Quality reference soil values for these elements from the state of Minas Gerais established by the Estate Council for Environment (COPAM, 2011) as well as industrial intervention values established by the national environment council (CONAMA, 2016) were added to this table in order to put the results in context.

7.1.2 Total metal concentrations in soil for every sampling area

Total concentrations of U showed similar arithmetic mean values around 100 mg kg^{-1} between the different sampling areas (Figure 20). Though, the median values were apparently higher in the areas A1, A2 and A3 than in the reference area (C). These concentrations were higher than natural U concentrations in soils in Brazil, which show a media between 0.78 and 0.96 mg kg^{-1} (PERÉZ et al., 1998). In Brazil, no quality reference values or intervention values for U in soil are established. The soil quality guideline value for human health for U established by the Canadian Council of Ministers of the Environment is 300 mg kg^{-1} (CCME, 2007). This value was passed in one sample in the reference area and one sample in area A3. Mainly because of this outlier values, reference area C and area A3 show high relative standard deviations between their U concentrations of over 100 % and high divergence between their media concentrations and median. In contrast, U values in area A1 and A2 showed lower variances (RSD = 44.1 % and RSD = 66.5 %, respectively). KS-test proofed

that the data of U concentrations of all samples is normally distributed (D = 0.157; p = 0.239). No statistically difference between the sampling areas could be proofed (One -factor ANOVA: f-ratio = 0.211; p = 0.889).

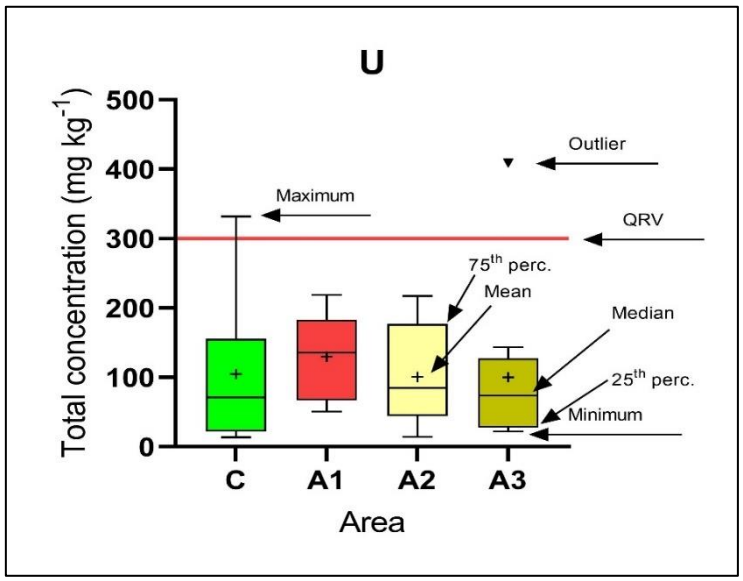

Figure 20: Boxplot diagrams for U concentrations in each sampling area compared with soil quality guideline value for human health (QRV) established by CCME (2007).

The Pb concentrations in all sampling areas showed significantly higher mean values than the quality reference value of 15.8 mg kg^{-1} for Pb in soils of Minas Gerais established by COPAM (2011). In area A1, A2 and A3, even minimum values were explicitly higher than this value (Figure 21). Mean Pb concentrations in area A1, A2 and A3 were higher than the prevention value of 72 mg kg^{-1} established by the national environment council (CONAMA, 2016). Outlier values in area A2 and A3 even passed the intervention values in residential soils of 240 mg kg^{-1} established by CONAMA (2016). Boxplot diagrams show that Pb concentrations in reference area have a low variance and an arithmetic media value which is near to the respective median (mean = 30.8 mg kg^{-1}). In contrast, mean values of area A1, A2 and A3 (mean = 82.0; 75.4 and 90.8 mg kg^{-1}, respectively) are distinctly higher than mean value of the reference area. While area A1 is showing a low variance in the Pb concentrations, area A2 and A3 have high standard deviations and high differences between mean and media values. This is due to a few very high outlier values. The KS-test showed that the data for the Pb concentration is not normally distributed (D = 0.217; p = 0.0358). Thus, a Kruskal-Wallis test was performed to investigate the statistical

difference of the U concentrations between the sampling areas. The result showed that there is a statistical difference between the sampling areas (H = 14.9; p = 0.0019). The performed post-hoc Student-Newman-Keuls test proofed that the results of the reference area differed significantly from the results of area A1, A2 and A3 (p = 0.002; 0.027 and 0.0068, respectively). No statistically significant difference was observed between area A1, A2 and A3. Thus, it was proven, that Pb concentrations from the areas A1, A2 and A3 were significantly higher than Pb concentrations in the reference area.

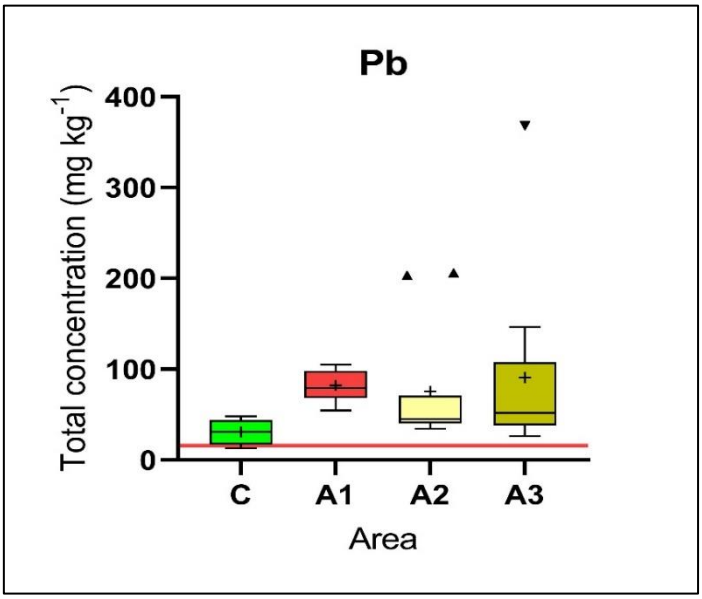

Figure 21: Boxplot diagrams for Pb concentrations in each sampling area compared with soil quality reference value (QRV) established by COPAM (2011).

Mean concentrations of Zn in all sampling areas were explicitly higher than the quality reference value of 31.04 mg kg^{-1} established by COPAM (2011). In all sampling areas, even minimum values showed significantly higher values than the quality reference values of Zn in soils for the state of Minas Gerais (Figure 22). Mean Zn concentrations in all sampling areas were higher than the prevention value of 86 mg kg^{-1} established by the national environment council (CONAMA, 2016). The mean Zn concentrations in all sampling areas were near the median and showed similar values between 91.5 and 99.6 mg kg^{-1}. The boxplot diagrams show that Zn concentrations in the reference area have a higher variance (RSD = 27.0 %) than in the other sampling areas. The KS-test showed that the data of Zn concentrations is normally distributed (D = 0.072; p = 0.974). The one-factor ANOVA test demonstrated that there is no statistically significant

difference between the Zn mean concentrations of the sampling areas (f-ratio = 0.447; p = 0.721).

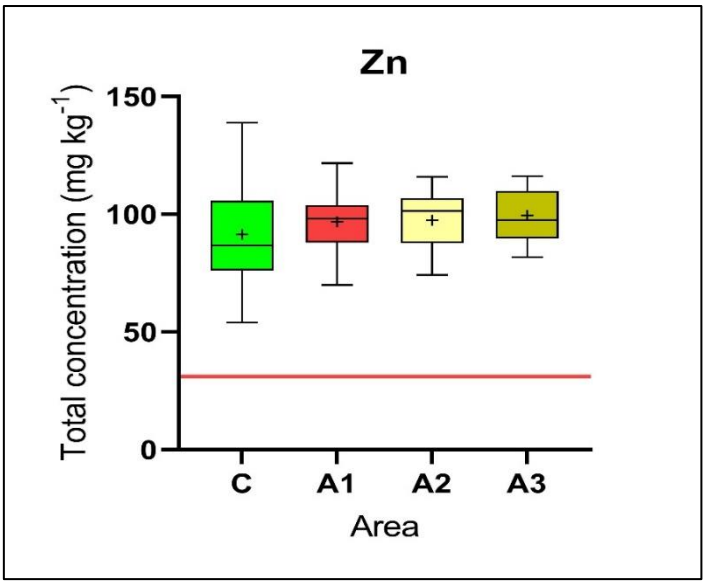

Figure 22: Boxplot diagrams for Zn concentrations in each sampling area compared with soil quality reference value (QRV) established by COPAM (2011).

Total concentrations of Cu in the soil samples showed similar mean values for the different sampling areas between 26.3 mg kg^{-1} (C) and 27.9 mg kg^{-1} (A3). These mean values were explicitly higher than the quality reference value of 13.22 mg kg^{-1} (COPAM, 2011) and all are close to their respective median values (Figure 23). Respectively, one value in area A2 and area A3 was under the respective detection limit. All sampling areas have similar relative standard deviations though the variance of area A1 is influenced by a very high single outlier value. The KS-test proofed that the data of Cu concentrations is normally distributed (D = 0.086; p = 0.911). The one-factor ANOVA test showed that there is no statistically significant difference between the Cu mean concentrations of the sampling areas (f-ratio = 0.185; p = 0.906).

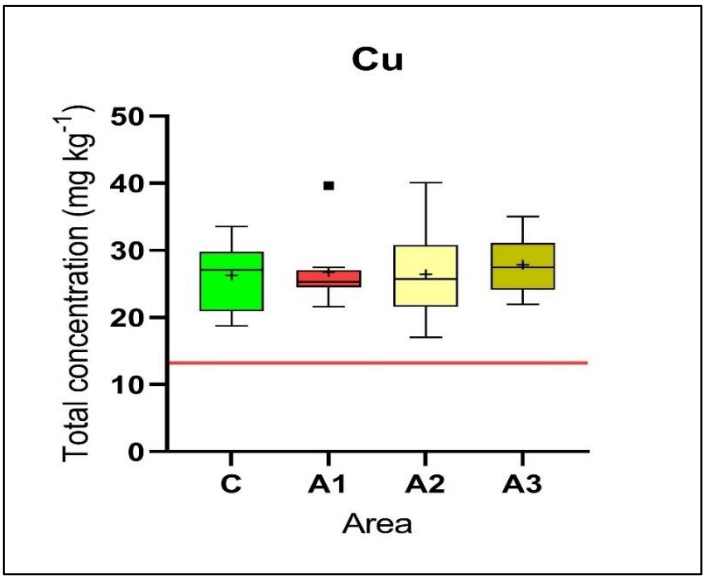

Figure 23: Boxplot diagrams for Cu concentrations in each sampling area compared with soil quality reference value (QRV) established by COPAM (2011).

The element Ni could not be detected in one sample in area A1 and area A2, respectively. In area A3, Ni could not be detected in five samples. The measured Ni concentrations in all sampling areas presented distinctly higher mean concentrations than the quality reference value of 23.04 mg kg^{-1} in Minas Gerais (COPAM, 2011). Mean Ni concentrations in all sampling areas were higher than the prevention value of 30 mg kg^{-1} established by the national environment council (CONAMA, 2016). The highest mean Ni concentrations were determined in area A1 with 73.7 mg kg^{-1} and the lowest mean Ni concentration were determined in the reference area with 49.1 mg kg^{-1} (Figure 24). Boxplot diagrams show that the mean concentration of the reference area is similar to the median. Furthermore, the variance of the Ni concentrations in the reference area were apparently lower in the reference area than in area A1, A2 and A3. In area A1, the 75-percentile was very close to the maximum value, as well was the 25-percentile to the minimum. The KS-test demonstrated that Ni concentrations in the soil samples are normally distributed (D = 0.215; p = 0.141). The one-factor ANOVA test showed that there is no statistically significant difference between the mean Ni concentrations of the sampling areas (f-ratio = 2.68; p = 0.089). The Ni concentrations of area A3 were not included in these calculations due to the high number of samples where Ni could not be detected.

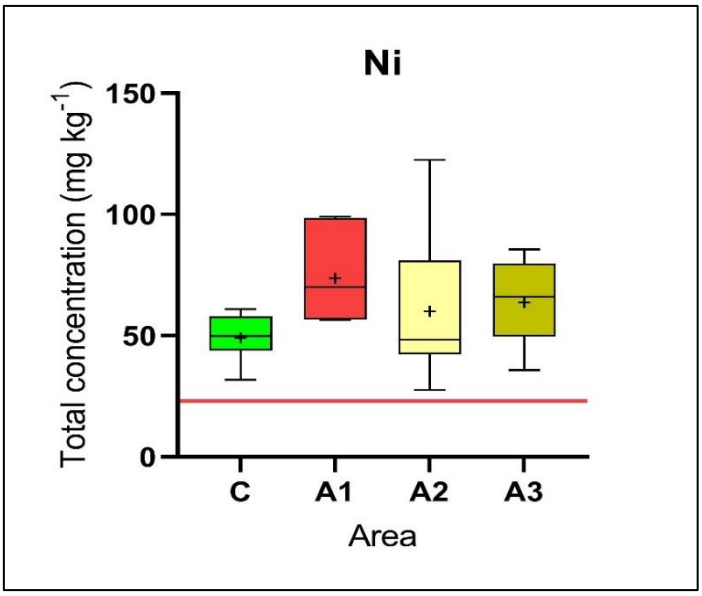

Figure 24: Boxplot diagrams for Ni concentrations in each sampling area compared with soil quality reference value (QRV) established by COPAM (2011).

Concentrations for the element Co in all samples showed explicitly higher values than the quality reference value of 17.5 mg kg^{-1} established by COPAM (2011). Mean Co concentrations in all sampling areas were higher than the prevention value of 25 mg kg^{-1} established by the national environment council (CONAMA, 2016). In area A2 and A3, mean Co concentrations were even higher than the intervention value for industrial soils of 90 mg kg^{-1}. In two samples in the reference area, as well as in one sample in area A1, the element Co could not be detected. The highest mean Co concentration was determined in area A3 with 119.7 mg kg^{-1}, while the lowest mean Co concentration was determined in the reference area with 73.8 mg kg^{-1} (Figure 25). Concentrations of Co in soil samples in area A1 have a very low variance (RSD = 8.2 %) with the 25-pecentile, the median, the arithmetic mean value and the 75-percentlie showing similar values. The Co concentrations in the soil samples of the reference area showed the highest variance with RSD = 34.6 %. As the KS-test showed that the Co concentrations in soil samples in all sampling areas are normally distributed ($D = 0.122$; $p = 0.583$), a one-factor ANOVA test was applied to investigate the differences of the mean Co concentrations between the sampling areas. Though, the one-factor ANOVA test failed due to the inequality of the variances ($p < 0.05$). Thus, a Kruskal-Wallis test was applied showing a statistically significant difference of the mean Co concentrations between the sampling areas ($H = 16.69$; $p = 0.0008$). The post-hoc Student-Newman-Keuls test showed in specific

that there was a statistically significant difference of the mean Co concentrations between the reference area and area A3 (p = 0.0005), and between area A1 and area A3 (p = 0.0019). This shows that Co concentrations in soil in area A3 were significantly higher than in the reference area and area A1.

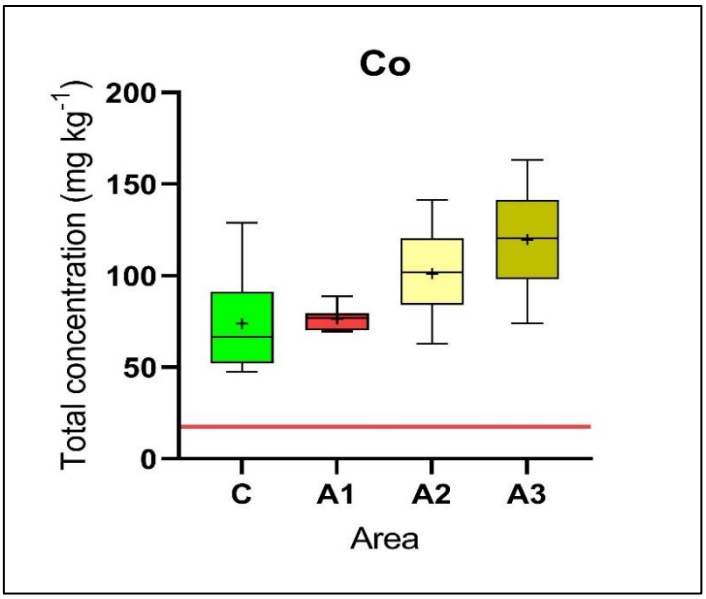

Figure 25: Boxplot diagrams for Co concentrations in each sampling area compared with soil quality reference value (QRV) established by COPAM (2011).

Fe concentrations in all sampling areas were explicitly lower than the quality reference value of 83,500 mg kg^{-1} in Minas Gerais (COPAM, 2011). The highest mean Fe concentrations were determined in area A3 with 43,111.2 mg kg^{-1} and the lowest in the reference area with 30,399.5 mg kg^{-1} (Figure 26). Area A1 showed the lowest variance in the Fe concentrations with an RSD of 13 % while the Fe concentrations in the reference area showed the highest variance with an RSD of 22.5 %. The boxplots of area A2 and area A3 demonstrate that their respective media, median and 75 % percentile are all close having a high number of samples in the concentration range of the mean concentration. The KS-test proofed that the data of Fe concentrations in the samples is normally distributed (D = 0.078; p = 0.938). The one-factor ANOVA test showed that the media Fe concentrations between the sampling areas statistically differ significant to each other (f-ratio = 7.36; p = 0.005). In specific, the post-hoc Tukey test demonstrated that mean Fe concentrations of area A2 and A3 differ significantly from mean Fe concentration of the reference area (p < 0.01,

respectively). This fact shows that Fe concentrations of area A2 and A3 were significantly higher than Fe concentrations of the reference area.

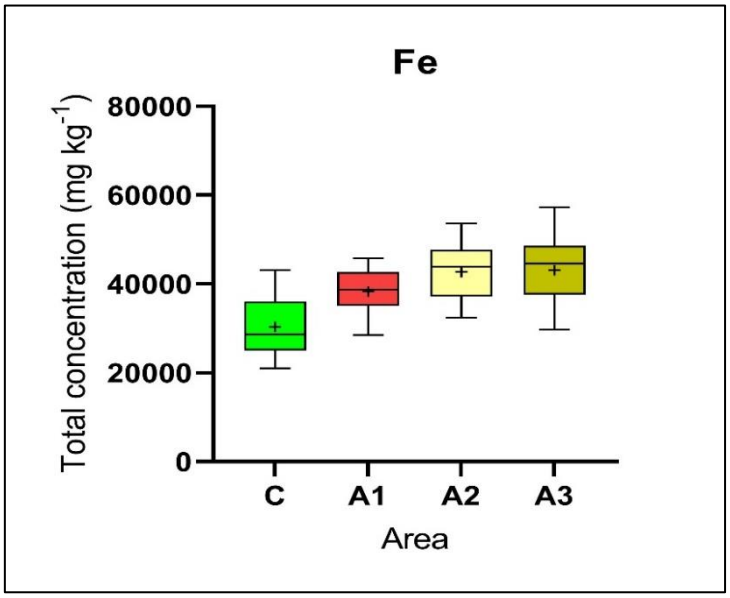

Figure 26: Boxplot diagrams for Fe concentrations in each sampling area.

Mean Mn concentrations in all sampling areas demonstrated higher values than the quality reference value of 446.91 mg kg^{-1} established by COPAM (2011). While mean Mn concentrations in area C, A1 and A2 were distinctly higher, the mean Mn concentration in soils in area A3 with 554 mg kg^{-1} was close to the quality reference value (Figure 27). In contrast to the other elements, the highest Mn concentration in terms of mean and maximum values were found in the reference area (mean = 1080.4 mg kg^{-1}; maximum = 2182.2 mg kg^{-1}). In this sampling area, the Mn concentrations in soil also showed the highest variance (RSD = 64.6 %). The KS-test showed that the Mn concentrations in the soil samples are normally distributed ($D = 0.185$; $p = 0.107$). The following one-factor ANOVA test failed due to the high inequality of the variances of the Mn concentrations between the sampling areas ($p < 0.05$). Thus, a Kruskal-Wallis test was applied which proofed that there is no statistically significant difference of the mean Mn concentrations between the sampling areas ($H = 3.78$; $p = 0.284$).

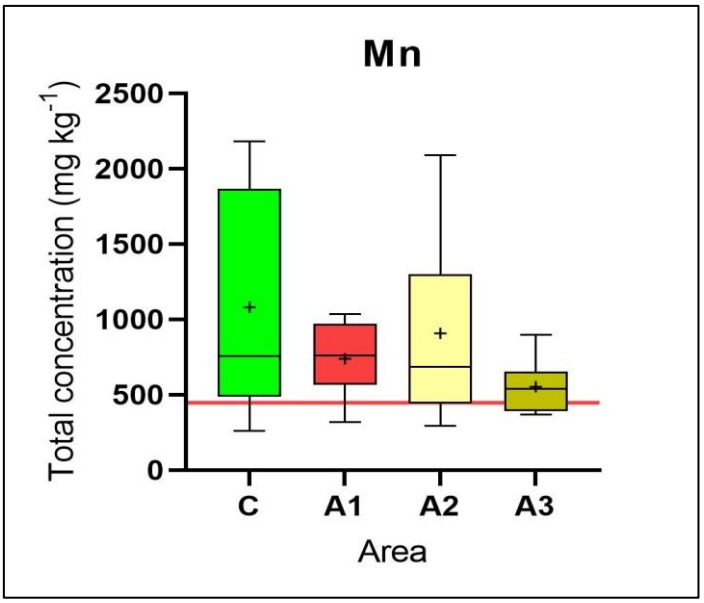

Figure 27: Boxplot diagrams for Mn concentrations in each sampling area compared with soil quality reference value (QRV) established by COPAM (2011).

The highest Al concentrations in the soil samples were determined in area A2 and A3 with mean values of 152,645 mg kg^{-1} and 152,087 mg kg^{-1}, respectively (Figure 28). The lowest mean concentration was determined in the reference area (126,045 mg kg^{-1}). Though, the highest variance in the Al concentrations was determined in this area (RSD = 12.1 %). The boxplot diagram for area A2 shows, that there is a big discrepancy between the mean and the media value. Furthermore, the range between 25- and 75-percentlie is remarkably high which indicates a high variance between the Al concentrations in this area. The KS-test showed that the Al concentrations in the soil samples in all sampling areas are normally distributed ($D = 0.109$; $p = 0.678$). The one-factor ANOVA test proofed that there is a statistically significant difference of the mean Al concentrations between the sampling areas (f-ratio = 8.715; $p = 0.0003$). In specific, the following pot-hoc Tukey test showed that there is a statistically significant difference between the mean Al concentrations of the reference area and area A2 ($p < 0.01$), as well as between the Al concentrations of the reference area and area A3 ($p < 0.01$). Thus, Al concentrations of area A2 and A3 were significantly higher than Al concentrations in the reference area.

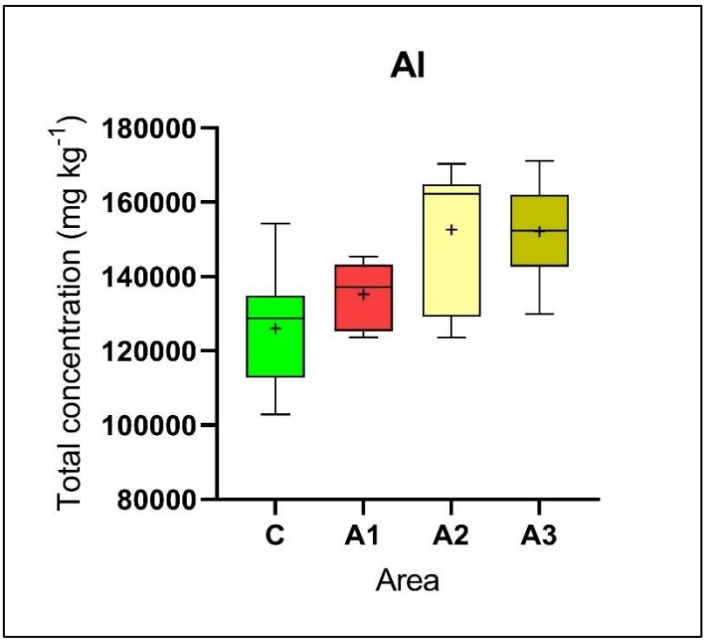

Figure 28: Boxplot diagrams for Al concentrations in each sampling area.

Mean total concentrations for Mo showed values far above the prevention value in soil of 5 mg kg^{-1} established by CONAMA (2016) in all sampling areas. The intervention value of 180 mg kg^{-1} established by CONAMA was passed in various samples in area A1, A2 and A3. The boxplot diagrams show that mean concentrations in these areas were higher than in the reference area (Figure 29). Though, these mean concentrations are much higher than their respective median, which shows that a few samples with high outlier concentrations are responsible for a high media concentration. Thus, a one-factor ANOVA test was realized in order to investigate if the mean Mo concentrations differ significantly from each other between the sampling areas. The one-factor ANOVA test was applied as the data showed to be normally distributed in a performed KS-test ($D = 0.126$; $p = 0.492$). The result demonstrated that there was no statistically difference between the mean concentrations of the four sampling areas (f-ratio = 1.671; $p = 0.19$).

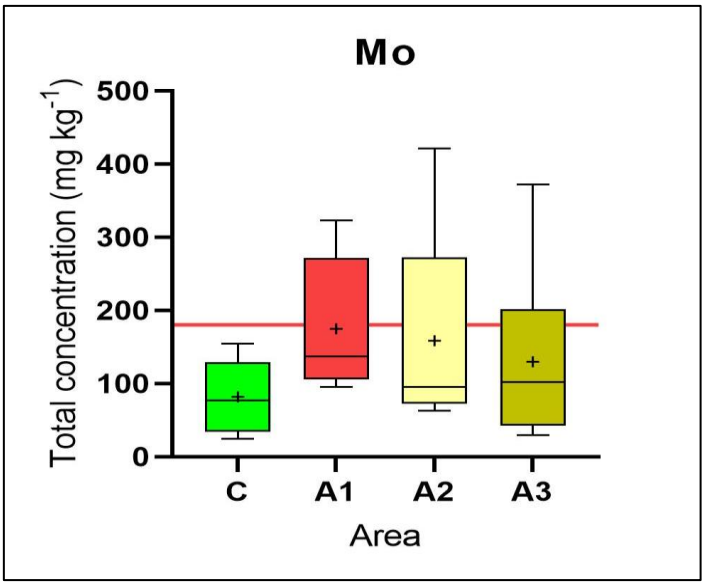

Figure 29: Boxplot diagrams for Mo concentrations in each sampling area compared with industrial intervention value (QRV) established by CONAMA (2011).

7.1.3 Discussion

In sampling area C, the metals with the highest total concentration were the following in the decreasing order Al> Fe> Mn> U> Zn> Mo> Co> Ni> Pb> Cu. For sampling areas A1 and A2 the order was Al> Fe> Mn> Mo> U> Zn> Pb> Co Ni> Cu. For sampling area A3, the order was Al> Fe> Mn> Mo> Co> U> Zn> Pb> Ni> Cu. In all sampling areas, mean total concentrations of the elements U, Pb, Zn, Mn, Cu, Ni, Co and Mo in soils were explicitly higher than quality reference values for soils in Minas Gerais (COPAM, 2011). The elements U, Pb, Zn, Ni, Co and Mo have to be emphasized here as their mean total concentrations were over the established prevention and intervention values in a variety of samples. Especially U and Pb are of concern as they are toxic trace elements for organisms. The elements Zn, Cu, Ni, Co, Fe and Al showed relatively low standard deviations under 40% relative to their mean values in all sampling areas. This indicates that there is a ubiquitous distribution of these elements in all sampling areas. The element Mn showed to be fairly ubiquitous distributed with relative standard deviations around 60% in area C and A2. Standard deviations for U are relatively high in every sampling area, especially for area C, A2 and A3 (RSD> 80%). This could be due to the punctual geogenic U enrichment processes described in the study area section, or also, the consequence of punctual redistribution of U by disposing of ore milling wastes. The element Pb

shows high relative standard deviation over 80% in area A2 and A3 with single contamination hotspots. The same pattern is found for Mo in sampling areas A1, A2 and A3. This could also be explained with the unusual, diversified geology of the study site, but also hints for anthropogenic influenced contamination by mining activities. With the evaluation of the results of the pore water, DGT and *Tree coring* analysis in the next chapters, it was attempted to assess if these local contaminations pose an even higher potential threat for the environment by showing high labile and potentially bioavailable metal contents.

Statistically significant differences between the sampling areas could not be detected for mean total concentrations in soil samples of the elements U, Zn, Cu, Mn and Mo, showing raised total concentrations compared to background values established by COPAM and CONAMA in all sampling areas. This can hint on the possibility that the processes of metal distribution being widespread with AMD as a principal cause. This is further supported by the high rainfalls in the region which could act as a vector for metal dispersion. For the elements Pb, Ni, Co, Fe and Al, the reference area showed significant lower mean total concentrations in the soil than at least one other sampling area, which were affected by the mining activities. This indicates that mining activities and AMD are with a very a high probability responsible for the enrichment of these elements in the soils of area A1, A2 and A3 in relation to the reference area.

7.2 Metal concentrations in soil pore water and labile metal concentrations

Results of metal concentrations in soil samples measured in pore water (C_{PW}) and by DGT application (C_{DGT}) are listed in Tables S3 to S10 in the Supplementary Material. Pore water analysis and DGT analysis were realized in 11 samples of the reference area, 8 samples of area A1, 11 samples of area A2 and 12 samples of area A3. Both measurement techniques were realized in replicas for each sample. The respective mean value of the results of both replicas were used for the statistical evaluation. In the case of results measured below the analytical detection limit, the value of the respective analytical detection limit divided by two was included to the statistical evaluation. To exemplify the

results, concentrations of both measurements for every element were illustrated in bar charts separated for every sampling area. In order to determine the labile fraction of the respective metal, the R-value of the respective element was calculated by Equation (6):

$$R = C_{DGT}/C_{PW} \times 100 \qquad (6)$$

where R is the ratio in % of C_{DGT}, the concentration of the metal measured by DGT, and C_{PW}, the concentration of the metal measured in pore water. The R-value is considered to be an indicator of the desorption rate of the respective metal from the soil solid phase to the pore water. A low R-value indicates a low desorption rate and high R-value indicates a high desorption rate. Thus, the R-value can hint to the amount of the labile and environmentally available fractions of the metal in the soil (DEGRYSE et al., 2009).

In order to validate the data for each element, C_{DGT} values were plotted against their respective C_{PW} values. If the metal concentrations in pore water are well buffered by resupply of the solid phase, a linear relationship between C_{DGT} and C_{PW} is obtained. A good linear relationship between both values also demonstrates that the same metal pools in the soil solid phase were assessed with the pore water extraction analysis and the DGT technique (ZHANG & DAVISON, 1998).

7.2.1 Uranium

The sample number of uranium quantified in pore water in area C was n= 8, for area A1 n= 8, for area A2 n= 11 and for area A3 n= 11. The sample number of U quantified using DGT in area C was n= 8, for area A1 n= 6, for area A2 n= 11 and for area A3 n= 11. The highest mean concentrations for U measured in pore water and measured by DGT were obtained in sampling area A1 (C_{PW}= 39.1 ± 38.6 µg L^{-1}, C_{DGT}= 21.3 ± 24.3 µg L^{-1}) (Figure 30). It was shown that C_{PW} values of area A1 in media were significantly higher than in the other sampling areas (KW-test: H= 8.3; p= 0.04; SNK-test: p(C-A1)< 0.01; p(A1-A2)< 0.05; p(A1-A3)< 0.05). No statistically significant difference was observed for C_{DGT} between all sampling areas (KW-test: H= 6.37; p= 0.09). The highest mean R values were

observed in area A2 and A3 (R= 74.7 ± 28.0 % and R= 77.2 ± 27.5 %, respectively). However, no statistically significant variances were detected between the sampling areas regarding the R-values (KS-test: H= 3.14; p= 0.37). In all sampling areas, mean R-values were higher or near 60 %. This shows that the desorption rate of U released from the soil solid phase to the pore water was high in all sampling areas and that the main fraction of U in the soils was labile and potentially environmentally bioavailable. This leads to the assumption that in all sampling sectors, the main part of the Uranium concentrations in the pore water were significantly resupplied from the solid phase, but it was insufficient to sustain fully the pore water concentrations. This is described as the partially sustained case (10 % < R < 95 %) (ZHANG et al., 1998). Though, three samples in the reference area, five samples in area A2 and four samples in area A3 applied for the fully sustained case (R> 0.95). Here, U concentration in pore water was fully resupplied by the soil solid phase. R-values of U from the present study were distinctly higher than R values reported in the study of Vandenhove et al. (2006) from soils of a soil covered Uranium waste dump in Germany (R= 11 %).

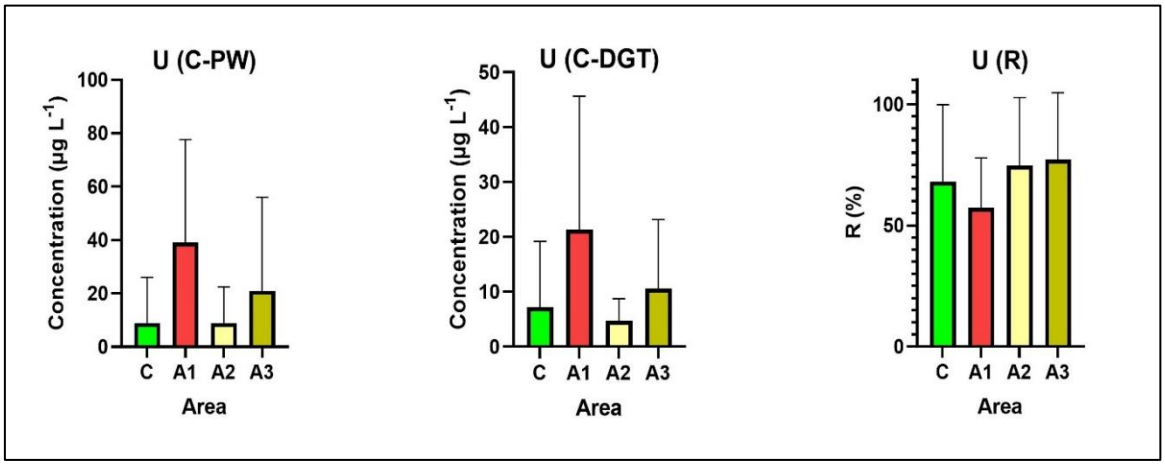

Figure 30: Bar charts for mean U concentrations measured in pore water (C-PW), U concentrations measured by DGT (C-DGT) and obtained R-values (R) for all sampling areas.

Values of C_{PW} and C_{DGT} for U show a high significant linear relationship (R^2> 0.9) in sampling areas C, A2 and A3 (Figure 31). This supports the assumption that U concentrations in pore water are well buffered from the soil solid phase in these areas. Values of C_{DGT} and C_{PW} are in a lower significant correlation in area A1 (R^2= 0.65) than in the other sampling areas. This observation agrees with the R-values, which were the lowest in area A1. Thus,

besides showing the highest U concentrations in pore water, it seems that the U species in this area are slightly less labile in soil.

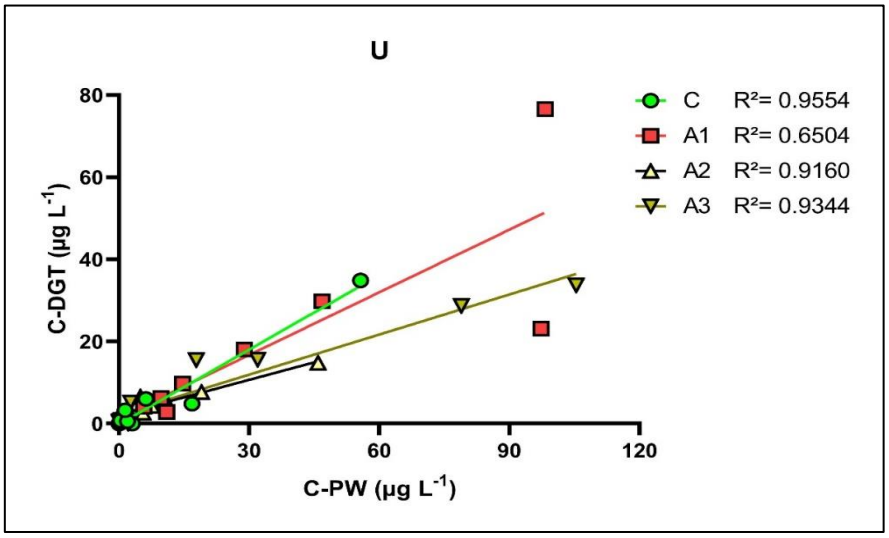

Figure 31: U concentrations measured by DGT (C-DGT) plotted against U concentrations measured in pore water (C-PW).

7.2.2 Lead

The sample number of lead quantified in pore water in area C was n= 7, for area A1 n= 8, for area A2 n= 11 and for area A3 n= 12. The sample number of Pb quantified using DGT in area C was n= 8, for area A1 n= 6, for area A2 n= 11 and for area A3 n= 12. The highest mean Pb concentration in pore water (C_{PW}) and the highest mean Pb concentration measured by DGT (C_{DGT}) were determined in area A3 (C_{PW}= 32.4 ± 52.9 µg L^{-1}; C_{DGT}= 13.0 ± 15.3 µg L^{-1}) (Figure 32). The lowest mean Pb concentration measured by DGT and in pore water on the other hand were determined in the reference area (C_{PW}= 2.5 ± 2.3 µg L^{-1}; C_{DGT}= 2.4 ± 2.0 µg L^{-1}). The SNK-test proofed that the Pb concentrations in pore water in area A3 were significantly higher than in area C ($p< 0.05$). Furthermore, C_{PW}-values were significantly higher in area A1 than in area C (SNK-test: $p< 0.05$). The same pattern was observed for the C_{DGT}-values. Pb concentration measured by DGT were significantly higher in area A1 than in area C (SNK-test: $p< 0.05$) and were also significantly higher in area A3 than in area C (SNK-test: $p< 0.01$). R-values were in similar ranges for all sampling areas between 70 and 80 %. No significant variances could be detected between the sampling areas regarding the R-values (KW-test: D= 1.99; p= 0.58). The high R-values in all

sampling areas indicate that that the main part of the Pb concentrations in the pore water were significantly resupplied from the solid phase. It indicates that the desorption rate of Pb released from the solid phase to pore water was extremely fast. Several samples in all three sampling sectors showed R values of over 95 % where the resupply of Pb from the soil solid phase was fast and fully sustained. Furthermore, the high R values indicated that the main part of Pb in soil is labile and potentially environmentally bioavailable in all sampling areas.

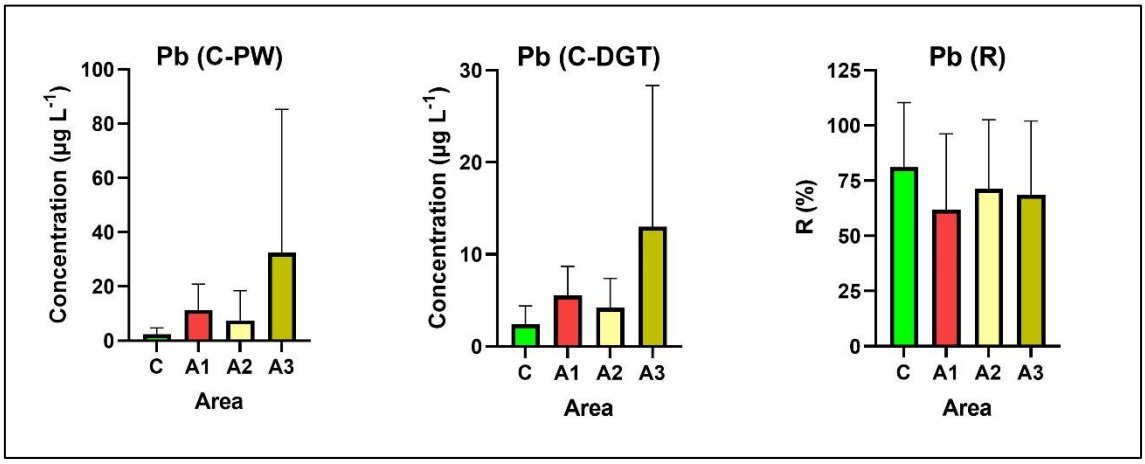

Figure 32: Bar charts for mean Pb concentrations measured in pore water (C-PW), Pb concentrations measured by DGT (C-DGT) and obtained R-values (R) for all sampling areas.

Values of C_{PW} and C_{DGT} for Pb showed a high significant linear relationship for sampling area A2 and A3 with $R^2 > 0.8$ (Figure 33). Here, the same metal pools were assessed with the DGT and pore water analysis. A moderate significant correlation was identified between the C_{PW}- and C_{DGT}-values in area C ($R^2 = 0.52$; n= 11), while no correlation could be detected between the two parameters in area A1 ($R^2 = 0.0004$; n= 8). This indicates a heterogeneity of the soil samples collected in area A1 and it shows that very likely not the same Pb pools were assessed with the DGT and pore water analysis here.

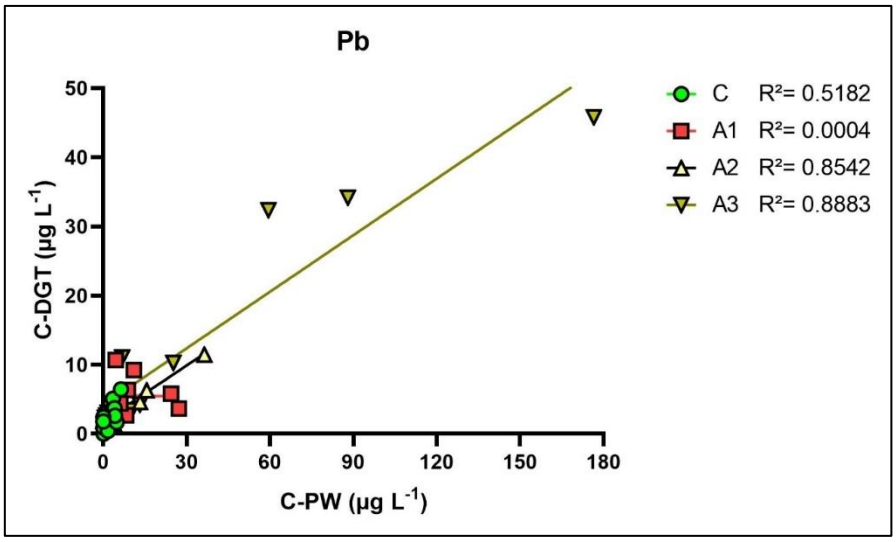

Figure 33: Pb concentrations measured by DGT (C-DGT) plotted against Pb concentrations measured in pore water (C-PW).

7.2.3 Zinc

Except for one sample in area C, Zinc was quantified in pore water in all samples of all sampling areas. Zinc was quantified using the DGT techniques in all samples of all sampling areas. The highest mean C_{PW}-values for Zn were observed in area A1 (C_{PW}= 989.9 ± 877.0 µg L^{-1}) and area A3 (C_{PW}= 738.6 ± 1084.4 µg L^{-1}) (Figure 34). However, no significant differences could be detected between all sampling areas regarding C_{PW} (KW-test: H= 4.0; p= 0.26). The highest mean C_{DGT}-values for Zn were also observed in area A1 (C_{DGT}= 161.3 ± 94.1 µg L^{-1}) and area A3 (C_{DGT}= 97.0 ± 122.3 µg L^{-1}). It was shown that C_{DGT} values in area A1 were significantly higher than in area C and area A2 (SNK- test: $p< 0.05$ and $p< 0.01$, respectively). R-values showed to be similar in all sampling areas ranging in media between 21.4 % and 33.8 %. No significant differences could be detected regarding the R-values between the sampling areas (KW-test: H= 4.4; p= 0.21). This demonstrates that Zn resupply in all sampling areas were mainly partially sustained from the soil solid phase to the pore water. Thus, desorption rate of Zn from the solid phase to pore water seemed to be low and just a small fraction of Zn in soil was labile and potentially environmentally bioavailable in all sampling areas. In the study of Degryse et al. (2003), even lower R values for Zn (between R= 7 % and R= 16 %) were reported in European

soils spiked with Zn, which showed C_{PW} values of Zn in similar ranges than C_{PW}-values of Zn of the present study.

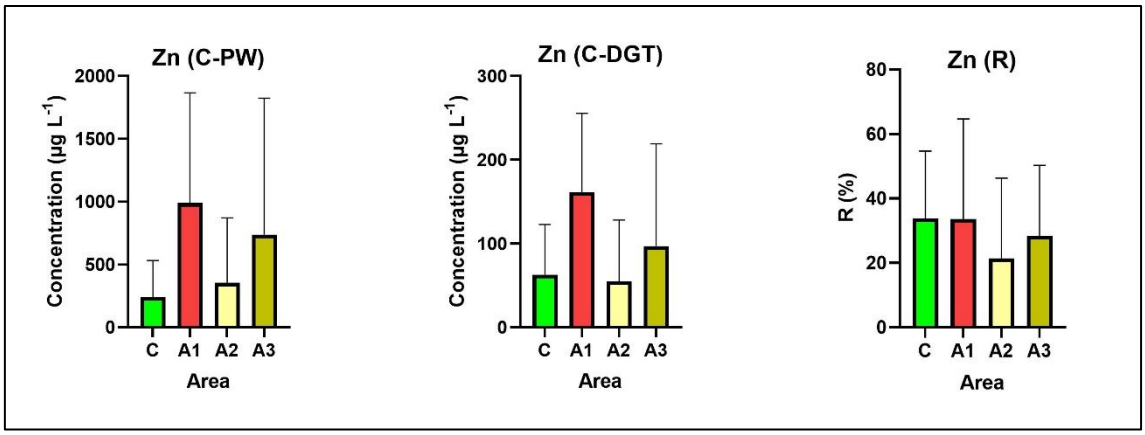

Figure 34: Bar charts for mean Zn concentrations measured in pore water (C-PW), Zn concentrations measured by DGT (C-DGT) and obtained R-values (R) for all sampling areas.

Values of C_{PW} and C_{DGT} for Zn were in a high significant linear relationship for sampling areas A1, A2 and A3 with $R^2 > 0.85$ (Figure 35). Here, the same metal pools were assessed in these areas with the DGT and pore water analysis. However, a moderate significant correlation was identified between the C_{PW}- and C_{DGT}-values in area C ($R^2 = 0.49$).

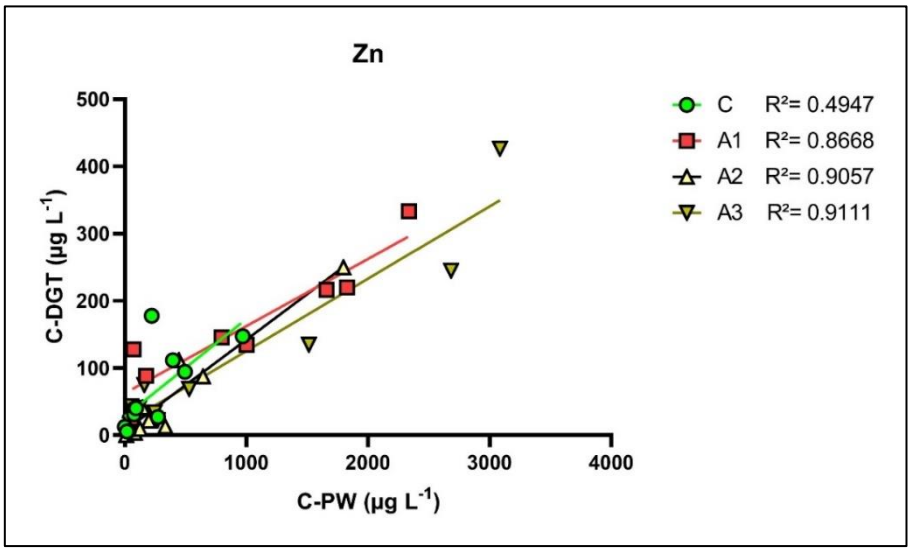

Figure 35: Zn concentrations measured by DGT (C-DGT) plotted against Zn concentrations measured in pore water (C-PW).

7.2.4 Cobalt

The sample number of Co quantified in pore water in area C was n= 10, for area A1 n= 8, for area A2 n= 6 and for area A3 n= 12. The sample number of Co quantified using DGT in area C was n= 10, for area A1 n= 8, for area A2 n= 9 and for area A3 n= 12. The highest mean C_{PW}-values and C_{DGT}-values for Co were observed in area A1 (C_{PW}= 61.7 ± 53.8 µg L^{-1}; C_{DGT}= 9.0 ± 5.8 µg L^{-1}) and area A3 (C_{PW}= 74.4 ± 86.4 µg L^{-1}; C_{DGT}= 9.8 ± 8.0 µg L^{-1}) (Figure 36). No statistically significant differences were found between the sampling areas regarding C_{PW} (KW-test: H= 6.8; p= 0.086). For the C_{DGT}-values, also no significant differences were detected between all sampling areas (KW-test: H= 5.2; p= 0.16). The R-values are in similar ranges in all sampling areas varying between 20.4 ± 10.4 % (area A1) and 34.9 ± 28.2 % (area C). Thus, no significant differences were detected using the KW-test (H= 3.1; p= 0.38). This demonstrates that the Co resupply from the soil solid phase to the pore water was partially sustained in all sampling areas. Desorption rate of Co released from the soil solid phase was relatively low and just a minor part of the Co in soil was labile and potentially environmentally bioavailable in all sampling areas.

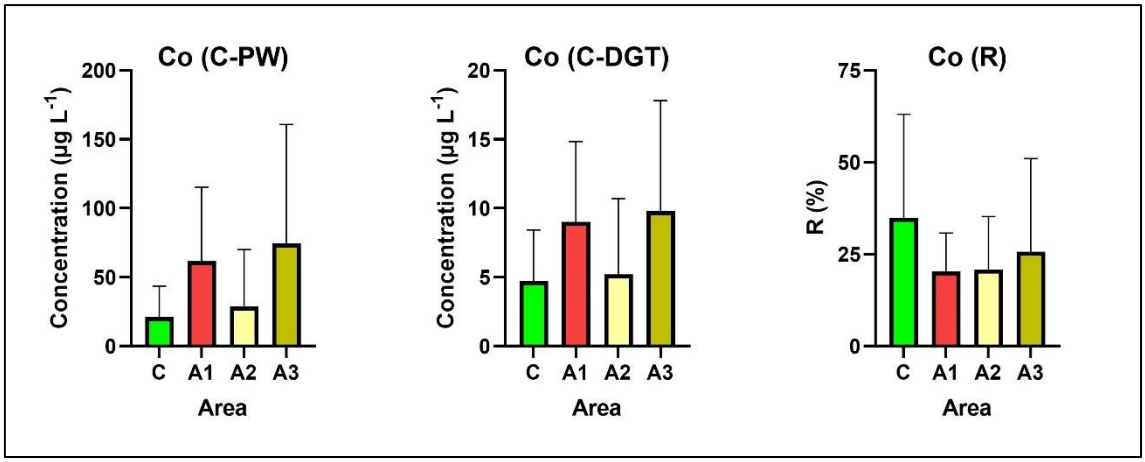

Figure 36: Bar charts for mean Co concentrations measured in pore water (C-PW), Co concentrations measured by DGT (C-DGT) and obtained R-values (R) for all sampling areas.

Values of C_{PW} and C_{DGT} for Co showed a high significant linear relationship for sampling areas A1, A2 and A3 with R^2> 0.83 (Figure 37). Here, the same metal pools were assessed in these areas with the DGT and pore water analysis. A moderate significant correlation was identified between the C_{PW}- and C_{DGT}-

values in area C (R^2= 0.48). It indicates that not necessarily the same Co pools were assessed with the DGT and pore water analysis in this area.

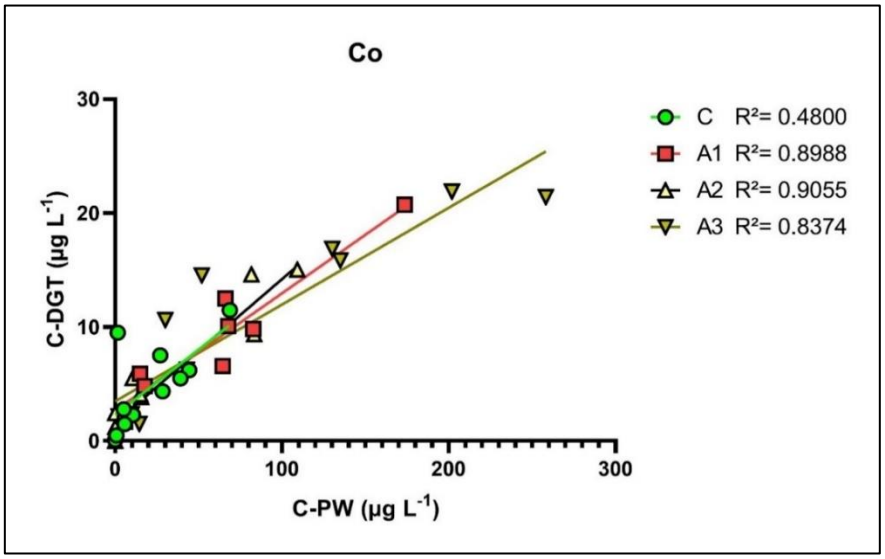

Figure 37: Co concentrations measured by DGT (C-DGT) plotted against Co concentrations measured in pore water (C-PW).

7.2.5 Iron

The sample number of Fe quantified in pore water in area C was n= 9, for area A1 n= 8, for area A2 n= 10 and for area A3 n= 12. The sample number of Fe quantified using DGT in area C was n= 11, for area A1 n= 8, for area A2 n= 11 and for area A3 n= 12. Mean concentrations for Fe in pore water showed apparently high differences between the sampling areas (Figure 38). While the mean C_{PW}-value for area A1 is 2435.1 ± 3350.8 µg L^{-1}, area A2 just shows a mean C_{PW}-value of 135.6 ± 128.6 µg L^{-1}. C_{PW}-values for area A2 were significantly lower than in area C, A1 and A3 (SNK-test: p< 0.05; p< 0.01; p< 0.01, respectively). The highest mean Fe concentrations by DGT were measured in area A1 (C_{DGT}= 349.3 ± 333.6 µg L^{-1}) and the lowest in area A2 (C_{DGT}= 41.7 ± 27.4 µg L^{-1}). C_{DGT}-values of area A2 were also significantly lower than in area C, A1 and A3 (SNK-test: p< 0.05; p< 0.01; p< 0.01, respectively). R-values ranged between 24.5 ± 27.2 % (area A3) and 37.7 ± 36.0 % (area A2). No statistical differences could be detected between the sampling areas regarding the R-values (KW-test: H= 1.4; p= 0.7). This indicates that the Fe resupply from the soil solid phase to the pore water was partially sustained in all sampling areas. Thus, the desorption rate of Fe released from the solid phase to the porewater was

relatively low. Summing up, just a minor part of the Fe species in soil was labile and potentially environmentally bioavailable in all sampling areas.

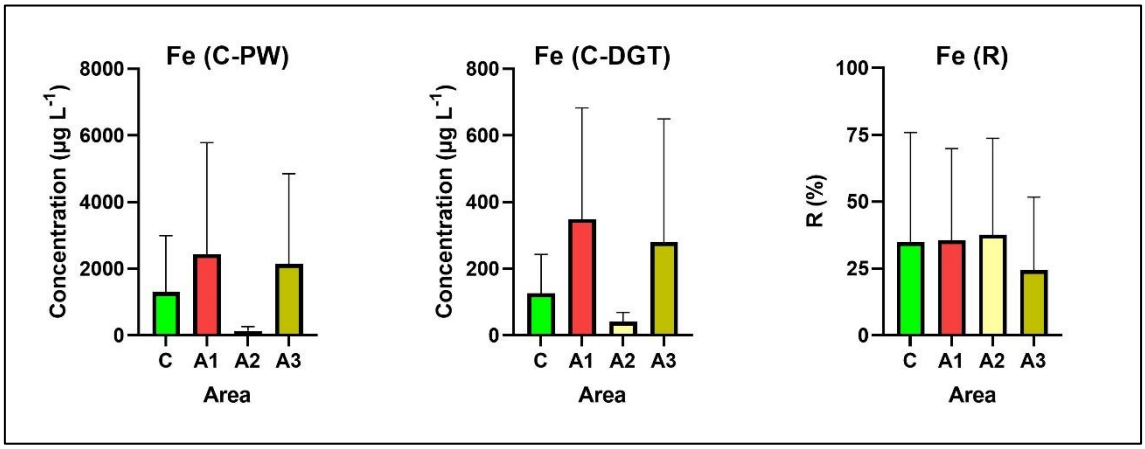

Figure 38: Bar charts for mean Fe concentrations measured in pore water (C-PW), Fe concentrations measured by DGT (C-DGT) and obtained R-values (R) for all sampling areas.

No correlation between C_{PW}-values and C_{DGT}-values in area C and area A3 could be detected and just a minor not significant correlation in area A1 and A3 (Figure 39). This observation together with the high standard variations found in all sampling areas indicates a heterogeneity of Fe species in the soil samples collected. Furthermore, it shows that basically not the same Fe pools were assessed with the DGT and pore water analysis.

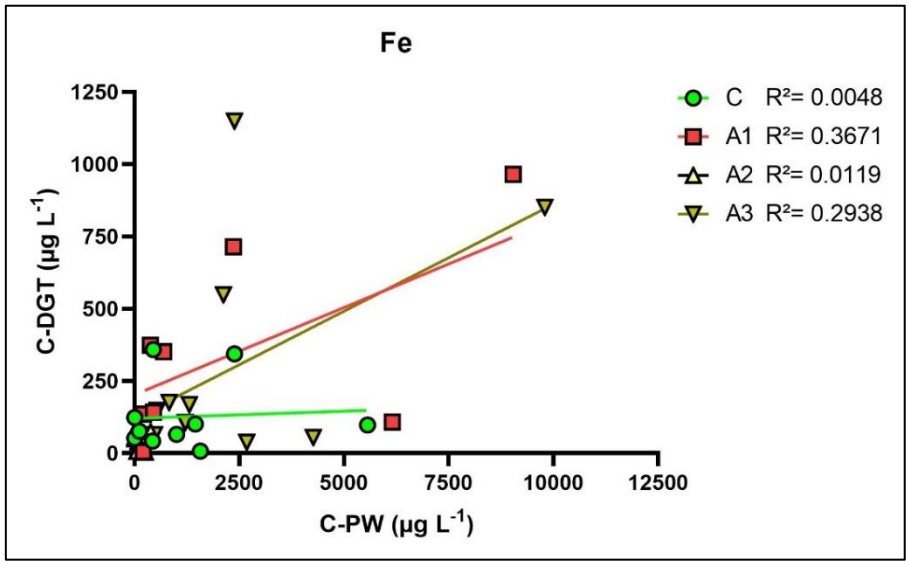

Figure 39: Fe concentrations measured by DGT (C-DGT) plotted against Fe concentrations measured in pore water (C-PW).

7.2.6 Manganese

Manganese analysed in pore water and analysed by using DGT was quantified in all samples of all sampling areas. The highest mean Mn concentration in pore water was observed in area A1 (C_{PW}= 100,807 ± 87,896 µg L^{-1}) (Figure 40). However, no statistical differences regarding C_{PW} were detected between the sampling areas (KW-test: H= 1.6; p= 0.65). Area A1 also showed the highest mean concentration for Mn measured by DGT (C_{DGT}= 5882 ± 3401 µg L^{-1}). Though, mean C_{DGT}-values of the other areas are close to this value and no statistical differences were observed between the sampling areas (One-factor ANOVA: F= 0.25; p=0.86). The mean R-values were very similar compared between the sampling areas with values between 14.8 ± 10.8 % (area A2) and 18.9 ± 21.4 % (area A3). Thus, no statistical differences were detected between the sampling areas (KW-test: H= 1.2; p=0.75). Resupply of Mn from the soil solid phase to the pore water was partially sustained in all sampling areas. The desorption rate of Mn from the soil solid phase to the pore water was extremely low in all sampling areas and just a small fraction of the Mn species in soil was labile and potentially environmentally bioavailable.

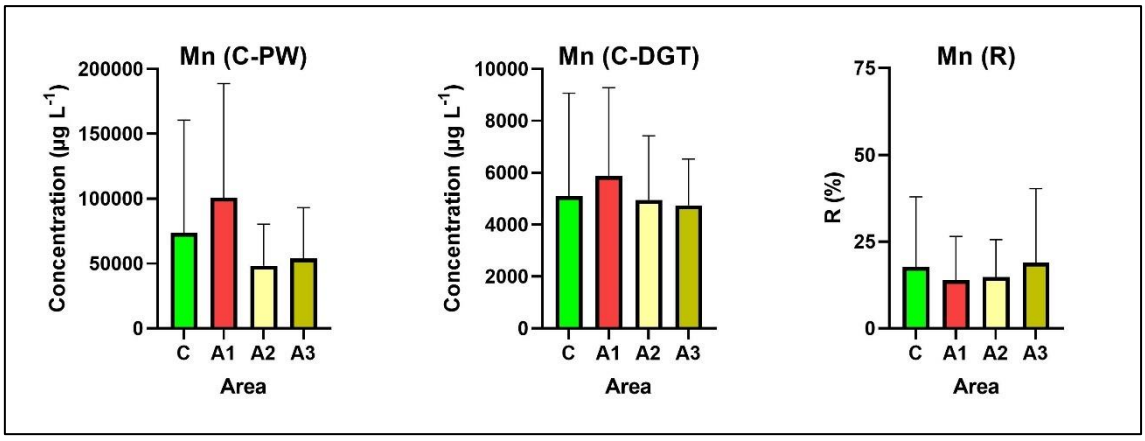

Figure 40: Bar charts for mean Mn concentrations measured in pore water (C-PW), Mn concentrations measured by DGT (C-DGT) and obtained R-values (R) for all sampling areas.

Moderate significant linear relationships could be detected between C_{PW} and C_{DGT} in area C, A1 and A2 (Figure 41). It is an indicator that fairly the same Mn pools in these sampling areas were assessed using pore water and DGT analysis. No significant correlation was detected between C_{PW} and C_{DGT} in area

A3. Here, probably different Mn pools were assessed with both analysis techniques.

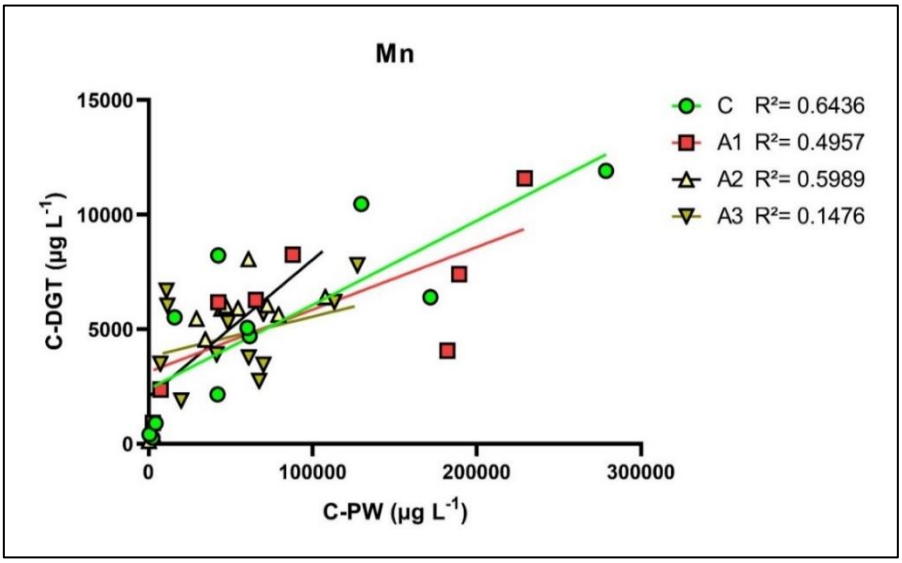

Figure 41: Mn concentrations measured by DGT (C-DGT) plotted against Mn concentrations measured in pore water (C-PW).

7.2.7 Aluminium

Aluminium in pore water could not be quantified in three samples in area C. For the other areas, Al in pore water was quantified in all samples. Using DGT, Aluminium could be quantified in all samples of all sampling areas. The highest mean Al concentration in pore water was observed in area A1 (C_{PW}= 20,253 ± 37,328 µg L^{-1}) (Figure 42). Mean Al concentration in pore water were significantly higher in area A1 than in area C (SNK-test: $p< 0.05$) and area A2 (SNK-test: $p< 0.01$). Furthermore, mean Al concentrations in pore water were significantly lower in area A2 than in area A3 (SNK-test: $p< 0.05$). Area A1 also showed the highest mean concentration for Al measured by DGT (C_{DGT}= 2166 ± 1808 µg L^{-1}). Here, C_{DGT}-values showed to be significantly higher in area A1 than in area A2 (SNK-test: $p< 0.01$). Furthermore, C_{DGT}-values in area A2 were significantly lower than in area C and area A3 (SNK-test: $p< 0.01$; $p< 0.01$, respectively). The mean R-values showed to be similar compared between the sampling areas with values between 38.4 ± 29.4 % (area A1) and 55.9 ± 36.8 % (area A2). Thus, no statistical differences were detected here (KW-test: H= 1.1; p=0.78). This indicates that the desorption rate of Al from the soil solid phase to the pore water was moderate in all sampling areas, and a considerable fraction of the Al species in soil was labile

and potentially environmentally bioavailable. Resupply of Al from the soil solid phase to the pore water was partially sustained in all sampling areas.

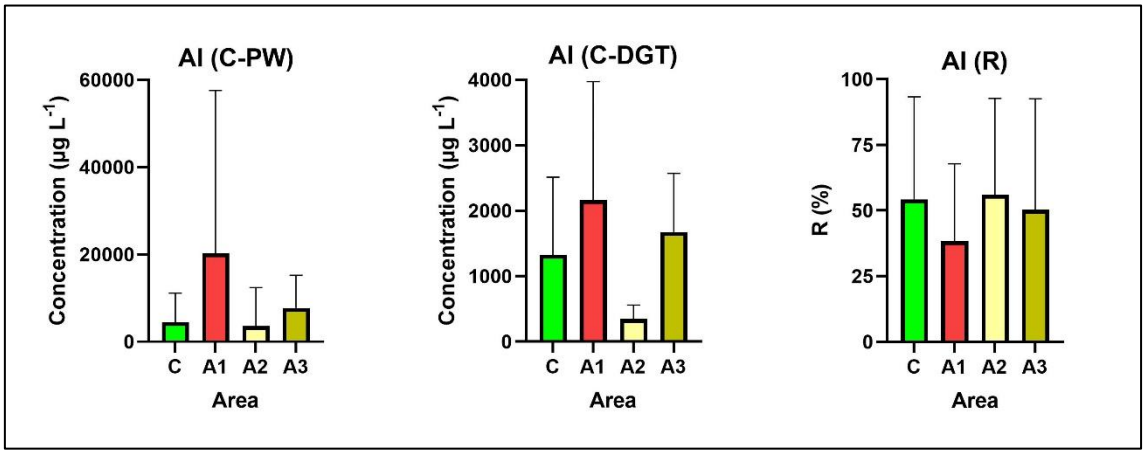

Figure 42: Bar charts for mean Al concentrations measured in pore water (C-PW), Al concentrations measured by DGT (C-DGT) and obtained R-values (R) for all sampling areas.

C_{PW}- and C_{DGT}-values were in a high significant linear relationship in area C (Figure 43). It seems that the same Al pools were assessed with the pore water analysis and DGT technique in this sampling area. However, no significant correlation was detected between C_{PW} and C_{DGT} in area A1, A2 and A3. Here, probably different Al pools were assessed with both analysis techniques.

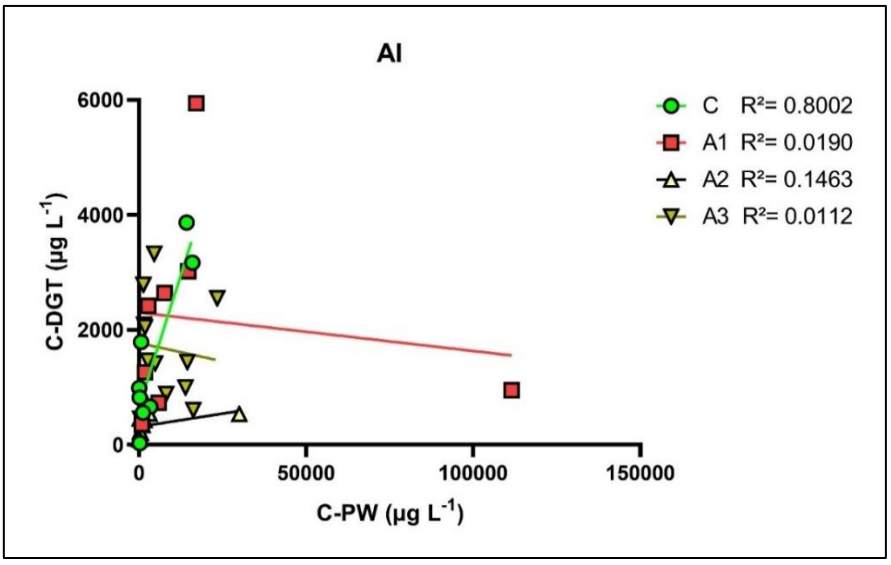

Figure 43: Al concentrations measured by DGT (C-DGT) plotted against Al concentrations measured in pore water (C-PW).

7.2.8 Copper

Copper in pore water could only be quantified in six samples from area C, in one sample from area A1, in none of 11 samples from area A2 and in 11 samples from area A3. Copper could only be quantified using DGT technique in seven samples from area C, in three samples from area A1, in two samples from area A2 and in 11 samples from area A3. Thus, descriptive statistics or calculation of R-values were not realized for areas A1 and A2. Mean concentrations of C_{PW} were similar in area C (C_{PW}= 3.3 ± 4.9 µg L^{-1}) and A3 (C_{PW}= 3.0 ± 3.1 µg L^{-1}) and no significant difference were detected (KW-test: H= 0.5; p= 0.46) (Figure 44). C_{DGT}-values in average were higher in area A3 (C_{DGT}= 0.6 ± 0.6 µg L^{-1}) than in area C (C_{DGT}= 0.3 ± 0.2 µg L^{-1}). However, no significant variances were observed between the two areas (KW-test: H= 1.2; p= 0.26). For area C, a mean R-value of 13.2 ± 2.1 % were obtained. As for area A3 a mean R-value of 26.0 ± 25.6 % were determined. This difference was not significant (KW-test: H= 2.1; p= 0.15). This fact indicates that the desorption rate of Cu released from the solid phase was low and just a minor part of the Cu species in relation to the accessible pool in soil was labile and potentially environmentally bioavailable in both sampling areas. However, this statement is questionable due to the low number of samples where Cu could be quantified.

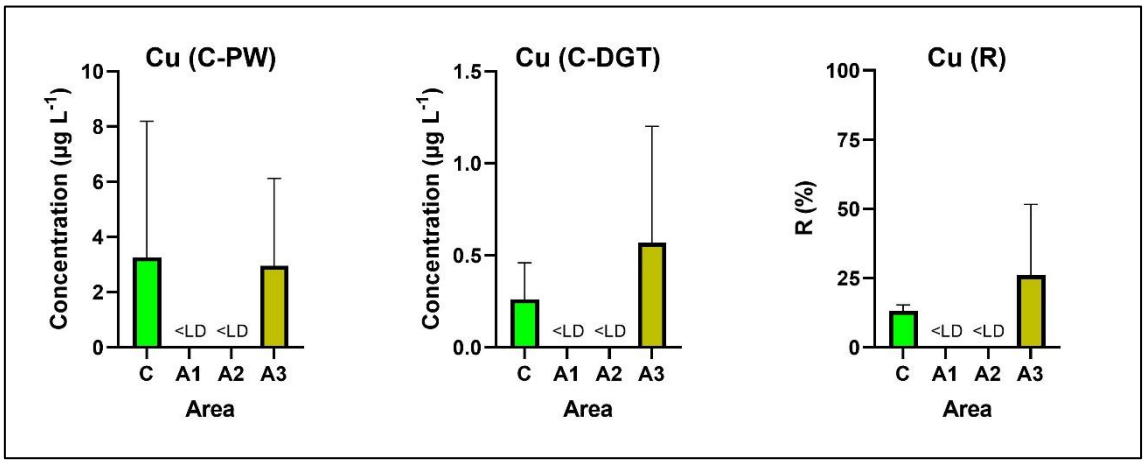

Figure 44: Bar charts for mean Cu concentrations measured in pore water (C-PW), Cu concentrations measured by DGT (C-DGT) and obtained R-values (R) for all sampling areas.

C_{PW}-values and C_{DGT}-values in area C and A3 showed a moderate linear relationship with R^2> 0.7 in both areas, which is not significant in area C and

significant in area A3 (Figure 45). Thus, probably mainly the same Cu pools were assessed with the pore water extraction by centrifugation and the DGT technique.

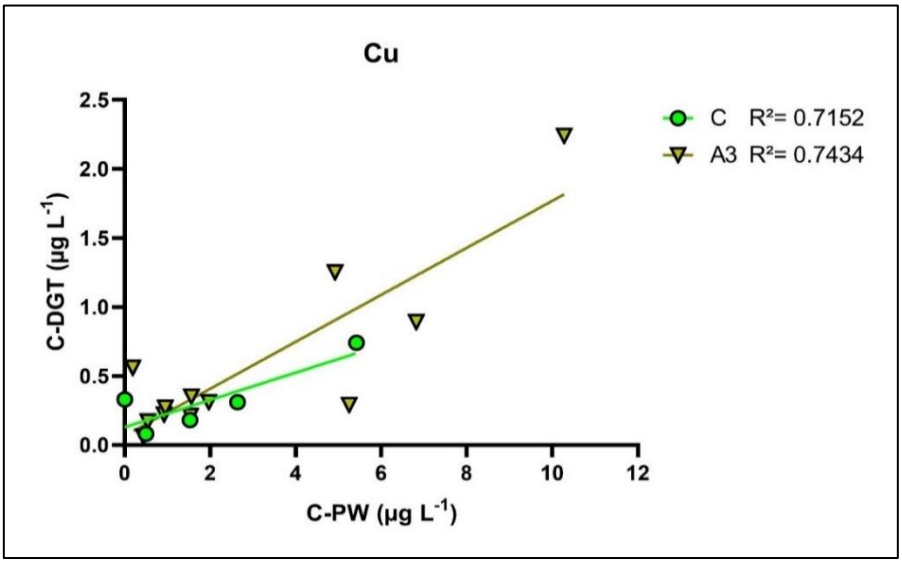

Figure 45: Cu concentrations measured by DGT (C-DGT) plotted against Cu concentrations measured in pore water (C-PW).

7.2.9 Nickel

The sample number of Ni quantified in pore water in area C was n= 5, for area A1 n= 6, for area A2 n= 6 and for area A3 n= 8. The sample number of Ni quantified using DGT in area C was n= 8, for area A1 n= 3, for area A2 n= 10 and for area A3 n= 11. Apparently, mean concentration for Ni in pore water was higher in area A1 than in the other sampling areas (C_{PW}= 78.3 ± 136.3 µg L^{-1}) (Figure 46). However, statistically no significant differences regarding C_{PW} were detected between the sampling areas (KW-test: H= 2.2; p=0.53). For the C_{DGT}-values, area A3 showed the highest mean concentration (C_{DGT}= 2.0 ± 2.6 µg L^{-1}). But also, no statistically significant differences regarding C_{DGT} were detected between the sampling areas (KW-test: H= 3.9; p= 0.28). Due to the low number of samples in area A1 in which Ni could be detected in pore water and by DGT, the R-value was not calculated for this area. Mean R-values were similar in all sampling areas ranging from R= 41.6 ± 38.9 % (area C) to R= 56.7 ± 28.4 % (area A3). These differences were also not significant (One factor ANOVA: F= 0.22; p=0.8). The R-values indicate that the desorption rate of Ni from the solid phase to the pore water was moderate in all sampling areas. Resupply of Ni from the soil solid

phase to the pore water was partially sustained in all sampling areas. Thus, a considerable fraction of the Ni species in all sampling areas in soil was labile and potentially environmentally bioavailable.

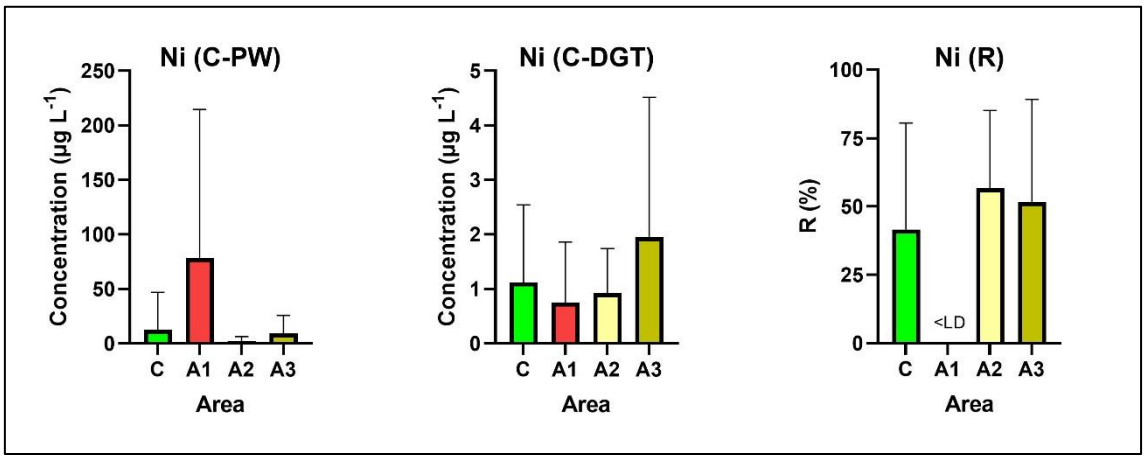

Figure 46: Bar charts for mean Ni concentrations measured in pore water (C-PW), Ni concentrations measured by DGT (C-DGT) and obtained R-values (R) for all sampling areas.

C_{DGT} and C_{PW} of Ni showed to be in a high significant linear relationship in area A2 and A3 (Figure 47). Here, apparently the same Ni pools were assessed with the pore water and DGT analysis. No significant correlation was obtained in area C and area A1. Probably, different Ni pools were assessed with the pore water extraction and DGT.

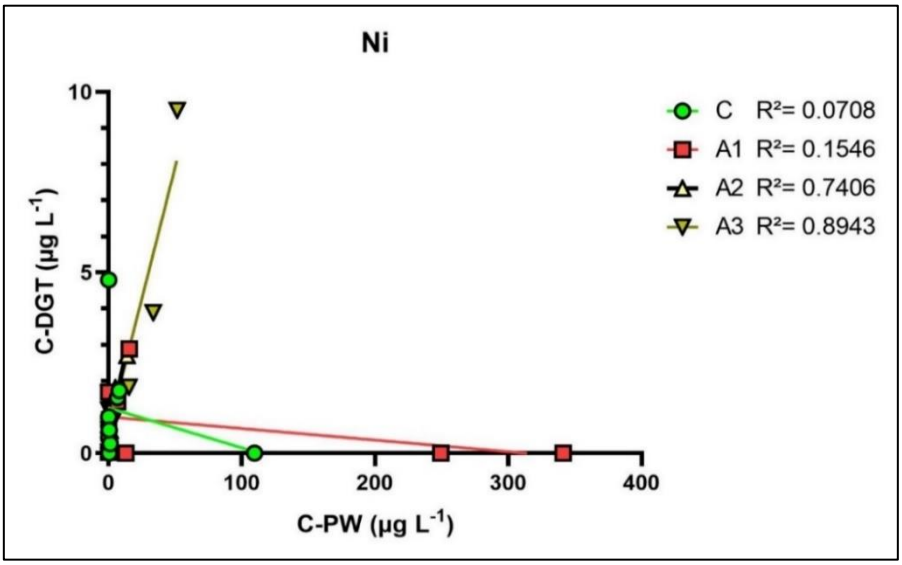

Figure 47: Ni concentrations measured by DGT (C-DGT) plotted against Ni concentrations measured in pore water (C-PW).

7.2.10 Discussion

Metal concentrations in pore water and metal concentrations measured by DGT in soil showed constantly very high relative standard deviations around or over 100% in all sampling areas for all elements. These variations were distinctively higher than compared to the variations of the total metal concentrations. This could hint to measurement variabilities in the techniques of the pore water and DGT analysis. However, C_{PW} and C_{DGT} correspond mainly well with each other with exception of Fe, Al and Ni in single sampling areas. Thus, it is more likely that desorption of metals from the soil matrix to the pore water is not ubiquitous in the sampling area. However, variations in metal concentrations measured by DGT are slightly lower than variations in metal concentrations in pore water, showing that DGT provides a more consistent measurement than the pore water analysis.

The AMD site of sampling area A1 showed significant higher C_{PW} values for the elements U, Pb and Al compared to the reference area (C). Furthermore, C_{DGT} values for the elements Pb and Zn were significantly higher in area A1 than area C. It is likely that AMD effluents caused a higher desorption rate of U and Al and raised the lability of Zn in soils in this sampling area. Total Pb concentrations in soil were also significantly higher in area A1 and A3 than in area C, so probably the C_{PW} and C_{DGT} values just mirror this trend. Area A2 showed high total concentrations of Fe and Al in soils. Surprisingly, C_{PW} and C_{DGT} values of these elements in area A2 were significantly lower than in the other sampling areas, indicating a mechanism for the depletion of labile Al and Fe in area A2.

Uranium is primarily transformed in soil by oxidation-reduction reactions that convert soluble U(VI) to insoluble U(IV). Reduction of U(VI) to U(IV) can occur as a result of microbial actions under anaerobic soil conditions, reducing the mobility and lability of U. However, the solubility and lability of U can be raised when complexing with inorganic or organic ligands. This can occur through the activity of microorganisms like *Thiobacillus ferrooxidans*. It can facilitate the oxidation of Fe^{2+} to Fe^{3+}. Then, Fe^{3+} ions can convert insoluble uranium dioxide to soluble UO_2^+. This reaction was described in soils of uranium mining and milling sites enhancing the lability of U (BARNES & COCHRAN, 1993; DE SILONIZ et al. 1991; ATSDR, 2013). Furthermore, Uranium can be removed from

pore water under sulphate reduction conditions influenced by microbial activity (BARNES & COCHRAN, 1993; ATSDR, 2013). The relatively high R-values as well as the good correlation between C_{PW} and C_{DGT} values of U in all sampling areas of the present study could indicate that a considerable fraction of the U in pore water consists of soluble UO_2^+.

The transport and lability of Pb in soils is influenced by the soil pH, the composition of the soil minerals, quantity and types of organic matter, presence of inorganic colloids and iron oxides. Lead is highly adsorbed on organic matter in soils. Furthermore, Pb can be immobilized by ion exchange with hydrous oxides or clay and as well by chelating with fulvic acids and humic substances in the soil. Also, inorganic Pb can be linked to crystalline matrices of rocks and remain immobile. The release of Pb from organic complexes is highly dependent on the soil pH. In soils with pH> 5 and a high organic matter content of > 5 %, Pb can form insoluble organic complexes. With soil pH conditions between 4 and 6, these organic complexes become soluble and labile and thus potentially bioavailable for plants (LIN et al., 1998; ATSDR, 2020; DE AZEVEDO & CHASIN, 2003). As latosols of the study site are acidic and low in organic matter, the high content of labile Pb in pore water with R> 70% in soils of all sampling areas can be explained. Concentrations of Pb in pore water and labile Pb in area A1 and A3 were significantly higher than in the reference area. However, the same trend was found regarding the total Pb concentrations. Thus, it is believed that AMD and mining activities had a possible impact on the enrichment of total concentrations of Pb in these areas, but not influenced the release mechanisms of labile Pb related to the total concentration in soil. As total Pb concentrations passed prevention values in a variety of samples and the labile Pb fraction in soils was very high, these areas need further attention as likely a considerable Pb fraction is environmentally bioavailable and thus has a potentially raised toxicity to soil organisms.

Zinc occurs naturally in the environment in the oxidation state of 2^+ (LINDSAY, 1979). It can form compounds with chlorine, oxygen, and sulphur. However, it is often found as ZnS in the nature (ATSDR, 1994). The mobility and lability of Zn in soils is highly dependent on the solubility of its compound, the soil pH and the soil solution salinity. Normally, Zn is absorbed strongly onto soil particulates. Thus, most of the Zn in soil is bound to the soil matrix and is not

dissolved in soil solution. However, in acidic soils with low pH, Zn is available in ionic forms and cation exchange processes influence its fate. Thus, Zn is more labile and bioavailable for plants in low soil pH conditions (DE AZEVEDO & CHASIN, 2003; ATSDR, 2005). This could explain the higher R-values found in the present study than compared to the reference studies, as the latosol soils in the study site have a low pH and a high presence of sulphur. Thus, a relatively higher fraction of labile Zn is present in the soils of the study site. Area A1 influenced by acid mine drainage showed significantly higher labile Zn concentrations than in the reference area and area A2. However, no differences regarding the total Zn concentrations in soil between these areas were detected. Therefore, it is very likely that the even more acidic conditions caused by AMD are responsible for a higher release of labile Zn in the pore water of soils from area A1 compared to the other sampling areas. Due to these findings, the area needs further attention as a high content of environmentally bioavailable Zn in soils is expected with higher potential of Zn toxicity to organisms.

Manganese in soil can be prevalent in many oxidation states in soils (0, II, III, IV, VI, VII). Divalent Mn is the most soluble species of Mn in soil and is thus the most bioavailable form of Mn in the soil. On the other hand, the solubility of Mn III and Mn IV in soil is very low. Mn oxides can form co-precipates with Fe oxides. Mn interacts both with cations and anions in oxidation-reduction reactions. These reactions are influenced by physical and chemical parameters as well as by microbiological processes (GUEST et al., 2002; BRADL, 2004; MILLALEO, 2010). In soils with low pH (<5.5) and increased redox potential, divalent Mn is predominant in the soil solution and Mn is mainly bioavailable. With increasing soil pH (up to pH 8), chemical Mn^{2+} auto-oxidation is favoured over $Mn0_2$, Mn_20_3, Mn_30_4 and even Mn_20_7, which are not normally available to plants. Furthermore, a higher soil pH leads to the adsorption of Mn to soil solid particles, decreasing the lability and bioavailability of Mn (ADRIANO, 2003; De AZEVEDO & CHASIN, 2003; ATSDR, 2005). R-values for Mn in the present study were relatively low and C_{PW} and C_{DGT} values of Mn correspond moderately with each other. This fact indicates that even in the acidic soils of the study site, a minor part of the Mn is divalent and the major fraction of Mn in pore water has an oxidation state of III or higher, which is less labile and less bioavailable.

The speciation of Co in soils depends on the nature of the soil, the soil pH, concentration chelating/complexing agents and the redox potential of the soil. Dissolved Co can be absorbed by ion exchange or form complexes with fulvic acids, humic substances or other organic ligands present in soils. Fulvic complexes with Co are not as stable compared to those of other metals. A low soil pH can result in the solubilization of precipitated cobalt and Co can be desorbed from the solid soil matrix. The presence of manganese oxides in the soil can lead to the oxidization of Co^{2+} to Co^{3+}, affecting the mobility and lability of Co (SMITH & CARSON, 1981; BRUSSEAU & ZACHARA, 1993, ATSDR, 2004). Total Co concentrations in soils of all sampling areas of the present study were very high passing prevention and intervention values in various samples. However, just a minor fraction of Co in pore water were accounted to be as labile by the R-value. Soils in the study site are rich in Mn and possibly rich in Mn oxides (with oxidation states of higher than III) in the soil solid matrix. This could be a reason that possibly a main part of Co in the soils is present as oxidation state of Co^{3+}, being immobilized in the soil matrix and mainly non-labile.

The mobilisation of Nickel in soils is also highly dependent on the soil pH. The major compounds of Ni are relatively soluble in pore water at soil pH< 6.5. Here, predominant solution species are likely Ni^{2+}, $NiSO_4$, and $NiHPO_4$. In pH> 6.7, Nickel mainly is present in insoluble forms like $Ni(OH)_2$ (SADIQ & ENFIELD, 1984; DE AZEVEDO & CHASIN, 2003; ATSDR, 2005). In sampling area A2 and A3, R-values for Ni were slightly over 50 % and C_{PW} corresponded very well with C_{DGT}. Thus, a considerable part of Ni in the pore water seemed to consist of labile Ni^{2+} and $NiSO_4$. An evaluation for the other sampling areas is difficult due to the low number of samples where Ni was detected by pore water and DGT analysis.

Most of the copper deposited in soils is absorbed in the upper 5-10 cm of the soil. The mobility of Cu is determined by physical and chemical interactions of copper with the soil components. In general, copper will adsorb to organic matter, carbonate minerals, clay minerals, or hydrous iron and manganese oxides. However, Cu binds strongly in soils with high organic contents and the soil pH has a lesser influence on the immobilization than it has on other metals. Though, when the content of organic matter is low, manganese and aluminium oxides are important adsorbents of Cu (DE AZEVEDO & CHASIN, 2003; ATSDR, 2004). The minor part of Cu in soils in the study site of the present study seemed

to be labile as indicated by the DGT measurements. As latosols are poor in organic matter, it is thus assumed that a major part of Cu in the soils of the study site is bound to manganese and aluminium oxides as well as clay minerals.

Aluminium is found in the soil mainly complexed with other anions, such as fluoride, sulphate, and phosphate. Soil acidification results in increased aluminium solubility. At moderately acidic levels (pH 5.5), aluminium appears as a cationic exchange initially as polynuclear hydroxide ions and, subsequently, as simple mononuclear ions. Most of the soluble forms of Al under acidic conditions is formed by non-silicate organic compounds bound to Al, with amorphous aluminium hydroxide being more soluble than crystalline forms (BODEK et al. 1988; DE AZEVEDO & CHASIN, 2003, ATSDR, 2008). Results of the present study suggest that about 50% of the Al in pore water in all sampling areas were labile. C_{PW} and C_{DGT} values did not correspond well in any sampling area. This could indicate that a great part of Al in the study site is bound to the soil minerals in form of fluoride, sulphate, and phosphates. On the other hand, a considerable part of Al seems to be soluble in pore water in form of Al^{3+}.

The oxidation state, whether iron (II) or iron (III), and the physical-chemical form determine the behaviour of Fe in the environment and its availability in the biota. The presence of dissolved organic matter (DOM) in soil solution has a large influence on the mobility and lability of Fe in soils (DE AZEVEDO & CHASIN, 2003). Fe(II) and Fe(III) can form very stable complexes with DOM by binding to multiple functional groups on one DOM molecule through coordination bonding. The creation of these strong complexes is believed to decrease the lability and bioavailability of Fe. The soil pH and redox potential of the soil are important factors (POHLMAN & MCCOLL, 1988; TAM & MCCOLL, 1991; STUMM & MORGAN, 1996). C_{PW} and C_{DGT} for Fe did not correspond well in all sampling areas of the present study. Furthermore, R-values are indicating that the minor part of Fe in pore water is labile. As organic matter is relatively low in the latosols of the study site, probably a considerable part of the Fe is immobilized in the clay minerals of the soil matrix, being responsible for the low mobility and lability of Fe.

7.3 Metal uptake in tree vegetation

7.3.1 Metal concentrations in tree core samples

Metal concentrations for every analysed tree core sample are demonstrated in Tables S11-S14 in the Supplementary Material. Mean concentrations and standard deviations for every sample area are shown in Table 6. For the calculation of these values, the concentrations which were below their respective analytical detection limit were considered as the analytical detection limit divided by two. In order to classify the results of the current study, obtained data was compared to data from the studies of Algreen et al. 2012 and Algreen et al. 2014. Though, these results have a limited function as comparative values as both studies were carried out under totally different climate, vegetation, soil and contamination conditions and fewer elements were analysed. The mentioned studies were realized in Norway and Denmark at sites contaminated by oil wastes as well as at dump, steel work and wood proofing facility sites. Tree species analysed in these studies were Populus sp. and Salix sp.

Table 6: Mean concentrations for elements determined in wood samples from all tree species for each sampling area.

	C			A1			A2			A3		
Element	**Mean**	**SD**	**n**	**Mean**	**SD**	**n**	**Mean**	**SD**	**n**	**Mean**	**SD**	**n**
U	<LD	<LD	0	5.6	9.2	2	<LD	<LD	0	3.7	4.5	2
Pb	26.0	20.0	7	31.4	18.2	8	90.5	157.7	10	100.1	108.0	10
Zn	1864.2	1799.4	9	985.9	867.5	8	1202.4	1296.4	10	1505.7	1028.4	11
Co	1.9	1.9	2	<LD	<LD	0	1.8	1.0	10	1.4	1.0	6
Fe	15023.0	17933.0	9	4486.8	4543.8	8	3767.6	2013.3	10	5436.4	4259.6	11
Mn	20530.9	26143.7	9	9665.3	6937.0	8	8190.8	6188.9	10	11893.3	8309.2	11
Al	1274.2	2753.7	4	324.0	363.5	3	254.0	133.1	8	123.4	71.7	1
Cu	258.3	358.2	9	103.5	97.5	8	95.4	28.0	10	109.5	59.8	10
Ni	17.4	23.0	5	80.9	161.5	7	<LD	<LD	0	6.7	7.7	5

The metals with the highest concentrations in wood samples in all sampling areas from the present study can be characterized with the following decreasing order: Mn> Fe> Zn> Al> Cu > Pb> Ni> Co.

Uranium was not detected in any of the sampled tree individuals in area C and area A2. In area A1 and A3, Uranium was detected in respectively two of the sampled tree individuals. Measured concentrations were slightly higher in area

A1. However, due to the low number of samples in which U was detected, a statistical comparison was not feasible.

Except for three tree individuals, Pb was quantified in all sampled tree individuals of all sampling areas. Mean concentrations of Pb were apparently higher in area A2 and A3 than in area C and A1. However, these differences were not significant (KW-test: H= 3.4; p= 0.33) as relative standard deviations in area A2 and A3 were remarkably high.

Zinc was quantified in all wood samples of all sampling areas. No statistically differences were detected between the sampling areas (One-factor ANOVA: F= 0.76; p= 0.53). Algreen et al. 2012 and Algreen et al. 2014 reported concentrations of Zn in wood samples obtained from *Populus sp.* and *Salix caprea* at contaminated sites in Denmark and Norway that were 10 times higher than in the present study. Though, total Zn concentrations in soils from these studies were not being exceedingly higher than Zn concentrations in soils from the present study. In Algreen et al. (2014), mean Zn concentrations in tree cores varied between 20.6 mg kg^{-1} and 25.3 mg kg^{-1} in unpolluted reference sites and varied between 19.4 mg kg^{-1} and 106 mg kg^{-1} in polluted test sites. In Algreen et al. (2012), mean Zn concentrations in tree cores varied between 15.0 mg kg^{-1} and 33.1 mg kg^{-1} in unpolluted reference sites, and between 24.7 mg kg^{-1} and 39.8 mg kg^{-1} in polluted test sites. In Pulford et al. (2001) even Zn concentrations over 200 mg kg^{-1} were measured in wood samples of *Salix sp.* on a sewage disposal site in the UK.

Cobalt could not be quantified in any wood sample from area A1 and just in two tree individuals from area C. However, the element was quantified in 10 tree individuals from area A2 and six tree individuals from area A3. Concentrations of Co in wood did not differ significantly between area A2 and A3 (KW-test: H= 0.38; p= 0.55).

Iron was quantified in all wood samples of all sampling areas. Area C showed apparently a higher mean Fe concentration in wood samples than the other sampling areas (C_{wood}= 15023 ± 17933 µg kg^{-1}). However, this mean concentration was raised by an exceedingly high outlier and differences between the sampling areas were not significant (KW-test: H= 6.5; p= 0.09).

Manganese was quantified in all wood samples of all sampling areas. Mean Mn concentration showed an apparently higher value than in the other

sampling areas (C_{wood}= 20531 ± 26144 µg kg^{-1}). Yet, the apparent differences with the other sampling areas were statistically not significant (KW-test: H= 1.5; p= 0.67).

Aluminium was quantified in most of the sampled tree individuals in area A2. However, in the other sampling areas, Al was quantified in just a few samples. The mean Al concentration did not differ significantly from each other between the sampling areas (KW-test: H= 5.0; p= 0.17).

Copper was quantified in nearly all sampled tree individuals of all sampling areas (except for one individual in area A3). The highest mean concentration of Cu in wood samples was detected in area C, though showing a very high standard deviation (C_{wood}= 258 ± 358 µg kg^{-1}). Mean Cu concentration in the other sampling areas were lower with lower variances within the areas. Differences of mean Cu concentrations in wood were not significant between the sampling areas (KW-test: H= 1.3; p= 0.7). In Algreen et al. (2014), mean Cu concentrations in tree cores varied between 1.11 mg kg^{-1} and 1.79 mg kg^{-1} in unpolluted reference sites, and between 0.43 mg kg^{-1} and 2.57 mg kg^{-1} in polluted test sites. In Algreen et al. (2012), mean Cu concentrations in tree cores varied between 1.33 mg kg^{-1} and 1.95 mg kg^{-1} in unpolluted reference sites, and between 1.66 mg kg^{-1} and 3.05 mg kg^{-1} in polluted test sites.

Nickel could not be quantified in any of the sampled tree individuals in area A2. In area A1, Ni was quantified in nearly all sampled tree individuals, except for one. Whereas in area C and A3, Ni was quantified in half of the sampled tree species, respectively. Area A1 showed an apparently higher mean concentration of Ni in wood samples than in the other sampling areas. However, this is due to an exceedingly high outlier in this area and differences between the sampling areas were not significant (KW-test: H= 5.7; p= 0.13). In Algreen et al. (2014), mean Ni concentrations in tree cores varied between 0.095 mg kg^{-1} and 0.51 mg kg^{-1} in unpolluted reference sites, and between 0.34 mg kg^{-1} and 0.74 mg kg^{-1} in polluted test sites.

7.3.2 Bioconcentration factors

The process of the accumulation of a substance in an organism in relation to the substance concentration in the external medium is called bioconcentration. The bioconcentration factor (BCF) is defined as the substance partition coefficient between the organism and its external medium in which the organism is exposed. Thus, the BCF describes the potential of an organism to accumulate a specific substance in a specific medium (PARAÍBA, 2007, PARAÍBA et al., 2010). In the present work, the BCF were derived from the average of the quotient from the metal concentration in wood samples and the respective total metal concentration in soil for every sampling area (Table 7). Zinc and manganese showed the highest BCF for all examined metals. Concentrations of these elements found in wood samples showed values between 1.25 % and 2.5 % of the total concentrations found in soil samples. These results distinguish Zn and Mn from the other metals whose BCF values were significantly lower showing values of concentrations in wood far below 1 % of the total concentrations in soil.

Table 7: Mean values BCF for every sampling area with their respective standard deviations (SD).

	C		A1		A2		A3	
	Mean	**SD**	**Mean**	**SD**	**Mean**	**SD**	**Mean**	**SD**
Pb	0.0012	0.0008	0.0004	0.0003	0.0010	0.0010	0.0026	0.0033
Zn	0.0250	0.0205	0.0126	0.0119	0.0122	0.0125	0.0159	0.0116
Co	0.0001	0.0001	<LD	<LD	0.00002	0.00001	0.00001	0.00001
Fe	0.0005	0.0007	0.00012	0.00012	0.00009	0.00004	0.00014	0.00011
Mn	0.0125	0.0090	0.0168	0.0190	0.0133	0.0142	0.0232	0.0172
Al	0.00003	0.00004	0.00001	0.000002	0.000002	0.000001	<LD	<LD
Cu	0.0095	0.0128	0.0038	0.0037	0.0038	0.0014	0.0044	0.0019
Ni	0.0005	0.0005	0.00172	0.003298	<LD	<LD	0.000293	0.000176

7.3.3 Relationship metal concentrations in wood vs. total metal concentrations in soil

The relationships between metal concentrations in wood (C_{wood}) and total metal concentrations in soil ($C_{tot.}$) were investigated calculating linear regression lines for every element and sampling area separately (Table 8). In the calculation, values under the analytical detection limit were considered as the actual value of the respective detection limit divided by two. If less than four sample pairs showed values over their actual detection, analysis of linear regression were not executed

for the respective sampling area as the representativeness would be highly questionable.

Table 8: Slopes of the linear regression between concentration in wood (C_{Wood}) and total metal concentration in soil ($C_{tot.}$) of all sampling areas, Y-intercepts of regression and coefficient of determination R^2 (in bold: significant).

	C			A1			A2			A3		
	Slope	**Y-int.**	**R²**	**Slope**	**Y-int.**	**R²**	**Slope**	**Y-int.**	**R²**	**Slope**	**Y-int.**	**R²**
Pb	0.00004	30	0.001	0.00009	24	0.01	0.002	-30	**0.463**	-0.001	201	0.27
Zn	-0.008	2380	0.02	-0.02	2943	0.12	0.013	-37	0.016	-0.043	5740	0.20
Co	-1E-05	3	0.02	-	-	-	2E-06	2	0.003	0.00001	-0.04	0.11
Fe	-0.0004	28050	0.02	-3E-05	5674	0.001	0.0002	-3304	0.351	-0.0001	11541	0.07
Mn	0.015	-1956	0.29	-0.006	13744	0.04	0.0003	7888	0.001	0.005	9356	0.01
Cu	0.029	-493	0.14	-0.002	147	0.01	-0.0001	99	0.001	0.006	-31	0.11
Ni	0.0006	-14	0.07	-0.003	337	0.13	-	-	-	2.4E-05	5	0.002

Slopes for all elements in all sampling areas showed low values (far below 1) and were even negative in several cases. Except for Pb in area A2, no significant regression could be detected between C_{wood} and $C_{tot.}$. Thus, C_{wood} and $C_{tot.}$ are mainly unrelated and the transfer of soil-to-plant is nonlinear considering the total metal concentration in soil. Similar results were obtained when all results were considered together without the separation in sampling areas (Table 9).

Table 9: Slopes of the linear regression between concentration in wood (C_{Wood}) and total metal concentration in soil ($C_{tot.}$) considering all tree individuals of all sampling areas together, Y-intercepts of regression and coefficient of determination R^2 (in bold: significant).

	All sampling areas			
	Slope	**Y-int.**	**R²**	**n**
Pb	0.0007	23	0.10	35
Zn	-0.0111	2418	0.02	37
Co	0.0000	2	0.02	27
Fe	-0.0003	20608	0.08	36
Mn	0.0062	6068	0.07	37
Al	-0.0001	9131	0.22	15
Cu	0.0061	-21	0.03	35
Ni	0.0001	32	0.00	21

In the regression analysis of Tables 8 and 9, no separation between the tree species were performed. However, these species belong to different families and orders in the taxonomy, and thus, are suspected to have different mechanisms of metal uptake and bioaccumulation. Hence, it was necessary to also perform a regression analysis for C_{wood} vs. $C_{tot.}$ considering all sampled

species separately. These results are demonstrated in Table S15 of the Supplementary Material. Here, notably the species *Alchornea triplinervia* showed increased values of R^2. A significant linear relationship between C_{wood} and $C_{tot.}$ was detected regarding the elements Pb and Mn for this species. For the case of Pb, a negative relationship was detected and a positive for Mn. No significant relationship was detected in the other tree species.

7.3.4 Relationship metal concentration in wood vs. labile metal concentrations in soil

The relationship between metal concentrations in wood (C_{wood}) and the labile metal concentrations in soil measured by DGT (C_{DGT}) was also investigated calculating linear regression lines for every element and sampling area separately (Table 10). As the labile metal species are considered to be environmentally available and thus possibly bioavailable for plants, a higher linear relationship was expected for C_{wood} vs. C_{DGT} than between C_{wood} and $C_{tot.}$. In the regression calculation, values under the analytical detection limit were also considered as the actual value of the respective detection limit divided by two. If less than four sample pairs showed values under their actual detection limit, analysis of linear regression were not executed for the respective sampling area.

Table 10: Slopes of the linear regression between concentration in wood (C_{Wood}) and concentration of labile metals in soil measured by DGT (C_{DGT}) of all sampling areas, Y-intercepts (Y-int.) of regression and coefficient of determination R^2 (in bold: significant).

	C			**A1**			**A2**			**A3**		
	Slope	**Y-int.**	**R^2**	**Slope**	**Y-int.**	**R^2**	**Slope**	**Y-int.**	**R^2**	**Slope**	**Y-int.**	**R^2**
Pb	-2.2	32	0.05	0.1847	30	0.001	12.8	37	0.07	-3.08	135	0.18
Zn	-8.9	2446	0.10	-5.357	1850	0.34	0.1	1196	0.00004	-1.49	1654	0.03
Co	-	-	-	-	-	-	-0.04	2	0.04	0.05	1	0.15
Fe	-6.2	15848	0.002	3.519	3258	0.07	36.6	2292	0.27	3.88	4262	0.12
Mn	1.7	11370	0.08	-0.1156	10345	0.00	0.7	4802	0.08	-1.74	20056	0.15
Cu	-354.9	330	0.02	-256.4	144	0.19	-	-	-	22.53	96	0.06

Slopes of regression lines of C_{wood} vs. C_{DGT} show distinctively higher values than slopes of regression lines of C_{wood} vs. $C_{tot.}$. However, various negative slopes are also present here. Values of R^2 were also exceptionally low and no significant relationship was recorded in any sampling area regarding all elements of interest. The same was the case for considering all sampling areas together

(Table 11). Thus, also the metal concentrations in wood and the labile metal concentrations in soil seem unrelated when no separation in tree species is realized. This is the case for both essential and toxic elements.

Table 11: Slopes of the linear regression between concentration in wood (C_{Wood}) and concentration of labile metals in soil measured by DGT (C_{DGT}) of all sampling areas together, Y-intercepts (Y-int.) of regression and coefficient of determination R^2 (in bold: significant).

	All areas, all tree individuals			
	Slope	**Y-int.**	**R^2**	**n**
Pb	-0.9	71	0.006	38
Zn	-3.1	1691	0.057	38
Co	-0.1	2	0.100	16
Fe	1.1	6844	0.001	38
Mn	0.8	8572	0.026	38
Al	0.1	953	0.002	15
Cu	-1.2	155	0.000	20
Ni	-2.9	27	0.005	10

The regressions of C_{wood} vs. C_{DGT} were also examined separately for every sampled tree species merging all sampling areas together (Table S16 in Supplementary Material). Noticeably, significant moderate linear relationships were detected for Fe, Mn and Zn in the species *Clethra scabra*. While Fe showed a positive relationship, Mn and Zn showed a negative relationship. This means that the higher the Fe labile concentration is in the soil, the higher the Fe concentration is in the wood samples of *Clethra scabra.* On the other hand, it is shown that the higher the labile Mn and Zn concentrations are in the soil, the lower are the Mn and Zn concentrations in wood samples of *Clethra scabra.*

7.3.5 Discussion

Manganese, iron, zinc and aluminium were the metals with the highest concentrations found in tree cores sampled in all sampling areas. Mn, Fe and Zn are three of the most important essential metals for plants as they play a beneficial role in plant growth and development. At optimum levels, these elements improve the nutrition levels of plants and are crucial for several mechanisms essential for growth and yield of plants. However, at highly increased concentration levels, these elements can show toxic effects on plants (ARIF et al., 2016). Considering the low total and labile Fe concentrations in soil,

as well as their low values of BCF in all sampling areas, it is excluded that these concentrations have toxic effects on the biota in soils of the study site. Total Zn concentrations in soil were elevated in every sampling area with a moderate percentage of labile Zn in pore water. Labile Zn concentrations were significantly higher in area AMD than in the other sampling areas. This trend was not mirrored by the Zn concentrations in wood and by the bioconcentration factors. However, bioconcentration factors of Zn, together with Mn, were by far the highest compared with the other elements. Considering the clearly elevated Zn concentrations in soil and wood, it is possible that these already have possible toxic effects on plants or soil organisms in the study area. Zinc is an essential element for plant growth. Absorption of Zn in plants is enzymatically regulated and big differences of Zn concentrations in wood between tree species were reported (HOLM et al., 2011). However, zinc phytotoxicity has been demonstrated on sites contaminated by mining wastes before (CHANEY, 1993). Zinc tends to be accumulated to a greater extent in roots. Here it interferes with root growth and elongation, thereby limiting plant uptake of water and nutrients (CASTIGLIONE et al.,2007; DISANTE et al., 2010; BEYER et al., 2013). Also, total Mn concentrations in soil were elevated compared to the quality reference value in all sampling areas. Considering this fact together with the high bioconcentrations factors found for Mn, potentially hazardous Mn levels could be present in the study site. For example, in its excess, Mn seems to be particularly damaging to the photosynthetic apparatus in plants (MUKHOPADHYAY & SHARMA, 1991).

The high total concentrations of Pb in soil with the high percentage of labile Pb in pore water gained attention especially in area A1 and A3, as Pb is one of the most toxic metals to plants and soil organisms. After entering the cells, Pb inhibits activities of many enzymes, upsets mineral nutrition and water balance, changes the hormonal status and affects membrane structure and permeability (SHARMA & DUBEY, 2005). Though, Pb showed moderate bioconcentration factors in wood between 0.0004 and 0.0025, it must be assumed that Pb levels in the soil of the study site cause toxic effects on the surrounding organisms, especially in area A1 and A3. It was reported that Pb tends to be immobilised and held primarily in the root system in various tree species. Roots have the ability to take up significant quantities of Pb whilst simultaneously greatly restricting its

translocation to above ground parts (LANE & MARTIN, 1977, PULFORD & WATSON 2003). Thus, Pb concentrations in wood not necessarily mirror the content of bioavailable Pb in the soil.

Cobalt is an essential element for plants as it is a crucial component of several enzymes and co-enzymes. However, exceeding Co concentrations can have toxic effects by inhibiting active ion transport in the plants. Toxic effects of Co on morphology are leaf fall, inhibition of greening, discoloured veins, premature leaf closure, and reduced shoot weight (PALIT et al., 1994). Total concentrations of Co in soils of the present study were in average remarkably high in every sampling area, passing prevention and even intervention values. However, the minor fraction of Co in soils seemed to be labile and bioconcentration factors of Co were exceptionally low in all sampling areas. It was reported that in higher plants, absorption of Co^{2+} by roots involves active transport. It is therefore questionable whether the measured total Co levels in soils in the present study cause toxic effects for the surrounding organisms.

In all sampling areas, uranium showed very high total concentrations in soil, as well as high concentrations in pore water with the major part very likely accounted as labile and possibly bioavailable UO_2^+. However, uranium in wood was just detected in two samples in area A1 and A3, respectively. Previous studies on different plant species showed that U mainly accumulates in the roots (LAROCHE et al. 2005; DOUSTALY et al. 2014). The study of Thiry et al. (2005) showed that 99.3 % of the U budget in *Pinus sylvestris* was stored in the root system. Furthermore, 97% of the U annual uptake returned to the soil through litterfall with the dominant fraction of the U ascending from roots to shoots passively through the xylem sap and steadily accumulating in the older foliage. It is very likely that also in case of the present study, nearly all bioavailable U was stored in the root system of the trees. Thus, U inside the wood samples could not be detected. However, this fact does not discard the possible phytotoxic effects of uranium stored in the roots. The exposure of U can cause physiological, biochemical, and molecular damage to plants and impact plant growth (GUPTA et al., 2019; VANDENHOVE et al., 2006).

It is known that Al absorbed by plants can inhibit root elongation severely (DELHAIZE & RYAN, 1995; IMADI et al. 2016). Total Al concentrations in the study site were elevated. However, the minor fraction of Al in pore water was

labile and bioconcentration factors in wood were extremely low. Thus, it is likely that Al levels in soils of the study site does not cause significant toxic effects on the biota.

Concentrations of Al, Co, Cu and Ni in wood were very low in relation to their total concentrations in soil. Furthermore, for all analysed elements, concentration in wood samples seemed to be mainly unrelated to total concentrations in soil and labile concentrations in pore water. The results agree with the findings of Algreen et al. (2014), McLaughlin et al. (2011) and Tuovinen et al. (2011). Here, it was reported that below a certain threshold, enzyme systems regulate essential metal uptake in the trees. If this threshold is passed, metals break through. This means that the respective metal concentrations in wood only correlate with the metal concentrations measured in the soil at spots with a highly elevated contamination. Furthermore, the mechanisms of the metal uptake by the tree roots must be considered. The roots act as buffer or barrier that regulate the uptake of phytotoxic metals or metalloids into the trees. This can be for instance due to the deposition of a thin layer of iron plaque on the exterior of the roots. The formation of this plaque layer is mainly from the oxidation of dissolved Fe^{2+} and has been known for a long time (GREEN & ETHERINGTON, 1977; ST-CYR & CAMPBELL, 1996). This plaque layer has also been detected on roots of plants at locations impacted by mine wastes as AMD often contains high concentrations of dissolved Fe (HANSEL et al. 2001). These facts also explain the findings that the significant differences of labile Pb and Zn in soils between the sampling areas were not mirrored in the concentrations measured in the wood samples. In order to realize an effective assessment of metal plant uptake in tree vegetation, it is therefore necessary to incorporate root and foliage analysis additionally to the tree coring analysis techniques.

Better results improving R^2 for regressions between C_{wood} vs. $C_{tot.}$ and C_{wood} vs C_{DGT} were obtained when tree species were observed separately. Significant linear relationships were detected for C_{wood} vs $C_{tot.}$ in the species *Alchornea triplinervia* regarding the element Mn and Pb. Regarding Pb, the regression slope was negative which means that with increasing Pb concentrations in the soil, the Pb concentrations in wood decreased. This observation could hint to a possible ability of phytoextraction of Pb by the species *Alchornea triplinervia*. Phytoextraction is the ability of plants to remove metals

from soils and to transport and concentrate them in their above-ground biomass (Nascimento & Xing, 2006). Root exudates in form of low-molecular weight organic acids play an important role in phytoextraction systems as they influence the acquisition of metals by either forming complexes with metal ions or decreasing the pH around the roots (NASCIMENTO & XING, 2006).

Observing the regression between C_{wood} vs. C_{DGT}, the tree species *Clethra scabra* showed significant negative linear relationships regarding the elements Mn and Zn. It is likely that through root exudates, the lability of Mn and Zn was reduced by forming complexes with organic acids followed by the accumulation of these complexes to the root system. This process is called phytostabilization (NASCIMENTO & XING, 2006). For the element Fe, the same species showed positive significant correlations between C_{wood} vs. C_{DGT}, showing that with an increased labile fraction of Fe in soil, Fe concentrations in wood samples are also increased. Thus, it seems that the species is able to predict the bioavailability of Fe in soils. However, all these assertions must be tested by analysing more tree individuals with a highly raised sample number for each species in different sampling areas with different contamination levels.

8 CONCLUSIONS

The present study represents one of the first applications of *Tree Coring* for the analysis of metals in the tropics and the southern hemisphere. For the first time, a comparison between DGT and *Tree Coring* was realized. The connection of the analysis of total metal concentration in soil, pore water analysis and DGT analysis of metals in soils gave a good insight about the pollution levels estimating the labile and potentially bioavailable fractions of the metals in the soils at the study site.

In all sampling areas, mean total concentrations of the elements U, Pb, Zn, Cu, Ni, Co, Mn and Mo in soils were explicitly higher than quality reference values for soils from Minas Gerais. The elements U, Pb, Co and Mo must be highlighted here as their concentrations even exceeded respective prevention and intervention values in various samples in all sampling areas. Pb, Ni, Co, Fe and Al showed significant higher total concentration in soils in area A1, A2 and A3 compared to the reference area, indicating an enrichment of these elements due

to the vicinity of acid mine drainage effluents and mining activities (e.g. redistribution through ore milling).

Study results suggest that labile concentrations of Zn in soils in area A1 are significantly higher than in the reference area, likely caused by the influence of AMD effluents in area A1. Highly labile fractions in soil together with high bioconcentration factors found in wood samples of the elements Mn, Pb and Zn indicate a high toxic potential of these elements to the biota in all sampling areas of the study site. The same is assumed for U, though this element barely could be quantified in wood samples as it is assumed that nearly all its bioavailable fraction was stored in the root system of the trees.

The comparison of the results from DGT and *Tree Coring* could not predict the uptake of metals into the xylems of the sampled tree individuals considering all sampled tree species together. Better results were obtained when tree species were observed separately. Significant linear relationships were detected for C_{wood} vs $C_{tot.}$ in the species *Alchornea triplinervia* regarding the elements Mn and Pb, and for C_{wood} vs C_{DGT} in the trees of species *Clethra scabra* regarding the elements Mn and Zn. The tree species *Alchornea triplinervia* seems to have the potential of phytoextraction of Pb from the soil. On the other hand, *Clethra scabra* seems to have the potential to predict bioavailability of Fe and to phyto-stabilize Mn and Zn in the rhizosphere. However, these assertions must be tested by analysing more tree individuals with a highly raised sample number for each species in different sampling areas with different contamination levels.

The combination of pore water and DGT analysis with *Tree Coring* showed to be a useful approach to measure metal pollution levels in soil and specify their risk for the environment. However, the use of *Tree Coring* technique was insufficient to evaluate the toxicological bioavailability of metals. In order to realize a more effective risk assessment of environmental and toxicological bioavailability of metals in soils, it is thus indicated to incorporate foliage and most importantly root analysis additionally to the suggested techniques.

9 REFERENCES

ABDEL-RAHMAN, M. A. E.; EL-MONGY, S. A. Ore Leashing Processing for Yellow Cake Production and Assay of their Uranium Content by Radiometric Analysis. **Journal of Inorganic and Organic Chemistry**, v. 644, p. 29-32, 2018.
ABEL, P. D. **Water Pollution Biology,** 2nd Edition**.** London: Taylor and Francis, 1996.

AKCIL, A.; KOLDAS, K. S. Acid Mine Drainage (AMD): Causes, treatment and case studies. **Journal of Cleaner Production**, v. 14, p. 1139-1146, 2006.

ADRIANO, D. C. **Trace Elements in Terrestrial Environments: Biogeochemistry, Bioavailability and Risks of Metals**, 2nd Edition. New York: Springer, 2003.

ADUMITROAEI, M. V.; IANCU, G. O.; RĂȚOI, B. G.; DORU, C. S.; SANDU, C. M. Spatial distribution and geochemistry of major and trace elements from Mohoș peatland, Harghita Mountains, Romania. **Holocene**, v. 28, 1936–1947, 2018.

AGBENIN, J. O.; WELP, G. Bioavailability of copper, cadmium, zinc, and lead in tropical savanna soils assessed by diffusive gradient in thin films (DGT) and ion exchange resin membranes. **Environmental Monitoring and Assessment**, v. 184, p. 2275–2284, 2012.

AGEITEC – AGÊNCIA EMBRAPA DE INFORMAÇÃO E TECNOLOGIA. **Latossolos Vermelho-Amarelhos**. Available at: https://www.agencia.cnptia.embrapa.br/gestor/solos_tropicais/arvore/CONT000g05ip3qr02wx5ok0q43a0r3t5vjo4.html. Accessed on 11th December of 2019.

ALBERTI, H. L. **Estudo hidroquímico e isotópico das águas subterrâneas impactadas pela drenagem ácida da mina de urânio - Osamu Utsumi, planalto de Poços de Caldas (MG)**. PhD thesis, Universidade Estadual de Campinas, 2017.

ALGREEN M.; REIN A.; LEGIND C. N.; AMUNDSEN C. E.; KARLSON U. G.; TRAPP S. Test of tree core sampling for screening of toxic elements in soils from a Norwegian site. **International Journal Phytoremediation**, v. 14(4), p. 305-319, 2012.

ALGREEN, M.; TRAPP, S.; REIN, A. Phytoscreening and phytoextraction of heavy metals at Danish polluted sites using willow and poplar trees. **Environmental Science and Pollution Research**, v.21, p. 8992-9001, 2014.

ARAIN, M. B.; KAZI, T. G.; JAMALI, M. K.; JALBANI, N.; AFRIDI, H. I. E.; SHAH, A. Total dissolved and bioavailable elements in water and sediment samples and their accumulation in *Oreochromis mossambicus* of polluted Manchar Lake. **Chemosphere**. V. 70, p. 1845-1856, 2008.

ARIF, N.; YADAV, V.; SINGH, S.; SINGH, S.; AHMAD, P.; MISHRA, R. K.; ... & CHAUHAN, D. K. Influence of high and low levels of plant-beneficial heavy metal ions on plant growth and development. **Frontiers in Environmental Science**, v. 4, p. 69, 2016.

ATSDR - AGENCY FOR TOXIC SUBSTANCES AND DISEASE REGISTRY. **Toxicological profile for cobalt**. U.S. Department of Health and Human Services, Public Health Service, Atlanta, GA, USA, 2004.

ATSDR - AGENCY FOR TOXIC SUBSTANCES AND DISEASE REGISTRY. **Toxicological profile for Copper**. U.S. Department of Health and Human Services, Public Health Service, Atlanta, GA, USA, 2004

ATSDR - AGENCY FOR TOXIC SUBSTANCES AND DISEASE REGISTRY. **Toxicological profile for Nickel**. U.S. Department of Health and Human Services, Public Health Service, Atlanta, GA, USA, 2005.

ATSDR - AGENCY FOR TOXIC SUBSTANCES AND DISEASE REGISTRY. **Toxicological profile for Aluminum**. U.S. Department of Health and Human Services, Public Health Service, Atlanta, GA, USA, 2008.

ATSDR - AGENCY FOR TOXIC SUBSTANCES AND DISEASE REGISTRY. **Toxicological profile for Uranium**.. U.S. Department of Health and Human Services, Public Health Service, Atlanta, GA, USA, 2013.

ATSDR - AGENCY FOR TOXIC SUBSTANCES AND DISEASE REGISTRY. 2020. **Toxicological profile for Lead**. U.S. Department of Health and Human Services, Public Health Service, Atlanta, GA, USA, 2020.

BARNES C. E.; COCHRAN J. K. Uranium geochemistry in estuarine sediments controls on removal and release processes. **Geochim Cosmochim Acta**, v. 57, p. 555-569, 1993.

BERTSCH, P. M.; HUNTER, D. B. Elucidating fundamental mechanisms in soil and environmental chemistry: The role of advanced analytical spectroscopic and microscopic methods. **Future prospects for soil chemistry**, v. 55, 1998.

BEYER, W. N.; GREEN, C. E.; BEYER, M.; CHANEY, R. L. Phytotoxicity of zinc and manganese to seedlings grown in soil contaminated by zinc smelting. **Environmental Pollution**, v. 179, p. 167-176, 2013.

BLUME, H.P.; BRUEMMER, G. Prediction of heavy metal behavior in soil by means of simple field tests. **Ecotoxicology and Environmental Safety**, v. 22, p. 164–174, 1991.

BMUB - GERMAN FEDERAL MINISTRY FOR THE ENVIRONMENT, NATURE CONSERVATION AND NUCLEAR SAFETY. **Federal soil protection and**

contaminated sites ordinance (Bundes-Bodenschutz- und Altlastenverordnung, BBodSchV), Berlin, Germany, 1999.

BODEK, I.; LYMAN, W.J.; REEHL, W.F.; et al. **Aluminum (Al). Environmental inorganic chemistry: Properties, processes, and estimation methods**. New York, NY: Pergamon Press, New York, 6.7-1 to 6.7-9, 1988.

BOLAN, N. S.; CHOPPALA, G.; KUNHIKRISHNAN, A.; PARK, J.; NAIDU, R. Microbial transformation of trace elements in soils in relation to bioavailability and remediation. **Reviews of environmental contamination and toxicology**, p. 1-56, 2013.

BRADL, H. Adsorption of heavy metal ions on soils and soils constituents. **J. Colloid. Interf Sci.**, v. 277, p. 1-18, 2004.

BRAND, E.; PEIJNENBURG, W.; GOENENBERG, B.; VINK, J.; LIJZEN, J.; TEN HULSCHER, D., et al. **Towards implementation of bioavailability measurements in the Dutch regulatory framework**. RIVM Report 711701084/2009, 2009.

BRUEMMER, G. W.; GERTH, J.; HERMS, U. Heavy metal species, mobility and availability in soils. **Journal of Plant Nutrition and Soil Science**, v. 149, p. 382–398, 1986.

BROWN, G.; FOSTER, A.; OSTERGREN, J. Mineral Surfaces and Bioavailability of Heavy Metals: A Molecular-Scale Perspective. **Proceedings of the National Academy of Sciences of the United States of America**, v. 96, p. 3388-3395, 1999.

BRUSSEAU M. L.; ZACHARA J. M. Transport of Co^{2+} in a physically and chemically heterogeneous porous medium. **Environmental Science & Technology**, v. 27, p. 1937-1939, 1993.

CASTIGLIONE, S.; FRANCHIN, C.; FOSSATI, T.; LINGUA, G.; TORRIGIANI, P.; BIONDI, S. High zinc concentrations reduce rooting capacity and alter metallothionein gene expression in white poplar (Populus albaL. cv. Villafranca). Chemosphere v. 67, p. 1117-1126, 2007.

CCME - Canadian Council of Ministers of the Environment. **Soil Quality Guidelines for the Protection of Environmental and Human Health**, 2007. http://st-ts.ccme.ca/en/index.html?chems=225&chapters=all. Accessed 10 September 2018.

CETESB - COMPANHIA DE TECNOLOGIA DE SANEAMENTO AMBIENTAL. **Áreas contaminadas**. 2002. Available at: http://www.cetesb.sp.gov.br/areas contaminadas/relacoes-de-areas-contaminadas/15-publicacoes. Accessed on 15 April 2018.

CETESB - COMPANHIA DE TECNOLOGIA DE SANEAMENTO AMBIENTAL. **USA Chemicals Ind. Com. Ltda – Campanhas de Amostragem de 2010. Informação técnica**. Agência Ambiental de Itu. CETESB, 2011.

CHANEY, R**. Zinc phytotoxicity**. In: Robson, A.D. (Ed.), Zinc in Soils and Plants: Proceedings of the International Symposium on Zinc in Soils and Plants, Held at the University of Western Australia, 27-28 September, 1993. Kluwer Academic Publishers, Dordrecht, the Netherlands, 1993.

CNA – CANADIAN NUCLEAR ASSOCIATION. **Uranium Mining**. Available at: https://cna.ca/technology/energy/uranium-mining/. Accessed on 23rd September of 2019.

COMMITTEE ON URANIUM MINING IN VIRGINIA; COMMITTEE ON EARTH RESOURCES; NATIONAL RESEARCH COUNCIL. **Uranium Mining in Virginia: Scientific, Technical, Environmental, Human Health and Safety, and Regulatory Aspects of Uranium Mining and Processing in Virginia**. Washington (DC): National Academies Press (US), 2011. (Available at: https://www.ncbi.nlm.nih.gov/books/NBK201030/)

CONAMA - COMPANHIA AMBIENTAL DO ESTADO DE SÃO PAULO. **Relatório à Diretoria nº 068/2016/E, de 21.11.2016 – Processo 95/2012/310 E**. 2016. Available at: https://www.cetesb.sp.gov.br/wp-content/uploads/2014/12/DD-256-2016-E-Valores-Orientadores-Dioxinas-e-Furanos-2016-Intranet.pdf. Accessed 20 May of 2019.

CONESA, H. M.; SCHULIN, R.; NOWACK, B. Suitability of using diffusive gradients in thin films (DGT) to study metal bioavailability in mine tailings: possibilities and constraints. **Environmental Science and Pollution Research**, v. 17, n. 3, p. 657-664, 2010.

COPAM - O Conselho Estadual de Política Ambiental. **Deliberação Normativa COPAM nº 166, de 29 de junho de 2011**. http://www.siam.mg.gov.br/sla/download.pdf?idNorma=18414. Accessed 20 May 2019.

DAVISON, W., ZHANG, H. In situ speciation measurement of trace components in natural waters using thin-film gels. **Nature**, v. 367, p. 546-548, 1994.

DE AZEVEDO, F. A.; CHASIN, A. A. D. M. **Metais - Gerenciamento da Toxicidade**. Editadora Atheneu, Brazil, 2003.

DEGRYSE, F.; SMOLDERS, E.; OLIVER, I.; ZHANG, H. Relating soil solution Zn concentration to diffusive gradients in thin films measurements in contaminated soils. **Environmental Science & Technology**, v. 37, n. 17, p. 3958-3965, 2003.

DEGRYSE, F.; SMOLDERS, E.; ZHANG, H.; DAVISON, W. Predicting availability of mineral elements to plants with the DGT technique: A review of experimental data and interpretation by modeling. **Environmental Chemistry**, v. 6, p. 198–218, 2009.

DELHAIZE, E.; RYAN, P. R. Aluminium toxicity and tolerance in plants. **Plant physiology**, v. 107, n. 2, p. 315, 1995.

DESAULES, A. Critical evaluation of soil contamination assessment methods for trace metals. **The Science of the Total Environment**, v. 426, p. 120–131, 2012.

DE SILONIZ M. I.; LORENZO P.; PERERA J. Distribution of oxidizing bacterial activities and characterization of bioleaching-related microorganisms in a uranium mineral heap. **Microbiologia**, v. 7, n. 2, p. 82-89, 1991.

DE SOUZA, J.; MENEGÁRIO, A. A.; DE ARAÚJO JÚNIOR, M. A. G.; FRANCIONI, E. Measurements of labile Cd, Cu, Ni, Pb, and Zn levels at a northeastern Brazilian coastal area under the influence of oil production with diffusive gradients in thin films technique (DGT). **Science of The Total Environment**, v. 500, p. 325-331 2014.

DGT RESEARCH LTD. **DGT - for measurements in waters, soils and sediments**. Lancaster, United Kingdom: DGT Research Ltd. p. 1–58, 2003.

DISANTE, K.; FUENTES, D.; CORTINA, J. Sensitivity to zinc of Mediterranean woody species important for restoration. **Science of the Total Environment**, v. 408, n. 10, p. 2216-2225, 2010.

DJINGOVA, R.; KULEFF, I.; MARKERT, B. Chemical fingerprinting of plants. **Ecological Research**, v. 19, n.1, p. 3-11, 2004.

DNPM - DEPARTAMENTO NACIONAL DE PRODUÇÃO MINERAL. **Economia Mineral do Brasil**, 2009. Available at: http://www.anm.gov.br/dnpm/publicacoes/serie-estatisticas-e-economia-mineral/outras-publicacoes-1/0-sumario-apresentacao-e-introducao. Accessed at 23rd September of 2019.

DOUSTALY, F.; COMBES, F.; FIEVET, J. B.; BERTHET, S.; HUGOUVIEUX, V.; BASTIEN, O.; ARANJUELO, I.; LEONHARDT, N.; RIVASSEAU C.; CARRIERE M.; VAVASSEUR A.; RENOU, J. P.; VANDENBROUCK, Y.; BOURGUIGNON J. Uranium perturbs signalling and iron uptake response in Arabidopsis thaliana roots. **Metallomics**, v. 6, p. 809–821, 2014.

ENE, A.; BOSNEAGA SION, A.; GEORGESCU, L. Determination of heavy metals in soils using XRF technique. **Romanian Journal of Physics**, v. 55, p. 815-820, 2010.

FANG, J.; WEN, B.; SHAN, X.Q.; Lin, J. M.; Owens, G. Is an adjusted rhizosphere-based method valid for field assessment of metal phytoavailability? Application to noncontaminated soils. **Environmental Pollution**, v. 150, p. 209–217, 2007.

FEAM - FUNDAÇÃO ESTADUAL DO MEIO AMBIENTE. **Mapa de solos do estado de Minas Gerais**. 1980. Available at: http://www.feam.br/banco-de-noticias/949-mapas-de-solo-do-estado-de-minas-gerais. Accessed 12 December 2019.

FERGUSSON, J. **The Heavy Elements: Chemistry, Environmental Impact and Health Effects**. Oxford: Pergamon Press, 1990.

FERNANDES, H. M.; FRANKLIN, M. R.; VEIGA, L. H. S.; FREITAS, P.; GOMIERO, L. A. Management of uranium mill tailing: Geochemical processes and radiological risk assessment. **Journal of Environmental Radioactivity**, v. 30, n. 1, p. 65-96, 1996.

FERNANDES H.M. **Subsídios ao descomissionamento da primeira indústria de mineração e beneficiamento de urânio no Brasil - O caso do Complexo Minero Industrial de Poços de Caldas – MG**. PhD thesis in Geosciences, Universidade Federal Fluminense. 1997.

FERNANDES, H. M.; FRANKLIN, M. R.; VEIGA, L. H. Acid rock drainage and radiological environmental impacts. A study case of the Uranium mining and milling facilities at Poços de Caldas. **Waste Management**, v. 18, n. 3, p. 169-181, 1998.

FERNANDES, H. M.; FRANKLIN, M. R. Assessment of acid rock drainage pollutants release in the uranium mining site of Poços de Caldas – Brazil. **Journal of Environmental Radioactivity**, v. 54, n.1 , p. 5-25, 2001.

FERRAZ, D.; POLESE, L.; PEDE, M. A. Z.; CHANG, H. K. Aplicação do método phytoscreening para determinação de hidrocarbonetos clorados em área tropical - Brasil – SP. **Águas Subterrâneas**, v. 31, n. 2, p. 74-88, 2017.

FERREIRA, D.; CIFFROY, P.; TUSSEAU-VUILLEMIN, M.-H.; BOURGEAULT, A.; Garnier, J.-M. DGT as surrogate of biomonitors for predicting the bioavailability of copper in freshwaters: an ex situ validation study. **Chemosphere**, v. 91, n. 3 , p. 241–247, 2013.

FOEFL - SWISS FEDERAL OFFICE OF ENVIRONMENT, FOREST AND LANDSCAPE. **Ordinance of 1 July 1998 on the Pollution of Soil (Verordnung ueber Belastungen des Bodens, VBBo)**. SR 814.01, Bern, Swiss 1998. Last amended on 1 June 2012.

FRAENKEL M. O.; SANTOS R. C.; LOUREIRO F. V. L.; MUNIZ W. S. Jazida de Urânio no Planalto de Poços de Caldas – Minas Gerais. **Principais depósitos minerais do Brasil**. NUCLEBRAS, Rio de Janeiro, 1:89-103, Anais. 1984.

FRANKLIN, M. R. **Modelagem numérica do escoamento hidrológico e dos processos geoquímicos aplicados à previsão da drenagem ácida em uma pilha de estéril da mina de urânio de Poços de Caldas – MG**. PhD thesis in Civil Engeneering, Universidade Federal do Rio de Janeiro, 2007.

GARY, L. T.; KOSSON, D. S.; ROCKNE, K. J.; SHOR, L. M. **Final Report: Bioavailability of organic contaminants in estuarine sediments to microbes and benthic animals.** 1999. Available at http://cfpub.epa.gov/ncer_abstracts/index.cfm/fuseaction/display.abstractDetail/abstract/160/report/F. Accessed 12 May 2018.

GOPALAKRISHNAN, G.; NEGRI, M. C.; MINSKER, B. S.; WERTH, C. J. Monitoring Subsurface Contamination Using Tree Branches. **Ground Water Monitoring & Remediation**, v. 27, n. 1, p. 65-74, 2007.

GREEN, M. S.; ETHERINGTON, J. R. Oxidation of Ferrous Iron by Rice (Oryza sativa L.) Roots: a Mechanism for Waterlogging Tolerance? **Journal of Experimental Botany**, v. 104, p. 678-690, 1977.

GRYSCHKO, R.; KUHNLE, R.; TERYTZE, K.; BREUER, J.; STAHR, K. Soil extraction of readily soluble heavy metals and As with 1 M NH_4NO_3-solution-evaluation of DIN 19730. **Journal of Soils and Sediments**, v. 5, p. 101–106, 2005.

GUEST, C.; SCHULZE, D.; THOMPSON, I.; HUBER, D. Correlating manganese X-ray absorption near-edge structure spectra with extractable soil manganese. **Soil Science Society of America Journal**, v. 66, p. 1172-1181, 2002.

GUPTA, D. K.; VUKOVIĆ, A.; SEMENISHCHEV, V. S. Uranium accumulation and its phytotoxicity symptoms in Pisum sativum L. **Environmental Science & Pollution Research**, v. 27, p. 3513–3522, 2020.

GWRTAC. **Remediation of metals-contaminated soils and groundwater**. Tech. Rep. TE-97-01, GWRTAC. Pittsburgh: GWRTAC-E Series, 1997.

HAN, F.; SHAN, X.; ZHANG, S.; WEN, B.; OWENS, G. Enhanced cadmium accumulation in maize roots - the impact of organic acids. **Plant and Soil**, v. 289, p. 355–368, 2006.

HANSEL, C. M.; FENDORF, S.; SUTTON, S.; NEWVILLE, M. Characterization of Fe plaque and associated metals on the roots of mine-waste impacted aquatic plants. **Environmental Science & Technology**, v. 35, n. 19, p. 3863-3868, 2001.

HARMSEN, J. Measuring Bioavailability: From a Scientific Approach to Standard Methods. **Journal of Environmental Quality**, v. 36, p. 1420-1428, 2007.

HOLM, O.; ROTARD, W.; TRAPP, S.; DÉSI, R. Arbeitshilfe zum Phytoscreening - Probenahme und chemische Untersuchung von Bohrkernen aus Bäumen zur Erkundung von Grundwasserschäden und Bodenbelastungen. **TASK - Terra-, Aqua- und Sanierungskompetenzzentrums**, 2011.

HOODA, P. S.; ZHANG, H.; DAVISON, W.; EDWARDS, A.C. Measuring bioavailable trace metals by diffusive gradients in thin films (DGT): soil moisture effects on its performance in soils. **European Journal of Soil Science**, v. 50, p. 285-294, 1999.

HOUBA, V. J. G.; LEXMOND, T. M.; NOVOZAMSKY, I.; VAN DER LEE, J. J. State of the art and future developments in soil analysis for bioavailability assessment. **The Science of the Total Environment**, v. 178, p. 21–28, 1996.

HUND-RINKE, K.; KOERDEL, W. Underlying issues in bioaccessibility and bioavailability: Experimental methods. **Ecotoxicology and Environmental Safety**, v. 56, p, 52–62, 2003.

IAC - INSTITUTO AGRONÔMICO. **Solos do Estado de São Paulo**. Available at: http://www.iac.sp.gov.br/solossp/pdf/Latossolos.pdf. Accessed 11 December of 2019.

IAEA – INTERNATIONAL ATOMIC ENERGY AGENCY. **Radioactive Waste Management – Status and Trends**. Issue 4, 2005.

IBGE - INSTITUTO BRASILEIRO DE GEOGRAFIA E ESTATÍSTICA. **Mapas de Bioma Brasil,** 2004.

IMADI, S. R.; WASEEM, S.; KAZI, A. G.; AZOOZ, M. M.; AHMAD, P. Aluminum toxicity in plants: an overview. **Plant Metal Interaction**, p. 1-20, 2016.

INAP - International Network for Acid Prevention. **Diffusive gradients in thin-films (DGT): A technique for determining bioavailable metal concentrations**. 2002. Available at: http://www.inap.com.au. Accessed 20 December 2017.

INB – INDÚSTRIAS NUCLEARES DO BRASIL. **Estudo Florístico e Fitossiológico**. Projeto de Drenagem Superficial – INB. Caldas (MG), 2015.

INB – INDÚSTRIAS NUCLEARES DO BRASIL **http://www.inb.gov.br/**. Accessed on 12 November 2018.

IUPAC - INTERNATIONAL UNION OF PURE AND APPLIED CHEMISTRY. **Glossary of terms used in physical organic chemistry (IUPAC Recommendations 1994)**, v. 66, p. 1077, 1994.

ISO – INTERNATIONAL ORGANISATION FOR STANDARDIZATION. **17402. Soil quality—requirements and guidance for the selection and application of methods for the assessment of bioavailability of contaminants in soil and soil materials**. Geneva, Switzerland, 2008.

IVANAUSKAS, N. M.; DE ASSIS, M. C. **Formações florestais brasileiras**. In: MARTINS, S. V. (Ed.). Ecologia de florestas tropicais do Brasil. Viçosa: Editora UFV, p. 74-108, 2009.

JOHNSON D. B. Chemical and microbiological characteristics of mineral spoils and drainage waters at abandoned coal and metal mines. **Water Air & Soil Pollution**, v. 3, p. 47–66, 2003.

JOHNSON, D. B.; HALLBERG, K. B. Acid mine drainage remediation options: a review. **Science of the Total Environment**, v. 338, p. 3-14, 2005.

KABATA-PENDIAS, A. **Trace elements in soils and plants**, 4th Edition. London, New York: CRC Press, 2011.

KIM, R. Y.; YOON, J. K.; KIM, T. S.; YANG, J. E.; OWENS, G.; KIM, K. R. Bioavailability of heavy metals in soils: definitions and practical implementation - a critical review. **Environmental Geochemistry and Health**, v. 37, n. 6, p. 1041-1061, 2015.

KIRPICHTCHIKOVA, T. A.; MANCEAU, A.; SPADINI, L.; PANFILI, F.; MARCUS, M. A.; JACQUET, T. Speciation and solubility of heavy metals in contaminated soil using X-ray microfluorescence, EXAFS spectroscopy, chemical extraction, and thermodynamic modeling. **Geochimica et Cosmochimica Acta**, v. 70, n. 9, p. 2163–2190, 2006.

KOSTER, M.; REIJNDERS, L.; VAN OOST, N.R.; PEIJNENBURG, W. J. Comparison of the method of diffusive gels in thin films with conventional extraction techniques for evaluating zinc accumulation. **Environmental Pollution**, v. 133, p. 103–116, 2005.

LANE, S. D.; MARTIN, E.S. A histochemical investigation of lead uptake in Raphanus sativus. **New Phytologist**, v. 79, n. 2, p. 281-286, 1977.

LANNO, R.; WELLS, J.; CONDER, J.; BRADHAM, K.; BASTA, N. The bioavailability of chemicals in soil for earthworms**. Ecotoxicology and Environmental Safety**, v. 57, p. 39–47, 2004.

LARSEN, M.; BURKEN, J.; MACHACKOVA, J.; GOSEWINKEL KARLSON, U.; TRAPP, S. Using Tree Core Samples to Monitor Natural Attenuation and Plume Distribution After a PCE Spill. **Environmental Science & Technology**, v. 42, n. 5, p. 1711-1717, 2008.

LAROCHE, L.; HENNER, P.; CAMILLERI, V.; MORELLO, M.; GARNIER-LAPLACE, J. Root uptake of uranium by a higher plant model (*Phaseolus vulgaris*) bioavailability from the soil solution. **Radioprotection**, p. 40, v. 33–39, 2005.

LEHTO, N.; DAVISON, W.; ZHANG, H.; TYCH, W. Theoretical comparison of how soil processes affect uptake of metals by diffusive gradients. **Journal of Environmental Quality**, v. 35, p. 1903–1913, 2006.

LIN, Z.; HARSBO, K.; AHLGREN, M.; QVARFORT, U. The source and fate of Pb in contaminated soils at the urban area of Falun in central Sweden. **Science of the Total Environment**, v., 209, n. 1, p. 47-58, 1998.

LINDSAY W.L. Inorganic equilibria affecting micronutrients in soils. **Micronutrients in agriculture**, v. 4, p. 89-112, 1991.

LING, W.; SHEN, Q.; GAO, Y.; GU, X.; YANG, Z. Use of bentonite to control the release of copper from contaminated soils. **Australian Journal of Soil Research**, v. 45, n. 8, p. 18–623, 2007.

LUOMA, S. N.; RAINBOW, P. S. **Metal contamination in aquatic environments: science and lateral management**. Cambridge: Cambridge University Press, p. 573, 2008.

MACHOLZ, R. M.; KAISER, D. B.; KOERDEL, W.; HUND-RINKE, K.; DERZ, K.; BERNHARDT, C. **Evaluation of existing assessment approaches and development of a concept for the integrated assessment of the effects of priority pollutants across all pathways on the basis of their bioavailability**. Text 59. Berlin: Umweltbundesamt, 2011.

MAIZ, I.; ARAMBARRI, I.; GARCIA, R.; MILLÁN, E. Evaluation of heavy metal availability in polluted soils by two sequential extraction procedures using factor analysis. **Environmental Pollution**, v. 110, n. 1, p. 3-9, 2000.

MCLAUGHLIN, M. J.; ZARCINAS, B. A.; STEVENS, D. P.; COOK, N. Soil testing for heavy metals. **Communications in Soil Science and Plant Analysis**, v. 31, n. 11–14, p. 1661–1700, 2000.

MCLAUGHLIN, M. J.; SMOLDERS, E.; DEGRYSE, F.; RIETRA, R. Uptake of metals from soil into vegetation. In: Swartjes, F. (ed) **Dealing with Contaminated Sites. From Theory towards Practical Application**. Dordrecht: Springer, pp 325–367, 2011.

MEERS, E.; SAMSON, R.; TACK, F. M. G.; RUTTENS, A.; VANDEGEHUCHTE, M.; VANGRONSVELD, J.; VERLOO, M. G. Phytoavailability assessment of heavy metals in soils by single extractions and accumulation by Phaseolus vulgaris. **Environmental and Experimental Botany**, v. 60, p. 385–396, 2007.

MEMOLI, V.; EYMAR, E.; GARCÍA-DELGADO, C.; ESPOSITO, F.; PANICO, S. C.; MARCO, A. D.; BARILE, R.; MAISTOA, G. Soil element fractions affect phytotoxicity, microbial biomass and activity in volcanic areas. **Science of the Total Environment**, v. 636, p. 1099–1108, 2018.

MENEGÁRIO A. A.; M. YABUKI, L. N.; S. LUKO, K.; WILLIAMS, P. N.; BLACKBURN, D. M. Use of diffusive gradient in thin films for in situ measurements: A review on the progress in chemical fractionation, speciation and bioavailability of metals in waters. **Analytica Chimica Acta**, v. 983, p. 54-66, 2017.

MENZIES, N. W.; DONN, M. J.; KOPITTKE, P. M. Evaluation of extractants for estimation of the phytoavailable trace metals in soils. **Environmental Pollution**, v. 145, p. 121–130, 2007.

MILLALEO, R.; REYES-DÍAZ, M.; IVANOV, A.G.; MORA, M. L.; ALBERDI, M. Manganese as essential and toxic element for plants: transport, accumulation and resistance mechanisms. **Journal of soil science and plant nutrition**, v. 10, n. 4, p. 470-481, 2010.

MITTERMEIER, R. A.; GIL, P. R.; HOFFMAN, M.; PILGRIM, J.; BROOKS, T.; MITTERMEIER, C. G.; ... & SALIGMANN, P. A. Hotspots revisited: earth's biologically richest and most endangered terrestrial ecoregions cemex. Mexico City, 2004.

MORRISSEY, C. **Mining's malignant menace**. Review Magazine, 6 St James' Square, London: Rio Tinto, v. 68, 2003.

MOUSAVI, S. M.; BAHMANYAR, M. A.; PIRDASHTI, H. Phytoavailability of some micronutrients (Zn and Cu), heavy metals (Pb, Cd), and yield of rice affected by sewage sludge perennial application. **Communications in Soil Science and Plant Analysis**, v. 44, p. 3246–3258, 2013.

MUKHOPADHYAY M.; SHARMA, A. Manganese in cell metabolism of higher plants. **The Botanical Review**, v. 57, p. 117-149, 1991.

MUNDUS, S.; LOMBI, E.; HOLM, P. E.; ZHANG, H.; HUSTED, S. Assessing the plant availability of manganese in soils using diffusive gradients in thin films (DGT). **Geoderma**, v. 183–184, p. 92–99, 2012.

NAGAJYOTI, P. C.; LEE, K. D.; SREEKANTH, T. V. M. Heavy metals, occurrence and toxicity for plants: a review. **Environmental Chemistry Letters**, v. 8, p. 199-216, 2010.

NASCIMENTO, C. W. A.; XING, B. Phytoextraction: a review on enhanced metal availability and plant accumulation. **Scientia Agricola**, v. 63, n. 3, p. 299-311, 2006.

NIELSEN, M. A.; TRAPP, S. Tree Coring as an initial screening tool for typical pollutants in the subsurface. **Tailored Improvement of Brownfield Regeneration in Europe**. Kopenhagen: Technical University of Denmark, 2014.

NÓBREGA, F. A; LIMA, H. M; LEITE, A. L. Análise de múltiplas variáveis no fechamento de mina - Estudo de caso da pilha de estéril BF-4, Mina Osamu Utsumi, INB Caldas, Minas Gerais. **REM: Revista Escola de Minas**, v. 61, n. 2, p. 197-202, 2008.

NOLAN, A. L.; ZHANG, H.; MCLAUGHLIN, M. J. Prediction of zinc, cadmium, lead, and copper availability to wheat in contaminated soils using chemical speciation, diffusive gradients in thin films, extraction, and isotopic dilution techniques. **Journal of Environmental Quality**, v. 34, p. 496–507, 2005.

NRC COMMITTEE - NATIONAL RESEARCH COUNCIL COMMITTEE ON BIOAVAILABILITY OF CONTAMINANTS IN SOILS AND SEDIMENTS. **Bioavailability of contaminants in soils and sediments: Processes, tools, and applications**. Washington, DC: The National Academic Press, 2003.

ORLOWSKI, N.; PRATT, D.; MCDONNELL, J. Intercomparison of soil pore water extraction methods for stable isotope analysis. **Hydrological Processes**, v. 30, n. 19, 2016.

PALIT, S.; SHARMA, A.; TALUKDER, G. Effects of cobalt on plants. **The Botanical Review**, v. 60, p. 149–181. 1994.

PANAGOS, P.; VAN LIEDEKERKE, M.; YIGINI, Y.; MONTANARELLA, L. Contaminated Sites in Europe: Review of the Current Situation Based on Data Collected through a European Network. **Journal of Environmental and Public Health**, Article ID 158764, 2013.

PARAÌBA, L.C. Pesticide bioconcentration modelling for fruit trees. **Chemosphere**, v. 66, n. 8, 2007.

PARAÍBA, L. C.; QUEIROZ, S. C. N.; MAIA, A. D. H. N.; FERRACINI, V. L. Bioconcentration factor estimates of polycyclic aromatic hydrocarbons in grains of corn plants cultivated in soils treated with sewage sludge. **Science of The Total Environment**, v. 408, n. 16, 2010.

PASCUCCI, S. **Soil Contamination**. Rijeka: InTech, 2011.

PÉREZ, D.V.; DA COSTA SALDANHA, M.F.; MOREIRA, J.C.; VAITSMAN, D.S. Concentração total de urânio e tório em alguns solos brasileiros. Pesquisa Agropecuária Brasileira, v. 33, n. 8, p. 1417-1423, 1998.

POHLMAN, A.A., MCCOLL, J.G. Soluble organics from forest litter and their role in metal dissolution. **Soil Science Society of America Journal**, v. 52, p. 265-271, 1988.

PRICE, H. L.; TEASDALE, P. R.; JOLLEY, D. F., An evaluation of ferrihydrite- and Metsorb™-DGT techniques for measuring oxyanion species (As, Se, V, P): Effective capacity, competition and diffusion coefficients. **Analytica Chimica Acta**, v. 803, p. 56-65, 2013.

PUEYO, M.; LÓPEZ-SÁNCHEZ, J. F.; RAURET, G. Assessment of $CaCl_2$, $NaNO_3$ and NH_4NO_3 extraction procedures for the study of Cd, Cu, Pb and Zn extractability in contaminated soils. **Analytica Chimica Acta**, v. 504, p. 217–226, 2004.

PULFORD, I.D.; WATSON, C.; MCGREGOR, S.D. Uptake of chromium by trees. Prospects for phytoremediation. **Environmental Geochemistry & Health**, v. 23, p. 307-311, 2001.

PULFORD, I.D.; WATSON, C. Phytoremediation of heavy metal-contaminated land by trees — a review. **Environment International**, v. 29, n. 4, p. 529-540, 2003.

QUI, H.; GU, H.; HE, E.; WANG, S.; QUI, R. Attenuation of Metal Bioavailability in Acidic Multi-Metal Contaminated Soil Treated with Fly Ash and Steel Slag. **Pedosphere**, v. 22, n. 4, p. 544-553, 2012.

RIEUWERTS, J. S.; THORNTON, I.; FARAGO, M. E.; ASHMORE, M. R. Factors influencing metal bioavailability in soils: Preliminary investigations for the development of a critical load approach for metals. **Chemical Speciation and Bioavailability**, v. 10, p. 61–75, 1998.

ROBERTS, D.; NACHTEGAAL, M.; SPARKS, D. L. **Speciation of metals in Soils**. In: Chemical Processes in Soils, Madison: SSA Book Series, n. 8, 2005.

SADIQ M.; ENFIELD C.G. Solid phase formation and solution chemistry of nickel in soils. 2. **Experimental. Soil Sci.**, v. 138, p. 335-340, 1984.

SCHALLER, C. **Ligand Field and Lability**. 2019. Available at: https://chem.libretexts.org/Bookshelves/Inorganic_Chemistry/Modules_and_Websites_(Inorganic_Chemistry)/The_Organometallic_Reader_(Michael_Evans)/Ligand_Binding_in_Coordination_Complexes/CC10._Ligand_Field_and_Lability. Accessed 12 September 2019.

SALAM, A. K.; HELMKE, P. A. The pH dependence of free ionic activities and total dissolved concentrations of copper and cadmium in soil solution. **Geoderma**, v. 83, p. 281– 291, 1998.

SCHULZE, D. G.; Bertsch, P. M. Synchrotron X-ray techniques in soil, plant, and environmental research. **Advances in agronomy**, v. 55, p. 1-66, 1995.

SHARMA, P.; DUBEY, R. S. Lead toxicity in plants. **Brazilian Journal of Plant Physiology**, v. 17, n. 1, p. 35-52, 2005.

SHOR, L.M.; KOSSON, D.S. **Bioavailability of organic contaminants in soils**. In: VALDES, J.J. (Ed.), Bioremediation. (pp. 15–43). Amsterdam: Kluwer Academics Publishers, 2000.

SMITH I. C.; CARSON B. L. **Trace metals in the environment**. Ann Arbor Science Publishers, Ann Arbor, MI, USA, 1981.

SOREK, A.; ATZMON, N.; DAHAN, O.; GERSTL, Z.; KUSHISIN, L.; LAOR, Y.; MINGELGRIN, U.; NASSER, A.; RONEN, D.; TSECHANSKY, L.; WEISBROD, N.; GRABER, E. R. “Phytoscreening": the use of trees for discovering subsurface contamination by VOCs. **Environmental Science & Technology**, v. 42, n. 2, p. 536-542, 2008.

SOUZA, A. M; SILVEIRA, C. S.; PEREIRA, R. M. Contribuições dos metais provenientes das pilhas de rejeito da mina Osamu Utsumi a drenagens do Complexo Alcalino de Poços de Caldas, Minas Gerais. **Geochimica Brasiliensis,** v. 27, n. 1, p. 63-76, 2013.

ST-CYR, L.; CAMPBELL, P. G. Metals (Fe, Mn, Zn) in the root plaque of submerged aquatic plants collected in situ: relations with metal concentrations in the adjacent sediments and in the root tissue. **Biogeochemistry**, v. 33, p. 45-76, 1996.

Stehmann, J. R. **Plantas da floresta Atlântica,** (Vol. 1). R. C. Forzza, A. Salino, M. Sobral, D. P. da Costa, & L. H. Y. Kamino (Eds.). Jardim Botânico do Rio de Janeiro, Rio de Janeiro, 2009.

STUMM, W.; MORGAN, J. J. **Aquatic Chemistry: chemical equilibria and rates in natural waters**. Wiley Interscience, New York, 1996.

TAM, S. H.; MCCOLL, J. G. Aluminum-binding ability of soluble organics in Douglas Fir litter and soil. **Soil Science Society of America Journal**, v. 55, p. 1421-1427, 1991.

TAUBE, H. **Electron transfer between Metal complexes**. Nobel lecture, 8th December of 1983, Nobel Foundation, Stockholm, 1984.

TAYLOR, H. E. **Inductively Coupled Plasma-Mass Spectrometry**. San Diego: Academic Press, 2001.

TEMMINGHOFF, E. J. M.; PLETTE, A. C. C.; VAN ECK, R.; VAN RIEMSDIJK, W.H. Determination of the chemical speciation of trace metals in aqueous systems by the Wageningen Donnan Membrane Technique. **Analytical Chimica Acta**, v. 417, p. 149–157, 2000.

THIRY, Y.; SCHMIDT, P.; HEES, M. V.; WANNIJN, J.; VAN BREE, P.; RUFYIKIRI, G.; VANDENHOVE, H. Uranium distribution and cycling in Scots pine

(Pinus sylvestris L.) growing on a revegetated U-mining heap. **Journal of Environmental Radioactivity**, v. 81, p. 201-219, 2005.

TUOVINEN, T.S., ROIVAINEN, P.; MAKKONEN, S.; KOLEHMAINEN, M.; HOLOPAINEN, T.; JUUTILAINEN, J. Soil-to-plant transfer of elements is not linear: results for five elements relevant to radioactive waste in five boreal forest species. **Science of the Total Environment**, v. 410, p. 191–197, 2011.

USEPA – UNITED STATES ENVIRONMENTAL PROTECTION AGENCY, OFFICE OF RADIATION PROGRAMS. **Report to Congress: Potential Health and Environmental Hazards of Uranium Mine Wastes**. U.S. Government Printing Office, Washington, DC, 1983.

USEPA - UNITED STATES ENVIRONMENT PROTECTION AGENCY. 2002. **Supplemental guidance for developing soil screening levels for superfund sites**. Washington DC. Available at: http://www.epa.gov/superfund/health/ conmedia/soil/pdfs/ssg_main.pdf. Accessed 14 September 2018.

USEPA - UNITED STATES ENVIRONMENT PROTECTION AGENCY. 2005. **Ecological soil screening level (Eco-SSL) guidance and documents**. Washington DC. Available at: http://www.epa.gov/oswer/riskassessment/ecorisk/ecossl.htm. Accessed 14 September 2018.

USEPA - UNITED STATES ENVIRONMENTAL PROTECTION AGENCY. **Method 3051A: Microwave assisted digestion of sediments, sludges, soils and oils**. 2007.

VANDENHOVE H.; CUYPERS, A.; VAN HEES, M.; KOPPEN, G.; WANNIJN, J. Oxidative stress reactions induced in beans (*Phaseolus vulgaris*) following exposure to uranium. **Plant Physiology and Biochemistry**, v. 44, p. 795–805, 2006.

VAN LEEUWEN, H. P. Revisited: the conception of lability of metal complexes. **Electroanalysis: An International Journal Devoted to Fundamental and Practical Aspects of Electroanalysis**, v. 13, n. 10, p. 826-830, 2000.

VAREDA, J. P.; VALENTE, A. J.; DURÃES, L. Assessment of heavy metal pollution from anthropogenic activities and remediation strategies: A review. **Journal of Environmental Management**, v. 246, p. 101-118, 2019.

VROBLESKY, D. A; YANOSKY, T. M. Use of tree-ring chemistry to document historical ground-water contamination events. **Ground Water**, v. 28, n. 5, p. 677–684, 1990.

VROBLESKY, D. A. **Chlorinated ethene uptake and loss in tree trunks**. U.S. Geological Survey Department of Defense Environmental Conservation (DODEC) meeting, May 4–8, Tampa, Florida, 1998.

VROBLESKY, D. A; NIETCH, C. T; MORRIS, J. T. Chlorinated ethenes from ground water in tree trunks. **Environmental Science and Technology**, v. 33, n. 3, p. 510–515, 1999

VROBLESKY, D. A. User's guide to the collection and analysis of tree cores to assess the distribution of subsurface volatile organic compounds. **U.S. Geological Survey Scientific Investigations Report**, v. 2008–5088, 2008.

WABER, N.; SCHORSCHER, H. D.; PETERS, **T. Mineralogy, Petrology and Geochemistry of the Poços de Caldas Analoguesites, MinasGerais, Brazil**. Technical Report TR90-11. Swedish Nuclear Fuel and Waste Management Co., 1993.

WARRINGTON, G. E.; SKOGLEY, E. O. **Bioavailability and the soil solution**. Warrington Ecological Systems Analysis (WECSA), Saint Ignatius, MT, 1997.

WENG, L.; TEMMINGHOFF, E.; RIEMSDIJK, W. Determination of the free ion concentration of trace metals in soil solution using a soil column Donnan membrane technique. **European Journal of Soil Science**, v. 52., p. 629 – 637, 2002.

WILLIAMS, P. N.; ZHANG, H.; DAVISON, W.; ZHAO, S. Z.; LU, Y.; DONG, F., ZHANG, L.; PAN, Q. Evaluation of in situ DGT measurements for predicting the concentration of Cd in Chinese field-cultivated rice: impact of soil Cd:Zn ratios. **Environmental Science and Technology**, v. 46, n. 15, p. 8009–8016, 2012.

WNA – WORLD NUCLEAR ASSOCIATION. **Uranium Mining Overview**. Available at: https://www.world-nuclear.org/information-library/nuclear-fuel-cycle/mining-of-uranium/uranium-mining-overview.aspx Accessed 3 September 2019.

WORSHAM, L.; MARKEWITZ, D.; NIBBELINK, N.; WEST, L. A Comparison of Three Field Sampling Methods to Estimate Soil Carbon Content. **Forest Science**, v. 58, p. 513-522, 2012.

WUANA, R. A.; OKIEIMEN, F. E. Heavy metals in contaminated soils: a review of sources, chemistry, risks and best available strategies for remediation. **Isrn Ecology**, 2011.

ZACCHINI, M.; IORI, V.; SCARASCIA MUGNOZZA, G.; PIETRINI, F.; MASSACCI, A. Cadmium accumulation and tolerance in Populus nigra and Salix alba. **Plant Biology**, v. 55, n. 2, p. 383-386, 2011.

ZHANG, H.; DAVISON, W. Performance characteristics of diffusion gradients in thin films for the in situ measurement of trace metals in aqueous solution. **Analytical Chemistry**, v. 67., p. 3391-3400, 1995.

ZHANG, H.; DAVISON, W.; KNIGHT, B.; MCGRATH, S. In Situ Measurements of Solution Concentrations and Fluxes of Trace Metals in Soils Using DGT. **Environmental Science and Technology**, v. 32, p. 704-710, 1998.

ZHANG, H.; LOMBI, E.; SMOLDERS, E.; MCGRATH, S. Kinetics of Zn Release in Soils and Prediction of Zn Concentration in Plants Using Diffusive Gradients in Thin Films. **Environmental Science Technology**, v. 38, n. 13, p. 3608-3613, 2004.

ZHANG, C., DING, S., XU, D.; TANG, Y.; WONG, M. H. Bioavailability assessment of phosphorus and metals in soils and sediments: a review of diffusive gradients in thin films (DGT). **Environmental Monitoring and Assessment**, v. 186, p. 7367–7378, 2014.

ZHANG, X.; WEI, S.; SUN, Q.; WADOOD, S. A.; GUO, B. Source identification and spatial distribution of arsenic and heavy metals in agricultural soil around Hunan industrial estate by positive matrix factorization model, principle components analysis and geo statistical analysis. **Ecotoxicology and Environmental Safety**, v. 159, p. 354-362, 2018.

10 SUPPLEMENTARY MATERIAL

Table S1: Mean detection limits (LD) in ug L^{-1} obtained in ICP-MS measurements for C_{PW}, C_{DGT} and C_{Wood} values.

	C_{PW} & C_{DGT}	C_{Wood}
Al	2.40	1.57
Co	0.03	0.04
Cu	0.14	0.16
Fe	1.82	0.71
Mn	0.89	0.80
Ni	0.07	0.08
Pb	0.03	0.05
U	0.03	0.05
Zn	0.17	0.49

Table S2: Total metal content in soil samples (mg kg^{-1}). Mean= mean concentration; SD= standard deviation; RSD= Relative standard deviation; Max= Maximum value; Min= Minimum value; n= Sample number.

			Reference Area (C)					
Element	**QRV MG***	**VI****	**Mean**	**SD**	**RSD**	**Max**	**Min**	**n**
Mo	-	180	82.0	44.8	54.6	154.8	24.6	10
U	-	300**	104.7	97.3	92.9	332.1	13.4	10
Pb	15.8	4400	30.8	12.7	41.4	48.3	12.9	10
Zn	31.04	1000	91.5	24.7	27	138.9	53.9	10
Cu	13.22	1000	26.3	4.8	18.3	33.5	18.8	10
Ni	23.04	3800	49.1	8.7	17.7	61	31.8	10
Co	17.5	90	73.8	25.5	34.6	129	47.4	8
Fe	83500	-	30399.5	6841.5	22.5	43144.5	21041.1	10
Mn	446.91	-	1080.4	697.9	64.6	2182.2	259.8	10
Cd	1.01	160	<LD	<LD	<LD	<LD	<LD	0
Al	-	-	126045.1	15266.6	12.1	154175.9	102877.2	10
			Area of Acid Mine Drainage (A1)					
Element	**QRV MG***	**VI****	**Mean**	**SD**	**RSD**	**Max**	**Min**	**n**
Mo	-	180	174.9	83.3	47.6	323.1	95.5	8
U	-	300''	129.6	57.1	44.1	219.1	50.6	8
Pb	15.8	4400	82.0	16.3	19.8	104.9	54.6	8
Zn	31.04	1000	96.8	13.9	14.4	121.6	70.0	8
Cu	13.22	1000	26.8	5.1	19.0	39.6	21.6	8
Ni	23.04	3800	73.7	17.4	23.7	99.2	56.6	7
Co	17.5	90	76.4	6.3	8.2	88.7	69.6	7
Fe	83500	-	38280.0	4989.0	13.0	45757.2	28532.8	8
Mn	446.91	-	737.9	228.2	30.9	1033.5	318.6	8
Cd	1.01	160	<LD	<LD	<LD	<LD	<LD	0
Al	-	-	135207.5	8346.1	6.2	145373.5	123661.7	8
			Area of Waste Rock Pile WR-8 (A2)					
Element	**QRV MG***	**VI****	**Mean**	**SD**	**RSD**	**Max**	**Min**	**n**
Mo	-	180	158.4	115.9	73.2	421.5	62.9	11
U	-	300''	100.5	66.9	66.5	217.5	14.4	11
Pb	15.8	4400	75.4	61.8	82.0	205.7	34.2	11
Zn	31.04	1000	97.4	11.9	12.2	115.9	74.2	11
Cu	13.22	1000	26.4	6.5	24.4	40.1	17.0	10
Ni	23.04	3800	60.0	28.7	47.8	122.5	27.5	10
Co	17.5	90	101.1	21.7	21.5	141.2	62.9	11
Fe	83500	-	42705.9	6634.3	15.5	53550.2	32376.6	11
Mn	446.91	-	906.6	528.5	58.3	2089.4	295.5	11
Cd	1.01	160	<LD	<LD	<LD	<LD	<LD	0
Al	-	-	152645.7	16766.4	11.0	170297.5	123527.7	11
			Area of Waste Rock Pile WR-4 (A3)					
Element	**QRV MG***	**VI****	**Mean**	**SD**	**RSD**	**Max**	**Min**	**n**
Mo	-	180	129.7	102.0	78.7	371.8	29.8	12
U	-	300''	100.3	104.2	103.9	409.3	21.8	12
Pb	15.8	4400	90.8	90.8	100.1	368.5	26.3	12
Zn	31.04	1000	99.6	10.3	10.4	116.2	81.9	12
Cu	13.22	1000	27.9	4.0	14.3	35.0	22.0	11
Ni	23.04	3800	63.7	16.7	26.2	85.6	35.8	7
Co	17.5	90	119.7	26.4	22.1	163.4	74.0	12
Fe	83500	-	43111.2	7571.8	17.6	57234.7	29767.5	12
Mn	446.91	-	554.0	163.6	29.5	897.0	370.8	12
Cd	1.01	160	<LD	<LD	<LD	<LD	<LD	0
Al	-	-	152087.4	11605.5	7.6	171137.7	129897.1	12

* Quality Reference Values for metals in soil in mg kg^{-1} Minas Gerais (75-Percentile) established by COPAM 2011

** Industrial Intervention Values for metals in soil in mg kg^{-1} established by CONAMA (2016)

'' Quality Reference Value of U for soils in mg kg^{-1} established by CCME (2007)

Table S3: Metal concentrations (µg L^{-1}) measured in pore water (C_{PW}) in soil samples from sampling area C.

C-PW	Al	Mn	Fe	Co	Ni	Cu	Zn	Pb	U
CT1 PW 1	n.a.	224394.8	158.0	1.4	49.5	LD	187.8	LD	0.5
CT1 PW 2	n.a.	119073.3	10964.7	20.0	2567.1	16.1	254.0	LD	4.5
Mean CT1	**n.a.**	**171734.0**	**5561.4**	**10.7**	**1308.3**	**16.1**	**220.9**	**LD**	**2.5**
CT2 PW 1	n.a.	9379.6	322.8	0.2	65.6	LD	26.0	LD	LD
CT2 PW 2	n.a.	22322.7	1677.9	3.1	153.3	LD	122.5	LD	LD
Mean CT2	**n.a.**	**15851.1**	**1000.3**	**1.6**	**109.5**	**LD**	**74.3**	**LD**	**LD**
CG1 PW 1	3588.7	143052.9	LD	29.7	LD	LD	433.3	2.0	17.2
CG1 PW 2	3089.6	116109.0	2454.9	24.6	LD	LD	357.4	1.8	16.5
Mean CG1	**3339.2**	**129581.0**	**1448.6**	**27.1**	**LD**	**LD**	**395.4**	**1.9**	**16.8**
CG2 PW 1	14667.0	62572.9	466.7	45.2	LD	LD	945.9	6.2	59.7
CG2 PW 2	13803.5	60762.4	417.2	43.7	LD	LD	995.5	6.5	51.7
Mean CG2	**14235.2**	**61667.6**	**441.9**	**44.4**	**LD**	**LD**	**970.7**	**6.4**	**55.7**
CP1 PW 1	113.5	2450.3	740.3	LD	LD	LD	LD	LD	LD
CP1 PW 2	201.4	2492.7	2399.0	LD	LD	LD	LD	LD	LD
Mean CP1	**157.5**	**2471.5**	**1569.6**	**LD**	**LD**	**LD**	**LD**	**LD**	**LD**
CP2 PW 1	LD	540.1	LD	0.8	1.6	5.0	16.6	0.1	0.4
CP2 PW 2	LD	610.0	LD	0.8	0.8	5.8	48.7	LD	0.4
Mean CP2	**LD**	**575.1**	**LD**	**0.8**	**1.2**	**5.4**	**32.6**	**0.04**	**0.4**
CM1 PW 1	1148.7	62724.3	LD	69.4	LD	LD	77.5	1.8	3.0
CM1 PW 2	1191.4	57760.0	LD	68.2	LD	LD	76.0	1.6	3.1
Mean CM1	**1170.0**	**60242.1**	**LD**	**68.8**	**LD**	**LD**	**76.7**	**1.7**	**3.1**
CM2 PW 1	6.9	4553.2	LD	6.0	LD	30.5	18.3	LD	LD
CM2 PW 2	LD	4037.7	LD	5.5	LD	LD	15.0	LD	LD
Mean CM2	**6.6**	**4295.4**	**LD**	**5.7**	**LD**	**15.9**	**16.7**	**LD**	**LD**
CE1 PW 1	15791.2	37802.6	2129.1	43.8	7.5	1.8	259.3	4.8	2.1
CE1 PW 2	16017.3	46249.2	2643.4	34.6	5.8	1.2	284.3	3.7	1.8
Mean CE1	**15904.2**	**42025.9**	**2386.3**	**39.2**	**6.6**	**1.5**	**271.8**	**4.2**	**2.0**
CV1 PW 1	975.6	286626.4	149.4	31.8	9.9	3.2	584.0	0.1	8.2
CV1 PW 2	219.7	270838.0	74.6	25.1	6.1	2.1	405.1	0.1	4.1
Mean CV1	**597.7**	**278732.2**	**112.0**	**28.5**	**8.0**	**2.6**	**494.5**	**0.1**	**6.2**
CV2 PW1	112.3	30135.9	3.9	4.5	0.1	0.8	132.2	0.1	1.2
CV2 PW 2	279.1	54701.6	4.1	5.7	0.7	0.2	54.1	0.1	1.6
Mean CV2	**195.7**	**42418.8**	**4.0**	**5.1**	**0.4**	**0.5**	**93.1**	**0.1**	**1.4**
Mean Area C	**4450.8**	**73599.5**	**1294.9**	**21.1**	**12.6**	**3.3**	**240.6**	**2.5**	**8.8**
SD Area C	**6655.3**	**86984.7**	**1693.4**	**22.5**	**34.2**	**4.9**	**291.6**	**2.3**	**17.2**

n.a.= not analysed

Table S4: Metal concentrations (µg L^{-1}) measured in pore water (C_{PW}) in soil samples from sampling area A1.

C-PW	Al	Mn	Fe	Co	Ni	Cu	Zn	Pb	U
A1T1 PW 1	8552.2	116251.8	652.4	57.4	24.3	LD	1561.5	4.8	98.9
A1T1 PW 2	20833.8	247966.3	4072.9	71.6	658.2	5.9	1754.1	4.2	97.7
Mean A1T1	**14693.0**	**182109.0**	**2362.6**	**64.5**	**341.2**	**3.1**	**1657.8**	**4.5**	**98.3**
A1T2 PW 1	71933.0	27045.5	476.4	17.2	498.5	LD	70.1	5.0	21.4
A1T2 PW 2	150986.8	58233.6	11832.5	12.7	LD	LD	71.1	11.6	0.6
Mean A1T2	**111459.9**	**42639.5**	**6154.5**	**15.0**	**249.3**	**LD**	**70.6**	**8.3**	**11.0**
A1P1 PW 1	2916.8	8014.2	221.8	18.7	LD	LD	190.8	28.1	28.5
A1P1 PW 2	2553.9	6690.7	194.1	16.6	LD	2.0	161.0	26.3	29.4
Mean A1P1	**2735.3**	**7352.4**	**208.0**	**17.6**	**LD**	**1.4**	**175.9**	**27.2**	**28.9**
A1V1 PW 1	6589.5	210849.6	357.5	61.7	13.9	LD	2126.4	8.0	15.0
A1V1 PW 2	8648.1	247592.2	389.1	74.0	17.2	LD	2545.5	9.8	14.4
Mean A1V1	**7618.8**	**229220.9**	**373.3**	**67.8**	**15.6**	**LD**	**2335.9**	**8.9**	**14.7**
A1G1 PW 1	2216.2	92393.6	447.7	70.3	6.9	LD	861.6	6.4	5.8
A1G1 PW 2	1331.6	83448.3	n.a.	61.9	6.4	LD	728.7	6.0	5.6
Mean A1G1	**1773.9**	**87920.9**	**447.7**	**66.1**	**6.6**	**LD**	**795.1**	**6.2**	**5.7**
A1G2 PW 1	850.3	2553.4	230.0	5.9	0.8	LD	56.5	0.5	10.5
A1G2 PW 2	783.5	2749.5	182.5	5.7	LD	LD	50.2	0.5	8.8
Mean A1G2	**816.9**	**2651.4**	**206.2**	**5.8**	**0.7**	**LD**	**53.3**	**0.5**	**9.7**
A1M1 PW 1	3097.3	50129.4	8723.1	169.9	LD	LD	986.7	23.8	95.7
A1M1 PW 2	8508.8	80654.3	9351.1	177.3	LD	LD	1017.7	25.0	99.0
Mean A1M1	**5803.0**	**65391.9**	**9037.1**	**173.6**	**LD**	**LD**	**1002.2**	**24.4**	**97.4**
A1M2 PW 1	17507.3	193486.6	164.4	84.9	9.7	LD	1863.4	7.7	49.6
A1M2 PW 2	16742.9	184856.5	1218.1	80.9	16.1	29.8	1793.2	14.3	44.1
Mean A1M2	**17125.1**	**189171.5**	**691.3**	**82.9**	**12.9**	**29.8**	**1828.3**	**11.0**	**46.9**
Mean Area A1	**20253.2**	**100807.2**	**2435.1**	**61.7**	**78.3**	**1.1**	**989.9**	**11.4**	**39.1**
SD Area A1	**37328.5**	**87896.4**	**3350.8**	**53.8**	**136.3**	**1.1**	**877.0**	**9.5**	**38.6**

Table S5: Metal concentrations (µg L^{-1}) measured in pore water (C_{PW}) in soil samples from sampling area A2.

C-PW	Al	Mn	Fe	Co	Ni	Cu	Zn	Pb	U
A2P1 PW 1	133.7	236.2	120.2	LD	LD	LD	18.2	1.5	10.9
A2P1 PW 2	240.3	294.0	254.4	LD	LD	LD	7.4	2.3	10.5
Mean A2P1	**187.0**	**265.1**	**187.3**	**LD**	**LD**	**LD**	**12.8**	**1.9**	**10.7**
A2P2 PW 1	238.1	43062.0	505.4	LD	LD	LD	585.6	1.4	2.5
A2P2 PW 2	295.6	45737.6	2.2	LD	LD	LD	81.5	1.3	2.6
Mean A2P2	**266.8**	**44399.8**	**253.8**	**LD**	**LD**	**LD**	**333.5**	**1.4**	**2.6**
A2T1 PW 1	29993.8	54603.4	LD	LD	LD	LD	83.7	3.2	0.2
Mean A2T1	**29993.8**	**54603.4**	**LD**	**LD**	**LD**	**LD**	**83.7**	**3.2**	**0.2**
A2E1 PW 1	1934.3	39407.5	116.4	82.4	1.3	LD	218.0	3.9	17.4
A2E1 PW 2	2376.0	29767.3	36.5	81.0	1.2	LD	177.4	3.9	20.6
Mean A2E1	**2155.1**	**34587.4**	**76.4**	**81.7**	**1.2**	**LD**	**197.7**	**3.9**	**19.0**
A2E2 PW 1	1143.0	2848.8	67.8	LD	LD	LD	146.4	37.6	5.9
A2E2 PW 2	918.6	2667.8	44.8	LD	LD	LD	101.2	35.2	5.1
Mean A3E2	**1030.8**	**2758.3**	**56.3**	**LD**	**LD**	**LD**	**123.8**	**36.4**	**5.5**
A2G1 PW 1	1483.0	113606.2	291.4	75.5	5.8	LD	611.2	14.9	1.3
A2G1 PW 2	1724.8	101762.9	324.0	91.2	4.3	LD	675.6	16.4	1.3
Mean A3G1	**1603.9**	**107684.6**	**307.7**	**83.3**	**5.0**	**LD**	**643.4**	**15.6**	**1.3**
A2G2 PW 1	285.0	76248.4	50.4	19.5	1.5	LD	97.4	7.0	0.6
A2G2 PW 2	68.9	68057.3	36.5	11.9	LD	LD	36.4	4.3	0.3
Mean A2G2	**177.0**	**72152.9**	**43.4**	**15.7**	**0.9**	**LD**	**66.9**	**5.6**	**0.5**
A2M1 PW 1	481.7	30185.3	43.9	16.5	1.8	LD	385.8	1.2	7.2
A2M1 PW 2	536.7	28440.0	106.8	13.7	0.3	LD	505.2	1.5	7.9
Mean A2M1	**509.2**	**29312.7**	**75.3**	**15.1**	**1.0**	**LD**	**445.5**	**1.4**	**7.5**
A2M2 PW 1	0.0	56626.8	19.2	LD	LD	LD	85.1	-0.1	0.7
A2M2 PW 2	17.6	37796.8	LD	LD	LD	LD	0.0	-0.1	0.9
Mean A2M2	**8.8**	**47211.8**	**9.6**	**LD**	**LD**	**LD**	**42.6**	**-0.1**	**0.8**
A2V1 PW 1	45.2	66642.1	153.3	12.8	LD	LD	165.6	0.6	5.2
A2V1 PW 2	37.5	55113.2	36.7	8.2	3.2	LD	124.8	0.6	4.6
Mean A2V1	**41.4**	**60877.6**	**95.0**	**10.5**	**1.8**	**LD**	**145.2**	**0.6**	**4.9**
A2V2 PW 1	3375.4	79317.4	377.3	112.3	15.1	LD	1798.4	14.1	48.0
A2V2 PW 2	2787.8	79038.6	391.4	106.1	12.7	LD	1798.0	12.4	43.8
Mean A2V2	**3081.6**	**79178.0**	**384.3**	**109.2**	**13.9**	**LD**	**1798.2**	**13.2**	**45.9**
Mean Area A2	**3550.5**	**48457.4**	**135.6**	**28.7**	**2.2**	**0.2**	**353.9**	**7.6**	**9.0**
SD Area A2	**8826.9**	**31926.4**	**128.6**	**41.3**	**4.1**	**0.0**	**516.5**	**10.9**	**13.5**

Table S6: Metal concentrations (µg L^{-1}) measured in pore water (C_{PW}) in soil samples from sampling area A3.

C-PW	Al	Mn	Fe	Co	Ni	Cu	Zn	Pb	U
A3P1 PW 1	4767.1	48195.6	10.5	131.6	LD	0.4	520.1	59.1	9.0
A3P1 PW 2	4810.5	48718.0	4.0	138.5	LD	LD	538.4	59.7	8.8
Mean A3P1	**4788.8**	**48456.8**	**7.2**	**135.0**	**LD**	**0.4**	**529.3**	**59.4**	**8.9**
A3P2 PW 1	351.6	n.a.	64.2	60.5	LD	1.1	31.5	5.2	3.0
A3P2 PW 2	296.1	11002.3	160.1	43.5	LD	LD	59.4	8.3	2.5
Mean A3P2	**323.9**	**11002.3**	**112.2**	**52.0**	**LD**	**0.9**	**45.4**	**6.8**	**2.8**
A3T1 PW 1	15346.1	121111.6	2981.4	135.4	52.9	9.6	3140.6	92.2	80.6
A3T1 PW 2	13505.2	105271.0	1783.1	125.0	50.1	10.9	3030.0	83.8	77.3
Mean A3T1	**14425.6**	**113191.3**	**2382.2**	**130.2**	**51.5**	**10.3**	**3085.3**	**88.0**	**78.9**
A3T2 PW 1	17089.3	134869.2	3320.1	212.2	17.0	LD	1612.9	14.3	16.5
A3T2 PW 2	15362.1	119745.8	2028.3	191.6	13.5	LD	1412.8	12.1	19.1
Mean A3T2	**16225.7**	**127307.5**	**2674.2**	**201.9**	**15.3**	**LD**	**1512.9**	**13.2**	**17.8**
A3E1 PW 1	21208.6	65430.6	1437.8	233.5	28.4	5.9	2368.6	161.8	83.7
A3E1 PW 2	25532.1	74454.4	2804.7	282.8	38.7	7.8	2998.7	191.1	127.2
Mean A3E1	**23370.4**	**69942.5**	**2121.3**	**258.1**	**33.5**	**6.8**	**2683.6**	**176.5**	**105.4**
A3E2 PW 1	22839.2	9389.6	7341.7	36.5	LD	5.1	212.4	39.1	43.4
A3E2 PW 2	4861.0	5074.1	1191.0	23.7	LD	4.7	108.0	11.4	20.6
Mean A3E2	**13850.1**	**7231.8**	**4266.4**	**30.1**	**LD**	**4.9**	**160.2**	**25.3**	**32.0**
A3G1 PW 1	1672.7	7618.4	1329.7	1.9	0.0	0.3	29.5	0.9	0.3
A3G1 PW 2	1233.1	15244.5	317.5	2.4	0.4	10.2	76.9	1.3	0.3
Mean A3G1	**1452.9**	**11431.4**	**823.6**	**2.1**	**0.2**	**5.3**	**53.2**	**1.1**	**0.3**
A3G2 PW 1	7798.8	81039.9	18410.2	43.4	LD	0.4	117.9	10.2	2.0
A3G2 PW 2	8364.8	58993.9	1184.1	42.7	LD	LD	119.2	10.3	2.2
Mean A3G2	**8081.8**	**70016.9**	**9797.1**	**43.1**	**LD**	**0.2**	**118.6**	**10.3**	**2.1**
A3M1 PW 1	1900.3	61584.6	1177.8	10.2	1.3	0.8	70.8	1.4	0.6
A3M1 PW 2	1607.0	60487.2	1233.7	9.9	1.9	3.2	141.2	1.9	0.6
Mean A3M1	**1753.7**	**61035.9**	**1205.8**	**10.0**	**1.6**	**2.0**	**106.0**	**1.6**	**0.6**
A3M2 PW 1	2764.4	22776.4	1522.3	9.0	2.5	2.5	428.3	3.0	1.0
A3M2 PW 2	2379.3	17104.4	1090.2	8.7	1.6	0.6	60.0	2.5	1.0
Mean A3M2	**2571.9**	**19940.4**	**1306.2**	**8.9**	**2.1**	**1.5**	**244.2**	**2.7**	**1.0**
A3V1 PW 1	1257.4	41460.8	474.6	6.7	0.8	0.2	20.8	0.5	LD
A3V1 PW 2	n.a.	n.a.	n.a.	6.9	1.2	0.8	87.9	0.7	LD
Mean A3V1	**1257.4**	**41460.8**	**474.6**	**6.8**	**1.0**	**0.5**	**54.4**	**0.6**	**LD**
A3V2 PW 1	4556.1	68324.9	880.1	14.9	3.0	2.0	442.0	3.7	1.4
A3V2 PW 2	4466.5	66548.4	194.1	14.2	2.2	1.1	98.7	3.4	1.3
Mean A3V2	**4511.3**	**67436.7**	**537.1**	**14.5**	**2.6**	**1.6**	**270.4**	**3.6**	**1.3**
A3V2 DGT 1	3769.1	2566.0	182.0	1.3	0.5	0.1	14.9	3.6	1.2
A3V2 DGT 2	2882.0	2931.0	115.4	1.7	1.2	0.6	29.9	4.1	1.2
Mean A3V2	**3325.6**	**2748.5**	**148.7**	**1.5**	**0.9**	**0.3**	**22.4**	**3.9**	**1.2**
Mean Area A3	**7717.8**	**54037.9**	**2142.3**	**74.4**	**9.0**	**2.9**	**738.6**	**32.4**	**20.9**
SD Area A3	**7487.5**	**39097.2**	**2710.3**	**86.4**	**16.7**	**3.2**	**1084.4**	**52.9**	**35.1**

Table S7: Labile metal concentrations (µg L^{-1}) measured by DGT in soils from sampling area C.

C-DGT	Al	Mn	Fe	Co	Ni	Cu	Zn	Pb	U
CT1 DGT 1	591.0	6426.6	22.2	2.4	LD	LD	185.3	2.3	21.5
CT1 DGT 2	1172.3	6371.0	172.7	2.2	LD	LD	170.0	7.8	31.9
Mean CT1	**881.6**	**6398.8**	**97.5**	**2.3**	**LD**	**LD**	**177.6**	**5.1**	**26.7**
CT2 DGT 1	1344.1	5392.3	50.8	8.8	LD	LD	35.3	3.2	1.1
CT2 DGT 2	1382.1	5640.1	80.0	10.2	LD	LD	38.6	4.2	1.6
Mean CT2	**1363.1**	**5516.2**	**65.4**	**9.5**	**LD**	**LD**	**37.0**	**3.7**	**1.4**
CG1 DGT 1	421.5	11552.1	107.6	8.0	0.8	0.4	115.6	1.6	5.1
CG1 DGT 2	905.5	9373.4	94.3	7.0	0.7	0.3	107.2	1.4	4.7
Mean CG1	**663.5**	**10462.8**	**101.0**	**7.5**	**0.8**	**0.4**	**111.4**	**1.5**	**4.9**
CG2 DGT 1	4284.6	4329.3	471.0	6.3	LD	LD	149.1	7.8	37.6
CG2 DGT 2	3454.6	5074.5	246.4	6.2	LD	LD	145.1	5.1	32.2
Mean CG2	**3869.6**	**4701.9**	**358.7**	**6.2**	**LD**	**LD**	**147.1**	**6.4**	**34.9**
CP1 DGT 1	34.2	251.7	8.7	0.1	0.4	0.3	11.4	LD	LD
CP1 DGT 2	25.9	281.7	5.0	0.1	0.5	0.3	13.7	LD	LD
Mean CP1	**30.1**	**266.7**	**6.8**	**0.1**	**0.4**	**0.3**	**12.5**	**LD**	**LD**
CP2 DGT 1	411.5	437.9	134.5	0.5	0.2	0.6	0.0	0.5	LD
CP2 DGT 2	422.9	385.7	108.9	0.5	0.4	0.9	12.3	1.2	LD
Mean CP2	**417.2**	**411.8**	**121.7**	**0.5**	**0.3**	**0.7**	**6.1**	**0.9**	**LD**
CM1 DGT 1	458.9	5352.3	LD	10.5	1.0	0.3	23.2	0.1	LD
CM1 DGT 2	664.6	4774.6	LD	12.4	1.1	0.3	38.8	0.7	LD
Mean CM1	**561.7**	**5063.5**	**LD**	**11.5**	**1.0**	**0.3**	**31.0**	**0.4**	**LD**
CM2 DGT 1	1167.2	986.9	44.9	1.7	LD	LD	6.0	2.5	1.0
CM2 DGT 2	814.9	816.3	58.8	1.2	9.5	LD	5.2	0.9	0.6
Mean CM2	**991.1**	**901.6**	**51.8**	**1.5**	**4.8**	**LD**	**5.6**	**1.7**	**0.8**
CE1 DGT 1	2249.7	2260.7	338.2	5.8	1.7	0.2	30.2	2.7	0.6
CE1 DGT 2	4093.4	2061.8	349.2	5.2	1.4	0.1	23.9	2.6	0.6
Mean CE1	**3171.5**	**2161.3**	**343.7**	**5.5**	**1.5**	**0.2**	**27.1**	**2.6**	**0.6**
CV1 DGT 1	1374.1	7218.2	73.6	3.3	1.9	0.3	82.8	1.9	5.9
CV1 DGT 2	2203.4	16604.3	79.0	5.5	1.6	0.3	105.9	3.0	6.2
Mean CV1	**1788.7**	**11911.2**	**76.3**	**4.4**	**1.7**	**0.3**	**94.4**	**2.4**	**6.1**
CV2 DGT1	526.5	10640.9	28.6	3.3	0.5	0.1	51.6	0.8	2.0
CV2 DGT 2	1118.7	5807.3	217.9	2.3	0.8	0.1	28.2	2.7	4.5
Mean CV2	**822.6**	**8224.1**	**123.2**	**2.8**	**0.6**	**0.1**	**39.9**	**1.8**	**3.3**
Mean Area C	**1323.7**	**5092.7**	**126.2**	**4.7**	**1.1**	**0.3**	**62.7**	**2.4**	**7.2**
SD Area C	**1190.9**	**3981.6**	**116.6**	**3.7**	**1.4**	**0.2**	**60.1**	**2.0**	**12.0**

Table S8: Labile metal concentrations (µg L^{-1}) measured by DGT (C_{DGT}) in soils from sampling area A1.

C-DGT	Al	Mn	Fe	Co	Ni	Cu	Zn	Pb	U
A1T1 DGT 1	2437.8	4076.1	554.6	6.8	LD	LD	218.0	8.5	66.7
A1T1 DGT 2	3605.6	4060.5	874.3	6.4	LD	LD	214.1	12.9	86.4
Mean A1T1	**3021.7**	**4068.3**	**714.5**	**6.6**	**LD**	**LD**	**216.1**	**10.7**	**76.6**
A1T2 DGT 1	871.58	5805.9	100.5	6.1	LD	LD	119.7	2.9	2.8
A1T2 DGT 2	1032.62	6547.5	114.5	5.7	LD	LD	135.8	2.5	2.9
Mean A1T2	**952.10**	**6176.71**	**107.50**	**5.89**	**LD**	**LD**	**127.77**	**2.66**	**2.83**
A1P1 DGT 1	2493.3	2395.7	139.0	4.8	LD	0.2	84.0	4.0	18.1
A1P1 DGT 2	2343.8	2346.0	131.5	4.8	LD	0.3	92.4	3.3	18.0
Mean A1P1	**2418.6**	**2370.9**	**135.2**	**4.8**	**LD**	**0.2**	**88.2**	**3.6**	**18.1**
A1V1 DGT 1	2998.1	11533.2	284.3	10.0	2.9	LD	323.4	7.2	LD
A1V1 DGT 2	2285.0	11630.4	463.5	10.2	2.9	LD	343.4	5.5	LD
Mean A1V1	**2641.5**	**11581.8**	**373.9**	**10.1**	**2.9**	**LD**	**333.4**	**6.3**	**LD**
A1G1 DGT 1	1422.2	7869.9	182.7	13.0	1.4	LD	151.5	4.9	LD
A1G1 DGT 2	1103.2	8642.2	101.3	12.0	1.4	LD	139.3	3.8	LD
Mean A1G1	**1262.7**	**8256.1**	**142.0**	**12.5**	**1.4**	**LD**	**145.4**	**4.4**	**LD**
A1G2 DGT 1	325.4	875.7	8.0	1.5	LD	0.2	24.7	0.8	6.1
A1G2 DGT 2	395.3	956.0	1.7	1.8	LD	0.2	25.7	1.8	6.4
Mean A1G2	**360.4**	**915.8**	**4.9**	**1.7**	**LD**	**0.2**	**25.2**	**1.3**	**6.2**
A1M1 DGT 1	450.2	5431.8	1029.1	17.3	1.5	0.4	115.2	4.2	19.1
A1M1 DGT 2	1010.1	7121.3	900.7	24.2	1.9	0.3	154.1	7.4	27.3
Mean A1M1	**730.2**	**6276.6**	**964.9**	**20.7**	**1.7**	**0.3**	**134.6**	**5.8**	**23.2**
A1M2 DGT 1	5149.6	7095.1	276.2	10.0	LD	LD	222.3	8.7	29.5
A1M2 DGT 2	6731.5	7724.5	426.7	9.6	LD	LD	217.5	9.7	30.2
Mean A1M2	**5940.5**	**7409.8**	**351.4**	**9.8**	**LD**	**LD**	**219.9**	**9.2**	**29.8**
Mean Area A1	**2166.0**	**5882.0**	**349.3**	**9.0**	**0.8**	**0.2**	**161.3**	**5.5**	**21.3**
SD Area A1	**1807.9**	**3401.3**	**333.6**	**5.8**	**1.1**	**0.2**	**94.1**	**3.2**	**24.3**

Table S9: Labile metal concentrations (µg L^{-1}) measured by DGT (C_{DGT}) in soils from sampling area A2.

C-DGT	Al	Mn	Fe	Co	Ni	Cu	Zn	Pb	U
A2P1 DGT 1	123.6	121.8	26.9	LD	LD	LD	0.0	4.6	5.3
A2P1 DGT 2	160.8	119.8	37.3	LD	LD	LD	0.0	7.8	6.4
Mean A2P1	**142.2**	**120.8**	**32.1**	**LD**	**LD**	**LD**	**0.0**	**6.2**	**5.8**
A2P2 DGT 1	117.4	5089.8	n.a.	0.7	0.3	LD	10.3	0.5	1.7
A2P2 DGT 2	335.4	6699.7	3.7	1.8	0.2	LD	15.6	1.5	2.9
Mean A2P2	**226.4**	**5894.8**	**3.7**	**1.2**	**0.2**	**LD**	**12.9**	**1.0**	**2.3**
A2T1 DGT 1	537.4	7181.9	54.8	1.3	0.1	LD	3.5	4.1	1.2
Mean A2T1	**537.4**	**5905.4**	**54.8**	**1.3**	**0.1**	**LD**	**3.5**	**4.1**	**1.2**
A2E1 DGT 1	610.2	5264.8	10.7	13.5	0.5	LD	26.4	1.1	6.6
A2E1 DGT 2	864.5	3837.8	12.8	15.8	0.7	LD	16.7	1.9	8.8
Mean A2E1	**737.3**	**4551.3**	**11.7**	**14.6**	**0.6**	**LD**	**21.6**	**1.5**	**7.7**
A2E2 DGT 1	376.6	382.2	9.5	LD	0.3	LD	5.2	14.0	2.9
A2E2 DGT 2	317.1	376.7	2.3	LD	0.4	LD	13.7	9.0	2.4
Mean A2E2	**346.8**	**379.4**	**5.9**	**LD**	**0.4**	**LD**	**9.5**	**11.5**	**2.7**
A2G1 DGT 1	461.4	6625.6	72.7	9.9	1.4	LD	92.4	6.8	3.1
A2G1 DGT 2	399.7	6190.7	45.6	8.8	2.2	LD	82.4	5.7	2.7
Mean A2G1	**430.5**	**6408.2**	**59.1**	**9.4**	**1.8**	**LD**	**87.4**	**6.3**	**2.9**
A2G2 DGT 1	476.5	5859.9	79.5	4.6	0.6	LD	23.3	6.9	1.4
A2G2 DGT 2	436.9	6243.1	97.6	3.0	0.5	LD	30.7	5.3	1.2
Mean A2G2	**456.7**	**6051.5**	**88.6**	**3.8**	**0.5**	**LD**	**27.0**	**6.1**	**1.3**
A2M1 DGT 1	233.5	5698.3	48.2	4.6	1.5	LD	125.6	1.4	4.6
A2M1 DGT 2	173.6	5215.3	30.7	3.5	1.0	LD	97.1	1.1	4.1
Mean A2M1	**203.6**	**5456.8**	**39.5**	**4.1**	**1.3**	**LD**	**111.4**	**1.3**	**4.3**
A2M2 DGT 1	96.2	5831.4	44.9	2.4	1.3	0.2	50.2	1.8	2.3
A2M2 DGT 2	100.9	6183.8	54.4	2.5	1.0	0.4	23.9	1.9	2.4
Mean A2M2	**98.6**	**6007.6**	**49.6**	**2.5**	**1.2**	**0.3**	**37.1**	**1.9**	**2.4**
A2V1 DGT 1	147.2	8244.7	46.7	5.0	1.4	0.2	38.8	2.2	7.3
A2V1 DGT 2	87.4	7867.1	31.7	6.0	1.3	0.1	43.3	1.4	5.9
Mean A2V1	**117.3**	**8055.9**	**39.2**	**5.5**	**1.3**	**0.2**	**41.1**	**1.8**	**6.6**
A2V2 DGT 1	601.6	5727.7	79.6	15.3	3.2	LD	243.4	5.2	15.9
A2V2 DGT 2	490.9	5545.8	68.6	14.7	2.2	LD	255.8	3.9	13.7
Mean A2V2	**546.2**	**5636.7**	**74.1**	**15.0**	**2.7**	**LD**	**249.6**	**4.6**	**14.8**
Mean Area A2	**349.4**	**4951.7**	**41.7**	**5.2**	**0.9**	**0.1**	**54.6**	**4.2**	**4.7**
SD Area A2	**209.5**	**2470.0**	**27.4**	**5.5**	**0.8**	**0.1**	**73.5**	**3.2**	**4.0**

Table S10: Labile metal concentrations (µg L^{-1}) measured by DGT (C_{DGT}) in soils from sampling area A3.

C-DGT	Al	Mn	Fe	Co	Ni	Cu	Zn	Pb	U
A3P1 DGT 1	1254.0	4896.8	10.2	16.6	0.7	LD	71.8	33.1	24.9
A3P1 DGT 2	1582.1	5695.2	44.5	15.1	0.6	LD	66.4	31.7	24.1
Mean A3P1	**1418.0**	**5296.0**	**27.3**	**15.9**	**0.7**	**LD**	**69.1**	**32.4**	**24.5**
A3P2 DGT 1	498.5	6726.4	28.4	15.2	LD	0.4	20.4	12.3	5.2
A3P2 DGT 2	418.2	6643.5	26.6	13.8	LD	0.1	15.9	9.8	5.1
Mean A3P2	**458.3**	**6685.0**	**27.5**	**14.5**	**LD**	**0.2**	**18.2**	**11.1**	**5.2**
A3T1 DGT 1	1482.3	6661.8	1070.7	17.8	10.2	2.3	474.9	29.6	27.2
A3T1 DGT 2	1405.1	5726.6	1226.7	15.9	8.7	2.2	377.9	38.7	30.3
Mean A3T1	**1443.7**	**6194.2**	**1148.7**	**16.9**	**9.5**	**2.2**	**426.4**	**34.2**	**28.7**
A3T2 DGT 1	583.4	8464.5	37.2	21.0	1.9	0.3	128.2	3.9	14.6
A3T2 DGT 2	635.6	7114.3	39.2	22.8	1.8	0.3	141.2	4.5	16.4
Mean A3T2	**609.5**	**7789.4**	**38.2**	**21.9**	**1.8**	**0.3**	**134.7**	**4.2**	**15.5**
A3E1 DGT 1	2479.1	3575.7	425.7	21.2	3.8	0.8	236.6	42.8	29.8
A3E1 DGT 2	2621.1	3337.3	670.6	21.7	4.0	1.0	253.5	48.8	37.7
Mean A3E1	**2550.1**	**3456.5**	**548.1**	**21.4**	**3.9**	**0.9**	**245.0**	**45.8**	**33.7**
A3E2 DGT 1	1081.0	2816.4	58.7	9.9	0.2	0.6	68.3	10.5	16.4
A3E2 DGT 2	913.8	4181.1	50.0	11.3	0.5	1.9	81.0	10.0	14.7
Mean A3E2	**997.4**	**3498.7**	**54.3**	**10.6**	**0.4**	**1.2**	**74.7**	**10.2**	**15.6**
A3G1 DGT 1	1423.1	7212.2	112.7	2.9	1.4	0.4	61.6	2.4	0.6
A3G1 DGT 2	2762.1	4854.1	239.0	1.4	1.0	0.2	25.4	2.9	0.8
Mean A3G1	**2092.6**	**6033.1**	**175.8**	**2.2**	**1.2**	**0.3**	**43.5**	**2.6**	**0.7**
A3G2 DGT 1	832.2	6430.7	1590.7	6.8	1.6	0.7	37.5	3.4	LD
A3G2 DGT 2	939.5	4932.8	110.9	5.8	1.7	0.5	44.1	3.4	LD
Mean A3G2	**885.9**	**5681.7**	**850.8**	**6.3**	**1.7**	**0.6**	**40.8**	**3.4**	**LD**
A3M1 DGT 1	2156.8	3997.4	120.4	2.5	1.1	0.4	23.5	3.8	1.0
A3M1 DGT 2	1942.6	3551.7	91.5	2.3	1.5	0.2	45.2	2.3	0.9
Mean A3M1	**2049.7**	**3774.6**	**106.0**	**2.4**	**1.3**	**0.3**	**34.4**	**3.0**	**1.0**
A3M2 DGT 1	1233.0	1586.4	138.6	2.2	1.1	0.3	23.2	2.8	0.8
A3M2 DGT 2	1697.9	2184.6	197.5	2.3	1.3	0.1	44.9	3.3	0.8
Mean A3M2	**1465.5**	**1885.5**	**168.1**	**2.2**	**1.2**	**0.2**	**34.1**	**3.1**	**0.8**
A3V1 DGT 1	4180.9	3191.1	99.6	1.7	0.8	0.1	22.4	3.0	0.7
A3V1 DGT 2	1388.5	4609.0	28.4	1.9	1.0	0.2	19.3	1.7	0.4
Mean A3V1	**2784.7**	**3900.0**	**64.0**	**1.8**	**0.9**	**0.2**	**20.9**	**2.4**	**0.5**
A3V2 DGT 1	3769.1	2566.0	182.0	1.3	0.5	0.1	14.9	3.6	1.2
A3V2 DGT 2	2882.0	2931.0	115.4	1.7	1.2	0.6	29.9	4.1	1.2
Mean A3V2	**3325.6**	**2748.5**	**148.7**	**1.5**	**0.9**	**0.3**	**22.4**	**3.9**	**1.2**
Mean Area A3	**1673.4**	**4745.3**	**279.8**	**9.8**	**2.0**	**0.6**	**97.0**	**13.0**	**10.6**
SD Area A3	**899.4**	**1783.9**	**370.1**	**8.0**	**2.6**	**0.6**	**122.3**	**15.3**	**12.5**

Table S11: Metal concentrations (µg kg^{-1}) in wood samples (C_{Wood}) from tree individuals from sampling area C.

C-Wood	Al	Mn	Fe	Co	Ni	Cu	Zn	Pb	U
CG1 I	LD	6271.3	1733.1	LD	LD	42.1	0.0	LD	LD
CG1 II	LD	8459.7	1618.9	LD	LD	21.5	0.0	LD	LD
Mean CG1	**LD**	**7365.5**	**1676.0**	**LD**	**LD**	**31.8**	**0.0**	**LD**	**LD**
CG2 I	840.6	13374.6	12755.0	LD	LD	63.2	942.9	17.1	LD
CG2 II	659.0	8371.8	11984.9	LD	LD	48.7	762.5	18.1	LD
Mean CG2	**749.8**	**10873.2**	**12370.0**	**LD**	**LD**	**56.0**	**852.7**	**17.6**	**LD**
CP1 I	LD	3558.7	9636.7	LD	38.7	52.7	7575.3	52.5	LD
CP1 II	LD	2509.7	16049.1	LD	63.5	55.9	3346.6	9.0	LD
Mean CP1	**LD**	**3034.2**	**12842.9**	**LD**	**51.1**	**54.3**	**5460.9**	**30.8**	**LD**
CP2 I	657.2	4319.9	20259.7	LD	58.4	61.3	3976.1	22.3	LD
CP2 II	1338.7	7392.6	36607.6	LD	112.6	110.6	9791.6	LD	LD
Mean CP2	**998.0**	**5856.2**	**28433.7**	**LD**	**85.5**	**85.9**	**6883.8**	**11.6**	**LD**
CM1 I	LD	6609.6	25711.4	LD	64.0	104.5	2283.9	9.1	LD
CM1 II	LD	6637.3	1231.1	LD	8.9	2106.2	1837.4	35.9	LD
Mean CM1	**LD**	**6623.4**	**13471.2**	**LD**	**36.4**	**1105.4**	**2060.6**	**22.5**	**LD**
CM2 I	438.1	8047.5	2025.4	LD	LD	40.7	0.0	23.5	LD
CM2 II	LD	6439.4	1952.5	LD	LD	33.8	0.0	41.3	LD
Mean CM2	**262.1**	**7243.5**	**1988.9**	**LD**	**LD**	**37.3**	**0.0**	**32.4**	**LD**
CT1 I	16959.7	14305.5	113456.1	11.6	LD	805.7	3209.7	26.1	LD
CT1 II	LD	12086.6	8109.4	1.5	LD	324.9	740.1	LD	LD
Mean CT1	**8525.7**	**13196.1**	**60782.7**	**6.5**	**LD**	**565.3**	**1974.9**	**13.1**	**LD**
CT2 I	LD	4446.3	5756.7	1.1	LD	138.8	647.5	30.4	LD
Mean CT2	**LD**	**4446.3**	**5756.7**	**1.1**	**LD**	**138.8**	**647.5**	**30.4**	**LD**
CV2 I	1521.9	95137.4	LD	17.8	197.4	3399.3	8.4	66.5	LD
CV2 II	1224.4	24351.9	LD	7.9	196.4	735.6	3.6	76.7	LD
Mean CV2	**1373.2**	**59744.6**	**LD**	**12.9**	**196.9**	**2067.5**	**6.0**	**71.6**	**LD**
CE1 I	LD	29176.6	LD	43.2	122.0	3222.1	2.8	LD	LD
CE1 II	LD	115326.4	LD	63.1	156.5	4204.5	2.6	LD	LD
Mean CE1	**LD**	**72251.5**	**LD**	**53.2**	**139.3**	**3713.3**	**2.7**	**LD**	**LD**
Media C	**1274.2**	**20530.9**	**15023.0**	**1.9**	**17.4**	**258.3**	**1864.2**	**26.0**	**LD**
SD C	2753.7	26143.7	17933.0	1.9	23.0	358.2	1799.4	20.0	LD

Table S12: Metal concentrations (µg kg^{-1}) in wood samples (C_{Wood}) from tree individuals from sampling area A1.

C-Wood	Al	Mn	Fe	Co	Ni	Cu	Zn	Pb	U
A1P1 I	1046.0	13167.3	3015.1	LD	22.7	98.5	1592.4	34.3	LD
A1P1 II	458.7	13792.8	3631.9	LD	27.2	65.8	1042.7	5.0	LD
Mean A1P1	**752.4**	**13480.0**	**3323.5**	**LD**	**24.9**	**82.2**	**1317.6**	**19.6**	**LD**
A1G1 I	641.6	9648.2	1260.9	LD	25.6	45.4	601.6	25.5	LD
A1G1 II	115.8	9188.9	2021.0	LD	25.5	56.3	0.0	10.7	LD
Mean A1G1	**378.7**	**9418.6**	**1641.0**	**LD**	**25.6**	**50.9**	**300.8**	**18.1**	**LD**
A1G2 I	935.1	20160.4	4070.3	LD	28.3	64.1	2280.4	29.8	8.5
A1G2 II	1079.0	18073.4	6916.1	LD	47.3	94.1	2904.3	38.7	11.7
Mean A1G2	**1007.0**	**19116.9**	**5493.2**	**LD**	**37.8**	**79.1**	**2592.4**	**34.2**	**10.1**
A1T1 I	LD	5323.5	15163.5	LD	53.0	187.5	1582.0	11.7	LD
Mean A1T1	**LD**	**5323.5**	**15163.5**	**LD**	**53.0**	**187.5**	**1582.0**	**11.7**	**LD**
A1T2 I	LD	2524.6	3504.8	LD	22.0	405.6	1109.0	26.0	LD
A1T2 II	LD	5033.1	5424.9	LD	26.9	211.4	1419.8	14.7	LD
Mean A1T2	**LD**	**3778.9**	**4464.9**	**LD**	**24.4**	**308.5**	**1264.4**	**20.4**	**LD**
A1V1 I	LD	22005.2	1720.2	LD	LD	55.8	255.0	86.0	LD
A1V1 II	LD	16854.2	1115.7	LD	LD	85.7	0.0	50.5	52.6
Mean A1V1	**LD**	**19429.7**	**1417.9**	**LD**	**LD**	**70.8**	**255.0**	**68.3**	**27.0**
A1M1 I	LD	1730.2	2653.9	LD	6.3	21.5	0.0	40.1	LD
A1M1 II	LD	1808.0	1197.1	LD	LD	20.3	0.0	40.4	LD
Mean A1M1	**LD**	**1769.1**	**1925.5**	**LD**	**6.3**	**20.9**	**0.0**	**40.3**	**LD**
A1M2 I	LD	4638.5	2276.8	LD	11.3	15.4	0.0	28.5	LD
A1M2 II	LD	5372.7	2653.7	LD	945.2	40.6	1150.6	48.3	LD
Mean A1M2	**LD**	**5005.6**	**2465.3**	**LD**	**478.3**	**28.0**	**575.3**	**38.4**	**LD**
Media A1	**324.0**	**9665.3**	**4486.8**	**LD**	**80.9**	**103.5**	**985.9**	**31.4**	**5.6**
SD A1	363.5	6937.0	4543.8	LD	161.5	97.5	867.5	18.2	9.2

Table S13: Metal concentrations (µg kg^{-1}) in wood samples (C_{Wood}) from tree individuals from sampling area A2.

C-Wood	Al	Mn	Fe	Co	Ni	Cu	Zn	Pb	U
A2M1 I	LD	2883.2	2808.3	3.3	LD	51.9	8.6	119.4	LD
A2M1 II	LD	2227.8	3273.8	2.7	LD	53.0	205.0	105.2	LD
Mean A2M1	**LD**	**2555.5**	**3041.1**	**2.3**	**LD**	**52.5**	**106.8**	**112.3**	**LD**
A2M2 I	205.2	685.8	4094.7	2.1	LD	86.7	129.1	1.3	LD
A2M2 II	230.0	418.3	1466.9	1.5	LD	79.3	192.3	1.8	LD
Mean A2M2	**217.6**	**552.1**	**2780.8**	**1.8**	**LD**	**83.0**	**160.7**	**1.6**	**LD**
A2G1 I	261.9	6567.8	7026.5	1.7	LD	93.8	349.4	69.6	LD
A2G1 II	412.6	6324.2	2495.5	1.8	LD	86.3	198.2	120.1	LD
Mean A2G1	**337.3**	**6446.0**	**4761.0**	**1.8**	**LD**	**90.1**	**273.8**	**94.9**	**LD**
Mean A2G2 I	245.9	11563.4	7439.8	4.5	LD	99.5	6528.6	32.4	LD
Mean A2G2 II	328.9	11701.7	3174.8	0.8	LD	70.9	577.7	45.1	LD
Mean A2G2	**287.4**	**11632.6**	**5307.3**	**2.6**	**LD**	**85.2**	**3553.2**	**38.7**	**LD**
A2E1 I	221.9	2250.1	1115.0	LD	LD	48.2	178.7	4.6	LD
A2E1 II	276.5	10973.3	2139.4	0.8	LD	84.4	235.9	5.7	LD
Mean A2E1	**249.2**	**6611.7**	**1627.2**	**0.4**	**LD**	**66.3**	**207.3**	**5.2**	**LD**
A2E2 I	473.5	7587.4	2207.3	0.8	LD	124.4	86.7	38.1	LD
A2E2 II	349.5	5535.5	3425.4	6.3	LD	115.5	1545.3	77.8	LD
Mean A2E2	**411.5**	**6561.5**	**2816.3**	**3.6**	**LD**	**120.0**	**816.0**	**58.0**	**LD**
A2P1 I	267.2	3694.0	1442.2	0.6	LD	111.4	353.5	702.7	LD
A2P1 II	425.5	2624.6	513.3	0.2	LD	85.1	697.9	350.5	LD
Mean A2P1	**346.3**	**3159.3**	**977.7**	**0.4**	**LD**	**98.3**	**525.7**	**526.6**	**LD**
A2P2 I	347.5	7078.0	2779.7	2.3	LD	124.0	5645.6	1.8	LD
A2P2 II	391.5	17843.0	3807.0	0.5	LD	182.0	910.0	11.0	LD
Mean A2P2	**369.5**	**12460.5**	**3293.4**	**1.4**	**LD**	**153.0**	**3277.8**	**6.4**	**LD**
A2V1 I	LD	10898.5	8349.1	1.3	LD	125.6	642.1	46.4	LD
A2V1 II	LD	9184.8	7089.4	1.7	LD	89.3	1683.7	29.3	LD
Mean A2V1	**LD**	**10041.6**	**7719.2**	**1.5**	**LD**	**107.5**	**1162.9**	**37.9**	**LD**
A2V2 I	246.7	22448.4	3382.8	1.8	LD	114.1	611.5	12.4	LD
A2V2 II	288.5	21326.7	7321.4	2.9	LD	82.3	3269.2	35.1	LD
Mean A2V2	**267.6**	**21887.6**	**5352.1**	**2.4**	**LD**	**98.2**	**1940.3**	**23.8**	**LD**
Media A2	**254.0**	**8190.8**	**3767.6**	**1.8**	**LD**	**95.4**	**1202.4**	**90.5**	**LD**
SD A2	133.1	6188.9	2013.3	1.0	LD	28.0	1296.4	157.7	LD

Table S14: Metal concentrations (µg kg^{-1}) in wood samples (C_{Wood}) from tree individuals from sampling area A3.

C-Wood	Al	Mn	Fe	Co	Ni	Cu	Zn	Pb	U
A3E1 I	LD	5158.0	5240.9	LD	LD	LD	193.7	16.9	LD
A3E1 II	LD	6738.0	657.8	LD	LD	LD	583.5	31.5	LD
Mean A3E1	**LD**	**5948.0**	**2949.3**	**LD**	**LD**	**LD**	**388.6**	**24.2**	**LD**
A3E2 I	LD	8113.2	887.9	LD	20.0	54.7	1195.9	38.5	30.6
A3E2 II	LD	7858.2	2289.0	LD	21.6	85.3	903.9	148.1	LD
Mean A3E2	**LD**	**7985.7**	**1588.4**	**LD**	**20.8**	**70.0**	**1049.9**	**93.3**	**15.9**
A3T1 I	LD	4701.6	6773.9	1.9	LD	227.8	1301.0	15.5	LD
A3T1 II	LD	4120.0	2320.7	LD	LD	169.3	1878.7	17.2	LD
Mean A3T1	**LD**	**4410.8**	**4547.3**	**1.0**	**LD**	**198.6**	**1589.9**	**16.3**	**LD**
A3T2 I	LD	6599.2	13186.9	2.3	LD	218.0	1786.7	LD	LD
A3T2 II	LD	5405.9	5220.2	0.0	LD	154.4	388.0	LD	LD
Mean A3T2	**LD**	**6002.6**	**9203.5**	**1.1**	**LD**	**186.2**	**1087.3**	**LD**	**LD**
A3P2 I	LD	10730.1	2527.1	LD	27.0	76.0	596.0	9.1	LD
A3P2 II	LD	8270.4	1722.6	LD	LD	96.1	1077.5	LD	LD
Mean A3P2	**LD**	**9500.3**	**2124.8**	**LD**	**13.5**	**86.0**	**836.8**	**4.9**	**LD**
A3G1 I	LD	12041.7	2262.0	LD	LD	124.5	1145.2	50.1	LD
A3G1 II	LD	9144.8	2712.9	LD	LD	180.4	694.4	47.3	LD
Mean A3G1	**LD**	**10593.3**	**2487.5**	**LD**	**LD**	**152.4**	**919.8**	**48.7**	**LD**
A3G2 I	LD	18350.1	11054.7	1.8	LD	178.3	3155.9	129.5	LD
A3G2 II	LD	12995.8	21042.8	3.0	LD	156.3	5157.3	111.2	LD
Media	**LD**	**15673.0**	**16048.8**	**2.4**	**LD**	**167.3**	**4156.6**	**120.3**	**LD**
A3M1 I	LD	3934.0	3565.7	1.5	LD	71.4	482.9	13.5	LD
A3M1 II	LD	2929.8	9223.1	LD	LD	62.4	1341.8	74.2	LD
Mean A3M1	**LD**	**3431.9**	**6394.4**	**0.7**	**LD**	**66.9**	**912.4**	**43.9**	**LD**
A3M2 I	LD	17841.6	4059.7	5.3	11.1	67.9	2843.4	182.5	LD
A3M2 II	LD	24757.7	2151.6	5.8	24.4	62.6	1827.1	153.2	LD
Mean A3M2	**LD**	**21299.7**	**3105.7**	**2.3**	**17.7**	**65.3**	**2335.2**	**167.9**	**LD**
A3V1 I	LD	25642.2	9281.8	LD	13.0	90.6	1697.3	221.1	LD
A3V1 II	381.7	35898.1	5733.8	1.3	LD	144.1	1881.1	311.6	LD
Mean A3V1	**289.6**	**30770.1**	**7507.8**	**0.8**	**10.4**	**117.3**	**1789.2**	**266.4**	**LD**
A3V2 I	LD	17519.3	6044.6	LD	5.5	93.9	992.4	341.8	LD
A3V2 II	LD	12902.3	1641.5	LD	7.0	80.2	2001.2	288.8	LD
Mean A3V2	**LD**	**15210.8**	**3843.0**	**LD**	**6.3**	**87.0**	**1496.8**	**315.3**	**LD**
Media A3	**123.4**	**11893.3**	**5436.4**	**1.4**	**6.7**	**109.5**	**1505.7**	**100.1**	**LD**
SD A3	71.7	8309.2	4259.6	1.0	7.7	59.8	1028.4	108.0	LD

Table S15: Slopes of the linear regression between concentration in wood and total metal in soil for all sampling areas together focusing on the tree species separately, Y-intercepts (Y-int.) of regression and coefficient of determination R2 (in bold: significant).

	Clethra scabra			*Myrsine sp.*			*Alchornea triplinervia*			*Piptocarpha axillaris*			*Eucalyptus sp.*			*Pinus sp.*		
	Slope	**Y-int.**	**R^2**	**Slope**	**Y-int.**	**R^2**	**Slope**	**Y-int.**	**R^2**	**Slope**	**Y-int.**	**R^2**	**Slope**	**Y-int.**	**R^2**	**Slope**	**Y-int.**	**R^2**
Pb	0.00012	40	0.008	-0.00014	65	0.006	-0.00006	22	**0.683**	-0.004073	327	0.289	0.00015	29	0.071	0.00217	-89	0.568
Zn	-0.03196	4880	0.193	-0.01622	2228	0.141	0.03353	-1878	0.520	0.033750	-1753	0.121	0.00067	552	0.001	-0.07291	9760	0.205
Co	0.00002	-0.1	0.096	0.00001	1	0.032	-0.00013	12	0.508	0.000004	1	0.010	-0.00005	7	0.705	0.00001	1	0.077
Fe	0.00011	1931	0.021	-0.00031	16712	0.342	-0.00090	46521	0.077	0.000262	-4273	0.109	-0.00011	6502	0.983	-0.00023	13666	0.462
Mn	-0.00427	15166	0.279	-0.00946	13274	0.221	0.00749	604	**0.745**	0.005893	19850	0.055	-0.00032	6906	0.002	0.00972	2158	0.552
Cu	0.00111	50	0.040	0.02641	-480	0.102	0.03899	-803	0.575	0.002049	59	0.016	-0.00516	213	0.252	-0.00029	102	0.003

Table S16: Slopes of the linear regression between concentration in wood and concentration of labile metals in soil (measured by DGT) for all sampling areas together focusing on the tree species separately, Y-intercepts (Y-int.) of regression and coefficient of determination R2 (in bold: significant).

	Clethra scabra			*Myrsine sp.*			*Alchornea triplinervia*			*Piptocarpha axillaris*			*Eucalyptus sp.*			*Pinus sp.*		
	Slope	**Y-int.**	**R^2**	**Slope**	**Y-int.**	**R^2**	**Slope**	**Y-int.**	**R^2**	**Slope**	**Y-int.**	**R^2**	**Slope**	**Y-int.**	**R^2**	**Slope**	**Y-int.**	**R^2**
Pb	3.668	31.88	0.035	-1.095	61.02	0.003	-0.01305	15	0.0002	-7.478	156	0.011	-0.02868	40	0.0002	10.45	72	0.041
Zn	-23.2	3402	**0.542**	-3.968	1070	0.095	2.099	966	0.3576	-2.719	1772	0.310	-4.701	1590	0.1043	-11.86	2597	0.041
Co	-0.115	2	0.122	-0.05162	1.575	0.099	-0.1927	4	0.4413	0.08	0.5	0.255	-0.06037	3	0.1760	0.30	1	0.676
Fe	16.32	2591	**0.728**	-4.15	5317	0.113	-12.12	21040	0.0650	-19.86	9799	0.217	6.245	2535	0.1990	-24.59	5522	0.078
Mn	-1.221	18791	**0.636**	-1.816	14409	0.385	0.5687	2767	0.0386	2.296	8617	0.324	-3.462	29689	0.0353	1.113	4913	0.473
Cu	98.87	66.64	0.157	778.3	11.33	0.055	-37.52	275	0.0441	-150.8	145	0.372	-51.56	105	0.3290	-213.2	126	0.707

Table S17: Code key for sampling spots and their respective geographical coordinates.

Sample Code	Area	Tree species sampled	Latitude	Longitude
A3E1	A3	*Eucalyptus sp.*	21.941920	46.494900
A3E2	A3	*Eucalyptus sp.*	21.932303	46.489634
A3G1	A3	*Clethra scabra*	21.939163	46.486944
A3G2	A3	*Clethra scabra*	21.938951	46.486991
A3M1	A3	*Myrsine gardineriana*	21.939144	46.486856
A3M2	A3	*Myrsine gardineriana*	21.939052	46.486736
A3P1	A3	*Pinus sp.*	21.941995	46.493614
A3P2	A3	*Pinus sp.*	21.947688	46.490218
A3T1	A3	*Alchornea triplinervia*	21.947055	46.494308
A3T2	A3	*Alchornea triplinervia*	21.940106	46.493099
A3V1	A3	*Piptocarpha axillaris*	21.939181	46.487058
A3V2	A3	*Piptocarpha axillaris*	21.938957	46.487004
A2E1	A2	*Eucalyptus sp.*	21.956168	46.512345
A2E2	A2	*Eucalyptus sp.*	21.948022	46.510533
A2G1	A2	*Clethra scabra*	21.954537	46.512620
A2G2	A2	*Clethra scabra*	21.954040	46.512870
A2M1	A2	*Myrsine gardineriana*	21.948808	46.513800
A2M2	A2	*Myrsine gardineriana*	21.953834	46.510216
A2P1	A2	*Pinus sp.*	21.948033	46.510462
A2P2	A2	*Pinus sp.*	21.951478	46.514041
A2T1	A2	*Alchornea triplinervia*	22.026445	46.563577
A2V1	A2	*Piptocarpha axillaris*	21.953688	46.510638
A2V1	A2	*Piptocarpha axillaris*	21.948832	46.513773
A1G1	A1	*Clethra scabra*	21.958596	46.511602
A1G2	A1	*Clethra scabra*	21.958000	46.511000
A1M1	A1	*Myrsine coriacea*	21.958000	46.511000
A1M2	A1	*Myrsine gardineriana*	21.958073	46.511027
A1P1	A1	*Pinus sp.*	21.957817	46.510628
A1T1	A1	*Alchornea triplinervia*	21.958061	46.511182
A1T2	A1	*Alchornea triplinervia*	21.958060	46.511160
A1V1	A1	*Piptocarpha axillaris*	21.958470	46.511086
CE1	C	*Eucalyptus sp.*	21.974314	46.509587
CG1	C	*Clethra scabra*	21.942776	46.508966
CG2	C	*Clethra scabra*	21.942779	46.508935
CM1	C	*Myrsine coriacea*	21.942173	46.507759
CM2	C	*Myrsine coriacea*	21.942248	46.507995
CP1	C	*Pinus sp.*	21.974603	46.509515
CP2	C	*Pinus sp.*	21.974000	46.500000
CT1	C	*Alchornea triplinervia*	21.942776	46.508965
CT2	C	*Alchornea triplinervia*	21.942678	46.508217
CV1	C	*Piptocarpha macropoda*	21.942850	46.508971
CV2	C	*Piptocarpha macropoda*	21.942860	46.509079